

Aus dem Institut für Prophylaxe und Epidemiologie der Kreislaufkrankheiten

der Ludwig-Maximilians-Universität München

Direktor: Prof. Dr. med. Christian Weber

The Role of MicroRNA-21 in Macrophages during Atherosclerosis

Dissertation

zum Erwerb des Doktorgrades der Humanbiologie

an der Medizinischen Fakultät

der Ludwig-Maximilians-Universität zu München

vorgelegt von

Richard Michael Blay

(M.Phil)

Aus

Bonyere, Ghana

2016

Mit Genehmigung der Medizinischen Fakultät
der Universität München

Berichterstatter: Prof. Dr. med. Andreas Schober

Unterschrift: _____

Mitberichterstatter 1: Prof. Dr. Heiko Adler

Mitberichterstatter 2: Prof. Dr. Daniel Teupser

Mitbetreuung durch den

promovierten Mitarbeiter: Dr. rer. nat. Maliheh Nazari-Jahantigh

Dekan: Prof. Dr. med. dent. Reinhard Hickel

Tag der mündlichen Prüfung: 25.07.2016

The Role of MicroRNA-21 in Macrophages during Atherosclerosis

Affidavit

Blay, Richard Michael

Surname, First Name

I hereby declare, that the submitted thesis entitled

The Role of MicroRNA-21 in Macrophages during Atherosclerosis

is my own work. I have only used the sources indicated and have not made unauthorised use of services of a third party. Where the work of others has been quoted or reproduced, the source is always given.

I further declare that the submitted thesis or parts thereof have not been presented as part of an examination degree to any other university.

Place, date

Signature doctoral candidate

Table of Contents

1	Introduction	5
1.1	Atherosclerosis	5
1.1.1	Cellular processes in atherosclerosis	6
1.1.2	Macrophages: apoptosis and efferocytosis	7
1.2	MicroRNAs and atherosclerosis	9
1.2.1	Biogenesis of microRNAs.....	9
1.2.2	MicroRNAs in macrophage function during atherosclerosis	10
1.2.3	<i>miR-21-3p</i> and <i>miR-21-5p</i> in atherosclerosis	11
1.3	The Circadian rhythm and atherosclerosis	12
1.4	Role of <i>Xaf1</i> and <i>Mbl2</i> in atherosclerosis.....	15
1.5	Aim of study	16
2	Materials and methods.....	17
2.1	General equipment.....	17
2.2	Chemicals	18
2.3	Antibodies.....	19
2.3.1	Primary antibodies.....	19
2.3.2	Secondary antibodies.....	19
2.4	Buffers and solutions	20
2.5	Kits Used	21
2.6	Mouse husbandry.....	22
2.7	Mouse strains.....	22

2.8	Animal models of atherosclerosis.....	22
2.8.1	Atherosclerosis in whole body knock-out mice	22
2.8.2	Atherosclerosis in bone marrow transplanted mice.....	23
2.8.3	Fixation of tissues.....	23
2.8.4	Serum analysis and blood cell count	24
2.9	Laser capture microdissection (LCM).....	24
2.10	Lesion characterization	25
2.10.1	Histology	25
2.11	<i>En face</i> preparation and oil red o staining	27
2.12	Immunofluorescence staining	27
2.12.1	TUNEL and MAC2 staining	28
2.13	In situ PCR.....	29
2.13.1	MAC2 immunostaining after in situ PCR	31
2.14	Global gene expression analysis by microarray.....	31
2.15	In vitro experiments	32
2.15.1	Cell culture of BM-derived macrophages (BMDMs).....	32
2.15.2	Synchronisation of BMDMs.....	33
2.15.3	Treatment of BMDMs with mimics	33
2.15.4	Stimulation of BMDMs to M1 and M2 macrophages.....	33
2.16	Quantitative real time polymerase chain reaction (qRT-PCR).....	34
2.17	Statistical analysis	34
3	Results.....	35
3.1	Role of <i>Mir21</i> in macrophages during atherogenesis.....	35

3.1.1	<i>miR-21-3p</i> and <i>miR-21-5p</i> expression in atherosclerotic lesions	35
3.1.2	Role of <i>Mir21</i> in macrophage polarization.....	36
3.1.3	The effect of hematopoietic deficiency of <i>Mir21</i> on lesion formation.....	39
3.1.4	The effect of <i>Mir21</i> deficiency on cellular content of atherosclerotic lesions	43
3.1.5	The effect of <i>Mir21</i> deficiency on lipid content in macrophages.....	45
3.1.6	The effect of <i>Mir21</i> deficiency on macrophage apoptosis in atherosclerosis	46
3.2	Targets of <i>Mir21</i> in macrophages during atherogenesis	47
3.2.1	Effect of <i>Mir21</i> deficiency on mRNA expression in atherosclerotic lesions	47
3.2.2	Differentially regulated circadian clock genes in aortic root lesions	50
3.2.3	Effect of BM deficiency of <i>Mir21</i> on circadian clock genes in lesional macrophages .	51
3.2.4	Effect of bone marrow deficiency of <i>Mir21</i> on <i>Xaf1</i> and <i>Mbl2</i> expression in lesional macrophages	52
3.3	Effect of <i>Mir21</i> on circadian clock in macrophages.....	53
3.3.1	Circadian rhythmic expression of <i>miR-21-3p</i> and <i>miR-21-5p</i>	53
3.3.2	Effect of <i>Mir21</i> deficiency on circadian clock genes in BMDMs.....	54
3.3.3	Circadian expression of <i>Xaf1</i> and <i>Mbl2</i>	56
3.3.4	Effect of <i>miR-21-3p</i> and <i>miR-21-5p</i> on circadian clock genes in macrophages.....	57
4	Discussion	62
4.1	Role of <i>Mir21</i> in macrophages and atherosclerosis.....	62
4.1.1	<i>miR-21</i> and macrophage polarization.....	62
4.1.2	The role of <i>Mir21</i> on atherosclerosis.....	63
4.1.3	The mechanism of <i>Mir21</i> in macrophages on atherosclerosis	64
4.2	Regulation of the macrophage clock by <i>Mir21</i> in atherosclerosis	68
4.2.1	<i>Mir-21</i> expression and circadian rhythm.....	68

4.2.2	Role of the clock genes in <i>miR-21-3p</i> and <i>5p</i> –regulated <i>Mbl2</i> and <i>Xaf1</i> expression ...	69
4.3	Clinical relevance	71
5	Summary	73
6	References	75
7	Acknowledgements.....	94

1 Introduction

Atherosclerosis is a maladaptive inflammatory response that occurs at susceptible sites in the walls of major conduit arteries to disturbed flow and increased plasma cholesterol¹⁻³. The process which is initiated by lipid retention in the intima and subsequent oxidation, promotes a chronic inflammatory response and ultimately forming advanced lesions that can cause stenosis or rupture and cause thrombosis^{4, 5}. Ischemic heart disease and cerebrovascular disease, two clinical consequences of atherosclerosis, are the leading causes of death in high-income countries as well as low and middle-income countries⁶. Micro-ribonucleic acids (miRNAs/microRNAs/miRs), a class of small endogenous non-coding RNAs that regulate gene expression play important roles in several physiological and pathological processes^{7, 8}. MicroRNAs are also implicated in various functions in different cell types and stages involved in atherogenesis⁹. The use of these small RNAs either as diagnostic markers or therapeutic measures presents a promising solution in the fight against atherosclerosis, its clinical complications and contribution to disease burden and mortality.

1.1 Atherosclerosis

The process of atherosclerosis develops over a long period of time and is initiated by the accumulation of lipoproteins which triggers the recruitment and differentiation of monocytes into macrophages and over time, inability of the immune cells to resolve this inflammatory response results in the deposition of lipid-laden macrophages (foam cells)^{10, 11}. In early atherosclerosis, apoptosis of the macrophages coupled with effective efferocytosis prevents further progression of the lesion but in late stages however, defective efferocytosis and increased inflammatory response lead to the formation of a necrotic core and more advanced lesions¹². Advanced lesions can grow through the increased accumulation of apoptotic debris and macrophages which may block the vessel, but also of clinical concern is the calcification, ulceration at the luminal surface, and haemorrhage from small vessels that grow into the lesion leading to thrombus resulting in ischemic heart disease (IHD) or stroke¹³.

IHD and stroke, the main cardiovascular diseases (CVD) constitute the leading cause of death worldwide¹⁴. Approximately 17 million people constituting 30%, died of CVD in 2010 worldwide¹⁵. Even as these statistics already present a great challenge and burden, it is projected to keep increasing due to rapid urbanization and higher prevalence of risk factors¹⁶. An estimate of the number of deaths due to IHD shows 80% and 100% increase in women and men respectively, whereas a 78% and 106% increase due to cerebrovascular disease in women and men respectively is projected by the year 2020¹⁶. This increase in the prevalence and mortality due CVDs according to Yusuf *et al.*¹⁷ are mainly due to; (1) the decrease in infant mortality; (2) rapid urbanization of low and middle income countries; (3) increasing life expectancy and a more ageing population and (4) increasing use of tobacco worldwide.

In spite of the extensive research into atherosclerosis, there are presently few therapeutic drugs to prevent or slow down the progression of atherosclerotic lesions and this mainly involves the use of statins to reduce blood cholesterol levels¹⁸. Although significant benefits are being achieved by statin therapy, a significant number of events still take place necessitating the need for more effective and new therapies¹⁹.

1.1.1 Cellular processes in atherosclerosis

In humans, the earliest form of atherosclerosis called the ‘fatty streak’ consists of the accumulation of cholesterol-engorged macrophages (foam cells) in the subendothelial space and can be found in the aorta within the first decade of life, the coronary arteries in the second decade, and the cerebral arteries in the third or fourth decades²⁰. Though fatty streaks are not clinically significant, they are the precursors of more advanced lesions¹³. Lesions form preferably at regions of the arteries in which laminar flow is disturbed by bends or branch point²¹⁻²³. From the decades of studies into atherosclerosis, three main hypotheses supporting its initiation have been postulated and these include the response-to-injury hypothesis, the response-to-retention hypothesis and the oxidative modification hypothesis²⁴.

According to the response-to-injury theory, atherosclerosis is initiated by the focal denudation of endothelial cells as a result of an “injury” to these endothelial cells²⁵. This is followed by the aggregation of platelets and the release of factors that enhances smooth muscle cell proliferation and advancement of lesion formation²⁵. It was later postulated that endothelial injury alone was not enough to initiate atherosclerosis, but the injury results in the initiation of functional modifications key to atherogenesis. These modifications include the attachment and activation of monocytes which enter the vessel wall early in atherogenesis and differentiate into macrophages²⁰ and the chemical modification of low density lipoprotein (LDL) by the endothelial cells through a free radical oxidation process thereby actively participating in foam cell formation²⁶.

The response-to-retention hypothesis states that the subendothelial retention of apolipoprotein B (apoB)-containing lipoproteins in focal areas of arteries as opposed to endothelial injury is the key pathological event in atherogenesis²⁴ and following the rapid induction of hypercholesterolemia, accumulation of LDL in the vessel wall is one of the earliest detectable changes²⁷. Modification of retained lipoproteins likely triggers inflammatory response leading to activation of endothelial and vascular smooth muscle cells (SMCs), recruitment of monocytes and accumulation of monocyte-derived macrophages, T-cells, B-cells, and dendritic cells in the subendothelial space⁵.

Evidence supporting the oxidative modification hypothesis suggests that native LDL does not enhance atherogenesis since it is not taken up by macrophages rapidly enough to generate foam cells, and so it was proposed that LDL is somehow ‘modified’ in the vessel wall²⁸.

LDL diffuses passively through endothelial cell to cell junctions and its retention involves interactions with negatively charged proteoglycans²⁹. LDL undergoes oxidation³⁰ making it susceptible to macrophage uptake through the scavenger receptor pathway, producing cholesterol ester-laden foam cells³¹. It is the accumulation of foam cells that forms the nest for the development of atherosclerotic lesions. Putting the evidence together, irrespective of the initiating event during atherogenesis and the subsequent cellular involvement, macrophage function seems to be central in the progression and formation of atherosclerotic lesions. Therapeutic targeting of macrophages and their functions in the arterial wall is therefore likely to provide several novel therapeutic solutions and possibilities.

1.1.2 Macrophages: apoptosis and efferocytosis

Even though atherosclerosis was for many years believed to be merely the passive accumulation of cholesterol in the vessel wall, it is considered today more as a chronic inflammatory disease³². The accumulation of oxidatively-modified low-density lipoprotein (oxLDL) in the vessel wall activates endothelial cells which send inflammatory molecular signals leading to the recruitment of cells responsible for innate immune response such as dendritic cells and monocyte-derived macrophages^{33, 34}. Macrophages infiltrate the subendothelial space as a response to inflammation with the purpose of engulfing oxLDL and to remove them³⁵. However, phagocytosis of oxLDL leads to the formation foam cells and further the progression of atherosclerosis when they persist in the subendothelial space^{13, 34, 36}.

Macrophage clearance of lipoproteins is thought to be beneficial at the initial stages of the immune response in atherosclerosis, but according to Moore *et al* there is little negative feedback following uptake³⁴ and thus the cells over time become grossly engorged with lipids thereby reducing their ability to emigrate from the subendothelial space resulting in failure to resolve the inflammation³⁷. The uptake of oxLDL mediated by the scavenger receptor A (SR-A) does not only lead to persistence of macrophages in lesions but more importantly to increased proliferation, a key factor that drives macrophage accumulation and atherosclerosis³⁸.

Persistence of macrophage foam cells in the lesion eventually leads to increased oxidative stress and endoplasmic reticulum (ER) stress³⁹. Activation of ER stress in lesional macrophages due to the accumulation of free cholesterol and saturated fatty acids triggers apoptosis through the cluster of differentiation 36 (CD36) and toll-like receptor 2 (TLR2) receptors⁴⁰. Prolonged ER stress activates the unfolded protein response (UPR) which triggers a second pathway of apoptosis through the activation of CEBP-homologous protein (CHOP) and subsequently the production of reactive oxygen species⁴¹. CHOP decreases the expression of the cell survival protein B-cell lymphoma 2 (Bcl2) leading to macrophage cell death in advanced atherosclerotic lesions⁵.

The central role played by macrophages in atherogenesis makes the number of macrophages in lesions a very important measure of atherosclerotic burden⁴². According to Tabas⁴², there are two factors that control lesional macrophage numbers namely factors that determine cellularity and factors that lead to macrophage depletion. Macrophage cellularity is determined by monocyte infiltration and macrophage proliferation whereas macrophage depletion is determined by apoptosis and removal of apoptotic macrophages, suggesting that altering macrophage content by reducing recruitment to atherosclerotic plaques or by promoting macrophage apoptosis may have therapeutic effects. However, this therapeutic effect may depend on the stage of atherogenesis that macrophage death occurs⁴³. In early lesions, blocking apoptosis in macrophages enhances atherosclerotic lesion formation^{44, 45}, indicating that macrophage apoptosis in the early stages of atherogenesis is beneficial. However, in advanced lesions, increased apoptosis combined with defective clearance of apoptotic macrophages (efferocytosis), leads to the formation of a necrotic core⁴⁶, which makes the lesion more vulnerable and dangerous by contributing further to inflammation, thrombosis and rupture⁴⁷.

To resolve inflammation, apoptotic cells are usually engulfed by macrophages through phagocytosis and removed from the sight of injury⁴⁸. In early lesions, efferocytosis is effective and apoptotic cells are removed, thus preventing lesion development; however, efferocytosis in advanced lesions is not efficient enough to clear apoptotic macrophages, leading to the accumulation of apoptotic cell debris and consequently necrotic core formation and increased atherogenesis¹². In LDL receptor knock-out (*Ldlr*^{-/-}) mice, increased macrophage survival in already existing lesions reduces necrotic core formation and the progression of atherosclerosis, indicating that macrophage apoptosis is pro-atherogenic in late atherosclerosis due to the defect in clearing apoptotic cells⁴⁹. The above discussed data implies an effective efferocytosis in early lesions, whereas in late atherogenesis, reduced efferocytosis may be an important promoter of necrotic core formation and atherogenesis⁴⁶. Efficient efferocytosis prevents the cytotoxic exposure of apoptotic bodies, triggers anti-inflammatory response and promotes survival of the efferocytes³⁹. These findings suggest possible therapeutic targets worthy of attention maybe to: (1) promote or increase macrophage apoptosis in early atherosclerosis, (2) enhance macrophage survival in late atherosclerosis and (3) to enhance efferocytosis in lesions.

Efferocytosis of apoptotic macrophages is mediated by the expression phagocytic receptors and apoptotic ligands that enhance recognition and uptake^{50, 51}. For example, targeting of MER proto-oncogene, tyrosine kinase (MERTK), a tyrosine kinase and low-density lipoprotein receptor-related protein 1 (LRP-1) in mouse atherosclerotic lesions increases the presence of apoptotic macrophages⁴⁶ suggesting that MERTK and LRP-1 mediate apoptotic clearance. The processes that lead to defective clearance of apoptotic macrophages during atherogenesis therefore need to be investigated and targeted as possible therapeutic pathways. Previous data suggests that not all lesional macrophages are transformed into foam cells, but some macrophages are responsible for the production of cytokines like interleukin-1 beta (IL-1 β) and tumour necrosis factor alpha (TNF α) and are involved in enhancing inflammation in

atherosclerotic lesions⁵². Macrophages were then later shown to exhibit plasticity and different phenotypes based on available signals and cytokines⁵³. Classical activation of macrophages (M1) which is pro-inflammatory, results in the presence of lipopolysaccharide (LPS) and interferon gamma (IFN- γ) whereas the alternative activation of macrophages (M2) occurs in response to interleukin-4 (IL-4)⁵³. Both M1 and M2 macrophage phenotypes, do exist in atherosclerotic plaques⁵⁴ and the activation and polarization of macrophages have significant effects on atherosclerosis⁵³.

1.2 MicroRNAs and atherosclerosis

MicroRNAs are a large family of small (~22 nucleotides) non-coding RNA molecules that are responsible for post-transcriptional regulation of gene expression⁷. The regulation of the expression of target genes occurs through imperfect base pairing to the 3' untranslated region (3' UTR) of messenger RNAs (mRNAs) thereby repressing mRNA expression. MicroRNAs are involved in several physiological processes including development, differentiation, metabolism, growth, proliferation and apoptosis^{8, 55-57}. Furthermore, several microRNAs expressed in various cells can regulate mechanisms including inflammation, cell proliferation, apoptosis and lipid metabolism, thereby playing important roles in atherosclerosis^{58, 59}. MicroRNAs therefore present several possibilities in the developing of therapeutic strategies to inhibit atherosclerosis.

1.2.1 Biogenesis of microRNAs

MicroRNA biogenesis is an evolutionary conserved mechanism which involves transcription of the primary microRNA (pri-miRNA) by RNA polymerase II (RNA pol II) from introns of protein coding genes or from non-coding regions^{60, 61} (Figure 1). Following transcription, the pri-miRNA is further processed by Drosha into a 60 – 100 nucleotide precursor namely the pre-miRNA⁶². This pre-miRNA is then recognized by Exportin-5 and Ran-GTP and transported from the nucleus to the cytoplasm⁶³ where it undergoes further cleavage by the RNase III enzyme Dicer into the 22 nucleotide mature guide strand microRNA and microRNA* its passenger strand⁶⁴. The guide strand is then loaded into the RNA-induced silencing complex (RISC) while the passenger strand is degraded^{60, 65}.

The strand selection and loading into the RISC is determined by their thermodynamic stability, abundance of microRNA target transcripts and tissue-specific regulatory mechanisms^{64, 66}. Contrary to earlier assertions that only the guide strand is loaded into the RISC complex, it is now known that both the guide strand and passenger strand can be functional⁶⁷. In certain cases, the two strands may target and inhibit similar mRNAs as is the

case for *miR-126-3p* and *miR-126-5p* in breast cancer⁶⁸ or may have different targets and functions in the case of *miR-28-3p* and *miR-28-5p* in colorectal cancer cells⁶⁹.

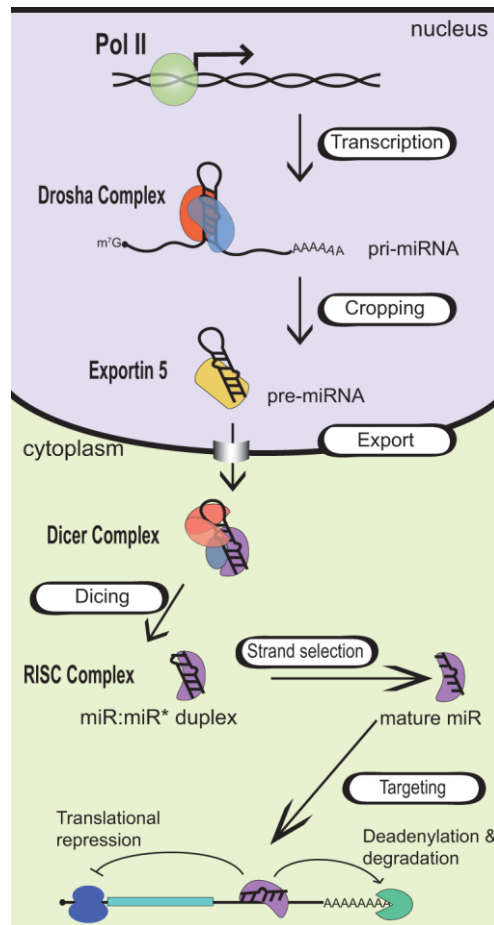


Figure 1: Biogenesis of microRNAs. RNA pol II transcribes the capped and polyadenylated pri-miRNAs. Pri-miRNAs are processed by Drosha to generate pre-miRNAs which are then translocated into the cytoplasm by exportin-5 in a RAN-GTP dependent manner where they are further processed by Dicer to give the mature microRNA/microRNA* duplex. After final processing, the guide strands of microRNAs are assembled into the RISC and where repression of mRNA through an imperfect binding to a complementary sequence within the 3'UTR of the mRNA occurs (Ref #60).

1.2.2 MicroRNAs in macrophage function during atherosclerosis

The microRNA expression profile in human atherosclerosis is differentially regulated compared to normal arteries with *miR-21*, *miR-34a*, *miR-146a*, *miR-146b-5p*, and *miR-210* being significantly upregulated⁷⁰. This dysregulation of microRNAs in atherosclerotic lesion suggests they play some important roles during atherogenesis. In endothelial cells for example, *miR-19a* is upregulated by laminar shear stress and regulates cell cycle by targeting cyclin D1⁷¹ and in the athero-susceptible inner aortic arch, *miR-10a* is downregulated and the knock-down of *miR-10a* in human aortic endothelial cells results in the upregulation of

nuclear factor-kappaB (NF- κ B) mediated inflammation⁷². In addition, *miR-126-5p* inhibits lesion formation at predilection sites by maintaining a proliferative reserve in endothelial cells by inhibiting delta-like homolog 1 (*Dlk1*)²².

In macrophages, microRNAs are also involved in the modulation of various functions during atherogenesis. Upon oxLDL treatment of human primary monocytes, several microRNAs including *miR-125a-5p*, *miR-9*, *miR-146a*, *miR-146b-5p*, and *miR-155* are significantly upregulated suggesting they may be involved in lipid uptake or metabolism by macrophages⁷³. *miR-155* is highly expressed in atherosclerotic lesions and in vitro, stimulation of macrophages with mildly oxidized LDL and IFN- γ upregulates *miR-155*⁷⁴ through the toll-like receptor (TLR) pathway⁷⁵. This upregulation through the TLR pathway indicates that *miR-155* mediates inflammatory response in macrophages. Furthermore, deficiency of *miR-155* in apolipoprotein E knock-out (*ApoE*^{-/-}) mice reduces atherosclerotic plaques and macrophage accumulation after partial ligation of the carotid artery⁷⁴. Atherosclerotic lesions and activated macrophages are characterised by the presence of enzymes that produce reactive oxygen species (ROS)^{76, 77} and the treatment of angiogenic progenitor cells with a nitric oxide synthase inhibitor upregulates *miR-21* leading to the enhanced extracellular signal-regulated kinase/mitogen-activated protein kinase-dependent (ERK/MAPK) reactive oxygen species formation⁷⁸. Moreover, macrophage activation in lesions through TLRs leads to the production of inflammatory cytokines as well as mediates foam cell formation⁷⁹, supporting the importance of macrophage activation during atherogenesis.

As mentioned earlier, uptake of modified lipoproteins by macrophages leads to inflammatory activation and this enhances atherosclerosis. In line with this, the metabolism of cholesterol and removal of cholesterol from the site of atherosclerotic lesion formation may be important in reducing lesion formation⁸⁰. Cholesterol enrichment of macrophages downregulates *miR-33*⁸¹ and the inhibition of *miR-33* in LDL receptor (*Ldlr*^{-/-}) mice increases circulating high density lipoprotein (HDL) levels, enhances reverse cholesterol transport to the plasma, liver, and faeces and subsequently reduces plaque formation⁸². These data indicate that microRNAs are critical in lipid uptake and metabolism in macrophages as well as inflammatory activation of macrophages during atherosclerosis. In addition to the previously outlined roles of microRNAs in macrophages during atherogenesis, several studies have also shown functional involvement in macrophage apoptosis and survival⁸³⁻⁸⁵.

1.2.3 *miR-21-3p* and *miR-21-5p* in atherosclerosis

MicroRNA-21 (*miR-21*) one of the first mammalian microRNA to be identified⁸⁶ is strongly conserved throughout evolution and is highly expressed in the cardiovascular system⁸⁷. *miR-21* is involved in the development of several cardiovascular diseases including myocardial disease⁸⁸, neointimal lesion formation⁸⁹, aortic aneurysm⁹⁰ and obesity⁹¹. Shear stress in

endothelial cells leads to overexpression of *miR-21* and decreased phosphate and tensin homolog (PTEN) expression and further increases endothelial nitric oxide synthase phosphorylation and nitric oxide production⁹². In vascular smooth muscle cells (VSMC), *miR-21* has anti-apoptotic and proliferative roles and this enhances neointimal formation in rodents⁸⁷.

In macrophages, *miR-21* is upregulated after stimulation with LPS through the adapter protein myeloid differentiation primary response protein (MyD88) and NF- κ B⁹³. This upregulation consequently regulates NF- κ B by targeting programmed cell death protein 4 (*Pdcd4*) thereby reducing inflammation. Furthermore, the suppression of *miR-21* increases tumor necrosis factor- α (TNF- α) and interleukin 6 (IL-6) while decreasing interleukin 10 (IL-10) levels after LPS stimulation⁹⁴. These data suggest a role for *miR-21* in inhibiting inflammatory polarization (M1) of macrophages and hence may play very important roles in macrophages during atherogenesis. The effect of suppressing *miR-21* on IL-10 indicates an anti-inflammatory role by *miR-21* and contribution to resolution of inflammation^{95, 96}.

In human atherosclerotic plaques, both strands of the pre-*miR-21*, *miR-21-5p* (*miR-21*) and *miR-21-3p* (*miR-21**) are highly expressed⁷⁰. In addition, *miR-21-3p* is one of the highly upregulated microRNAs in early atherosclerotic lesions compared to healthy arteries⁹⁷. Both *miR-21-5p* and *miR-21-3p* are upregulated in flow-induced atherosclerotic lesions after carotid artery partial ligation of *ApoE*^{-/-} mice and *miR-21-3p* is upregulated in diet induced atherosclerosis^{74, 98}. Moreover, *miR-21-3p* is selectively upregulated in macrophages in response to oxidative stress⁹⁹ whereas *miR-21-5p* is downregulated upon oxLDL stimulation¹⁰⁰. These data suggest that both strands of *miR-21* are functional and may play specific roles in macrophages during atherosclerosis.

1.3 The Circadian rhythm and atherosclerosis

Light sensitive organisms have developed an internal time-sensing process, known as the circadian clock, that allow them to anticipate daytime and night-time in order to prepare the body for each period^{101, 102}. Metabolic processes therefore exhibit a 24-hour diurnal cycle which may have evolved as a way for the cell to optimize metabolic events according to physiological needs and the environment¹⁰³. In mammals, specialized neurons in the suprachiasmatic nuclei (SCN) receive light photons through the retina via synaptic transmission, converts this information into chemical information and that alters the expression of so-called clock genes¹⁰⁴. The neurons generate a rhythm and soon synchronize other neurons and transmit this to peripheral organs like the liver, pancreas, heart, kidney and skeletal muscles. The SCN cells therefore serve as the master pacemaker, directing all the other clocks within the organism to realign to the new light/dark cycle¹⁰⁵.

Even though the SCN acts as the master pacemaker, peripheral organs also exhibit a circadian rhythm that regulates their functions at the cellular level¹⁰⁶. In mammalian cells, the mechanism of the circadian clock is autonomous, involving an auto-regulatory negative-feedback transcriptional network where two core clock genes, circadian locomotor output cycles kaput (*Clock*) and aryl hydrocarbon receptor nuclear translocator-like (*Arntl* or *Bmal1*) or neuronal PAS domain-containing protein 2 (*Npas2*) encode proteins that are members of the basic helix-loop-helix (bHLH)-PAS (Period-Arnt-Single-minded) transcription factor family^{107, 108}. The proteins CLOCK or NPAS2 heterodimerize with ARNTL in the cytoplasm, translocate to the nucleus and activate the transcription of *Period* genes (*Per1*, *Per2*, and *Per3*), as well as *Cryptochrome* genes (*Cry1* and *Cry2*)¹⁰⁹⁻¹¹¹. PER proteins form heterodimers with CRY, translocate into the nucleus and inhibits the ARNTL/CLOCK complex and thus forms a negative feedback loop to regulate its own transcription. As PER and CRY proteins are gradually degraded, the repression on ARNTL and CLOCK is suppressed thereby releasing them to begin a new 24-hr cycle¹¹² (Figure 2A, Loop 1).

Moreover, ARNTL induces the expression of *RAR*-related orphan receptor alpha ($ROR\alpha$) and nuclear receptor subfamily 1, group D, member 1 (NR1D1; also known as REV-ERB α), which in turn regulates the expression of ARNTL. In addition, the transcriptional activator albumin D-box binding protein (DBP), also regulated by ARNTL, and the repressor nuclear factor interleukin 3 (NFIL3), regulated by $ROR\alpha$ and REV-ERB α , both synergistically regulate the *Period* genes (Figure 2A, Loop 3)¹¹². The heterodimerization of ARNTL with NPAS2 or CLOCK occurs during the day and leads to high levels of PER and CRY expression in the day whereas at night the PER-CRY repressor complex is degraded¹¹³.

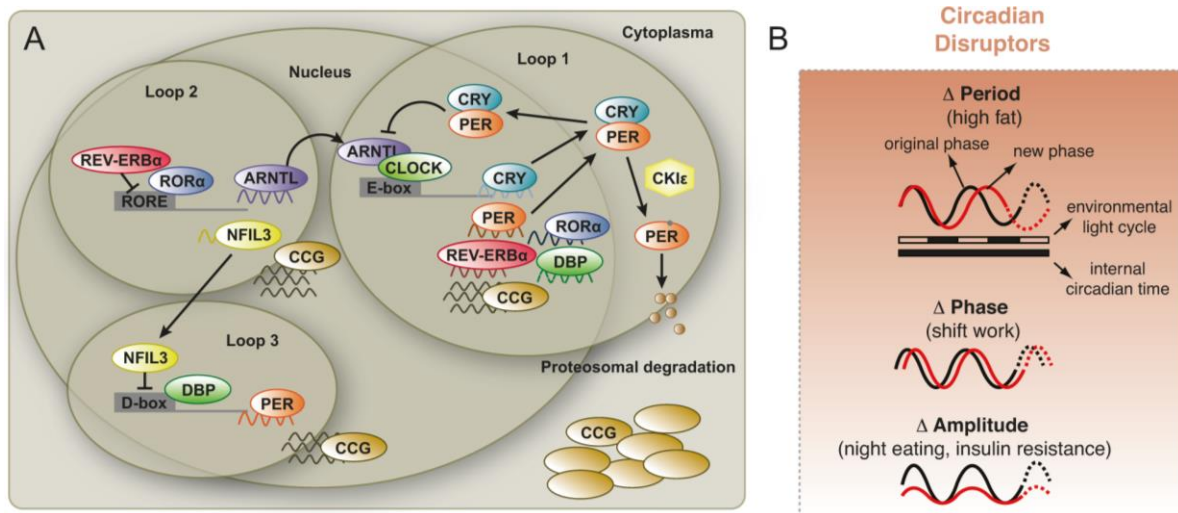


Figure 2: Circadian rhythm pathway. (A) Shows the auto-regulatory feedback loops of the circadian pathway consisting of three mechanisms of transcriptional regulation and control of molecular clock signaling (Ref #94). (B) Shows the different ways that the circadian clock could be disrupted and the stimulants that drive this disruption (Ref #97).

The circadian cycle is intimately connected to metabolism in humans and evidence supports the fact that several clock genes are involved in metabolic homeostasis^{114, 115}. This relationship between circadian clock and metabolism suggests that the circadian clock is sensitive to food and drugs¹¹⁶ and in mRNA microarray analysis of mice with disrupted clock in the liver, the expression of several transcripts are also disrupted¹¹⁷. These results together suggest that disruption of the circadian clock in peripheral tissues may affect their function and lead to disorders. Disruption of the circadian rhythm which can be manifested as changes in the period, phase and amplitude of the pathway can be brought about through high fat diet (HFD) consumption, shift work and night eating (Figure 2B)¹¹⁵. In experimental animal models of jet-lag, disrupted circadian clock leads to faster tumour growth¹¹⁸, increased mortality¹¹⁹ and lowered survival rate in the presence of cardiomyopathy¹²⁰.

The cardiovascular system exhibits rhythmic oscillations in function within the 24-hour period, for example blood pressure is highest mid-morning and progressively falls through the day^{121, 122}. Furthermore, cardiovascular events such as myocardial infarction, stroke, sudden cardiac death and unstable angina occur more frequently in the morning suggesting the involvement of circadian pathway in the function and physiology of the cardiovascular system^{123, 124}. Dysfunctional circadian rhythm is associated with cardiovascular diseases in humans and this leads to increased cardiovascular risk in shift workers especially night and early morning workers^{125, 126}. In several mouse models of dysregulated circadian rhythms, various pathways and mechanisms that lead to atherosclerosis are affected. *Bmal1* knock-out and *Clock* mutant mice exhibit increased pathological vascular remodelling, injury and endothelial dysfunction¹²⁷ and age-related decrease in nitric oxide (NO) production could lead

to dysregulated circadian rhythm suggesting that not only shift work but NO can affect the circadian rhythm¹²⁸.

Clock mutant gene in mice enhances hypercholesterolemia due to increased intestinal absorption of cholesterol and further increases atherosclerosis¹³⁰. Bone marrow (BM) knock-down of another circadian gene *Rev-Erba* increases atherosclerosis in *Ldlr*^{-/-} mice after regular chow diet¹³¹. The cell specific expression of circadian oscillation also exists in macrophages and dendritic cells¹³² and upon LPS stimulation, the expression of the cytokines IL-6, IL-12(p40), CXCL1, CCL5, and CCL2 show significant circadian-dependent upregulation via *Rev-Erba* activity¹³³. Moreover, macrophages with disrupted circadian rhythm exhibit increased uptake of modified LDL due to increased expression of the scavenger receptors CD36 and SR-A1¹³⁰ and overexpression of *Rev-Erba* in BM mononuclear cells decreases M1 markers while increasing M2 markers¹³¹. These data provides evidence for a role of macrophage circadian clock in atherosclerosis.

1.4 Role of *Xaf1* and *Mbl2* in atherosclerosis

XIAP-associated factor 1 (XAF1) a protein that increases caspase-3 activation by inhibiting the activities of X-linked inhibitor of apoptosis (XIAP) is ubiquitously expressed in normal tissues but has lowered expression in several cancer cell lines^{134, 135}. Over-expression of XAF1 activates the transcription factor p53 via post-translational modification and enhances apoptosis in vitro¹³⁶. XAF1 also inhibits proliferation and induces apoptosis of cancer cells thereby improving the survival times of tumour-bearing mice¹³⁷.

In human coronary vascular SMCs, *Xaf1* is regulated in a signal transducer and activator of transcription (STAT3)-dependent manner by IFN- γ ¹³⁸ and in endothelial cells, the upregulation of *miR-513a-5p* via LPS/TNF- α stimulation is associated with the inhibition of XIAP and increase in caspase-3 expression¹³⁹. This effect on XIAP with the subsequent increase in caspase-3 expression indicates that *miR-513a-5p* may increase XAF1 in endothelial cells. These results suggest that *Xaf1* could play important roles in various vascular cells during atherosclerosis and that *Xaf1*-induced apoptosis could be a potential therapeutic target and should be further investigated.

Mannose-binding lectin (MBL) is a secreted pattern recognition receptor from the collectin family that binds to late apoptotic and necrotic cells and enhances their engulfment by macrophages by binding to exposed DNA fragments and apoptotic blebs¹⁴⁰⁻¹⁴². In a study that provided early evidence for the possible association of MBL deficiency and atherosclerosis, 13% of patients with severe coronary artery atherosclerosis were observed to be homozygous defective for *Mbl*, compared with 3% of control healthy donors¹⁴³. This homozygous defect tended to occur in younger patients whereas older patients carried one or two copies of the normal. Genetic variations in the *Mbl* gene resulting in lowered expression of the protein is now known to be associated with coronary artery disease (CAD)¹⁴⁴ and high MBL decreases the likelihood of myocardial infarction¹⁴⁵.

MBL is highly expressed in mouse atherosclerotic lesions and is decreased in late lesions, whereas MBL deposition in human atherosclerotic lesions occurs in ruptured plaques around necrotic debris¹⁴⁶. In addition, *Ldlr*^{-/-} mice transplanted with BM cells deficient of an *Mbl* transcript show increased atherosclerosis after HFD¹⁴⁶. Moreover, in human monocytes and macrophages, MBL enhances macrophage binding and clearance of modified LDL but not native LDL¹⁴⁷. These data taken together suggest the importance of MBL in macrophage clearance of oxLDL and apoptotic cells in atherosclerotic lesions. *Xaf1* and *Mbl* function in macrophages may therefore combine to mediate apoptosis and efferocytosis and inhibit atherosclerosis.

1.5 Aim of study

Macrophages play a central role in atherosclerosis and the persistence of macrophages in lesions lead to increased accumulation and chronic inflammatory response thereby enhancing the development of advanced lesions. Macrophage apoptosis and efferocytosis are therefore critical in inhibiting lesion development and it has been suggested that altering macrophage content by reducing macrophage recruitment to atherosclerotic plaques or by promoting macrophage apoptosis may have therapeutic effects. *miR-21* a member of a family of small (~22 nucleotide) non-coding RNA molecules that regulate post-transcriptional gene expression and highly expressed in the cardiovascular system has been shown to inhibit apoptosis and enhance proliferation of cells. Moreover, *miR-21* is upregulated in macrophages upon LPS stimulation and mediates inflammatory response. The hypothesis was therefore tested that *miR-21* plays a role in macrophage phenotypes and function during atherogenesis in the current study. The study aimed at studying the effect of *miR-21* in macrophages on the development of atherosclerosis by knocking out *Mir21* in bone marrow cells of *Apoe*^{-/-} mice and feeding them with HFD for 12 weeks. The study also aimed at identifying possible novel mRNA targets of *miR-21* in lesional macrophages by performing gene expression profiling studies in mice transplanted with *Mir21* knock-out bone marrow cells.

Both strands of the pre-miR-21, *miR-21-5p* (*miR-21*) and *miR-21-3p* (*miR-21**) are highly upregulated in human atherosclerotic plaques as well as in different mouse models for atherosclerosis. However, their role in macrophages during atherosclerosis remains unclear. It was hypothesized in this study that the *miR-21/miR-21** pair may play specific roles in macrophages by either targeting same or different mechanisms during atherosclerosis. The cell specific expression of *miR-21-5p* and *miR-21-3p* in lesions was studied. Several studies focused on *miR-21-5p* strand and identified various targets in macrophages but the targets of *miR-21-3p* in macrophages during atherosclerosis have not received much attention. The study therefore investigated the effect of upregulation of both strands in macrophages during atherosclerosis.

2 Materials and methods

All solutions were prepared with millipore water (Milli-Q Integral 3/5/10/15, Millipore, Billerica, USA). The reagents were purchased from Sigma-Aldrich (Steinheim, Germany), Carl Roth (Karlsruhe, Germany), Merck (Darmstadt, Germany), and Fluka (Buchs, Switzerland) unless stated otherwise in the text.

2.1 General equipment

Balance -	Precisa 92SM-202A (Sartorius mechatronics, Göttingen, Germany)
Centrifuges -	Heraeus Pico 17 (Thermoscientific, Massachusetts, USA), Heraeus Megafuge 1.0R (Thermoscientific, Massachusetts, USA), Eppendorf 5430R and Eppendorf 5415D (Eppendorf AG, Hamburg, Germany),
Microscopes -	Leica M60, Leica DM6000B, Leica LMD7000 (Leica-Microsystems, Wetzlar, Germany) and Olympus IX50 (Olympus optical, Hamburg, Germany)
Laminar flow hood -	Herasafe (Heraeus, Osterode, Germany) and Maxisafe (Thermoscientific, Massachusetts, USA),
pH-meter -	WTW ph 526 (Weilheim, Germany)
Spectrophotometer -	Nanodrop 1000 (PeqLab, Erlangen, Germany)
PCR thermocyclers -	Master Cycler Nexus (Eppendorf AG, Hamburg, Germany), Thermal Cycler 2720 and 7900HT fast real-time PCR system (Applied Biosystems, Darmstadt, Germany)
Tissue homogenizer -	TissueLyserLT (Qiagen, Hilden, Germany)
Autoclave -	system VX-95 (system, Wetzlar, Germany)
Microtome -	Leica RM2235 (Leica Biosystems, Nussloch, Germany)
Plate reader -	microplate reader SpectraFluor Plus (Tecan, Crailsheim, Germany)
Imaging system -	LAS AF (Leica Biosystems, Nussloch, Germany)

Thermoblocks -	Thermostat Plus (Eppendorf AG, Hamburg, Germany)
Tissue processor-	MTM I/II (SLEE medical GmbH, Mainz, Germany)
Embedding center-	Leica EG1160 (Leica-Microsystems)
Syringes-	BD Discardit II (Becton, Dickinson and Company, NJ, USA), Omnican F (B. Braun AG, Melsungen, Germany)
X-ray irradiation system-	Faxitron CP-160 (Faxitron, Arizona, USA)
CO ₂ Incubator-	Galaxy S (RS Biotech, Irvine, UK)

2.2 Chemicals

β-Mercaptoethanol (Sigma-Aldrich, Steinheim, Germany)

Dimethyl sulfoxide (DMSO) (Carl Roth, Karlsruhe, Germany)

Dithiothreitol (DTT) (Carl Roth, Karlsruhe, Germany)

Horse serum (Vector Laboratories, California, USA)

Ketamin Hydrochloride (Bela-pharm GmbH and Co. KG, Vechta, Germany)

Lipofectamin, Invitrogen (ThermoFisher Scientific, California, USA)

Mounting medium with DAPI (Vector Laboratories, California, USA)

NP-40 alternative (Merck, Darmstadt, Germany)

Paraformaldehyde (PFA) (Carl Roth, Karlsruhe, Germany)

Paxgene tissue container (PreAnalytiX, Hombrechtikon, Switzerland)

Phosphate-buffered saline (PBS), Dulbecco (Biochrom AG, Berlin, Germany)

RNaseZap® decontamination solution (ThermoFisher Scientific, California, USA)

RNAlater® Ambion, (ThermoFisher Scientific, California, USA)

Triton X-100 (Sigma-Aldrich, Steinheim, Germany)

Tween® 20 (Merck, Darmstadt, Germany)

Vitro Clud® (R. Langenbrinck, Emmendingen, Germany)

Borgal solution 24% (Virac, Carros, France)

2.3 Antibodies

2.3.1 Primary antibodies

Monoclonal mouse anti-human smooth muscle actin (SMA) (Dako, California, USA)

Monoclonal anti-mouse MAC2 (Cedarlane, Ontario, Canada)

Monoclonal rat anti-human CD3 (AbD Serotec, Puchheim, Germany)

Normal mouse IgG (Santa Cruz Biotechnology, California, USA)

Normal rat IgG (Santa Cruz Biotechnology, California, USA)

Normal mouse IgG (Santa Cruz Biotechnology, California, USA)

Normal goat IgG (Santa Cruz Biotechnology, California, USA)

Normal rabbit IgG (Santa Cruz Biotechnology, California, USA)

Polyclonal rabbit anti-mouse perilipin-2 (Novus Biologicals, Colorado, USA)

Rabbit anti-mouse collagen type I (Cedarlane, Ontario, Canada)

Rabbit polyclonal anti-XAF1 antibody (Abcam, Cambridge, UK)

2.3.2 Secondary antibodies

Cy3-AffiniPure donkey anti-rat IgG (Jackson ImmunoResearch, Pennsylvania, USA)

Cy3-AffiniPure goat anti-rabbit IgG (Jackson ImmunoResearch, Pennsylvania, USA)

Cy3-AffiniPure donkey anti-mouse IgG (Jackson ImmunoResearch, Pennsylvania, USA)

Cy3-AffiniPure donkey anti-goat IgG (Jackson ImmunoResearch, Pennsylvania, USA)

Cy5-AffiniPure donkey anti-rat IgG (Jackson ImmunoResearch, Pennsylvania, USA)

Cy5-AffiniPure donkey anti-goat IgG (Jackson ImmunoResearch, Pennsylvania, USA)

Fluorescein (FITC)-conjugated AffiniPure donkey anti-mouse IgG (Jackson ImmunoResearch, Pennsylvania, USA)

Fluorescein (FITC)-conjugated AffiniPure donkey anti-rat IgG (Jackson ImmunoResearch, Pennsylvania, USA)

Fluorescein (FITC)-conjugated AffiniPure donkey anti-goat IgG (Jackson ImmunoResearch, Pennsylvania, USA)

Fluorescein (FITC)-conjugated AffiniPure donkey anti-rabbit IgG (Jackson ImmunoResearch, Pennsylvania, USA)

Dylight 549 labelled Streptavidin (KPL, Gaithersburg, USA)

2.4 Buffers and solutions

20× SSC buffer: 3 M NaCl, 0.3 M Na citrate (pH 7.0).

Tris/EDTA buffer: 100 mM Tris (pH 7.4), 10 mM EDTA
(pH 8.0).

Ago2-IP lysis buffer: 100 mM KCl, 5 mM MgCl₂, 10 mM HEPES (pH 7.0), 0.5% NP40, 5 mM DTT, 250 U/ml RNase OUT (Invitrogen), 400 μM vanadyl ribonucleoside complexes (New England Biolabs), and protease inhibitors (Complete Protease Inhibitor Cocktail Tablets; Roche).

Citrate buffer: 630 ml UP water, 12.6 ml solution A (2.101 g citric acid in 100 ml UP water), 57.4 ml solution B (14.70 g sodium citrate in 500 ml UP water), 320 μl Tween 20, pH 6.

EVG staining solutions:

Solution A: 10 g of hematoxylin was dissolved in 100 ml of 96% ethanol

Solution B: 29% Iron (III)-Chloride solution (145 g of Iron (III)-Chloride was dissolved in 500 ml of UP water) and 7.5 ml of 37% HCL was added to 950 ml of UP water.

4% PFA:

16 g of PFA was added to 184 ml of Millipore water and dissolved by adding 5 ml of 10 M NaOH during heating at 100°C. The pH was decreased to 7.4-8 by adding 25% HCl. Subsequently, an equal volume of 2×PBS was added and the solution was filtered through a filter paper.

Immunofluorescence staining:

Blocking solution A: 5.4 ml PBS, 600 µl 10% BSA (SERVA Electrophoresis GmbH, Heidelberg, Germany) 3 drops 2.5% normal horse serum (Vector laboratories, INC., Burlingame, USA)

Oil red O stock solution:

1 g Oil red O powder (Sigma-Aldrich, St. Louis, USA) was dissolved in 200 ml 99% isopropanol

Oil red O working solution:

160 ml Oil-Red-O stock solution was mixed with 120 ml UP water and stored at room temperature for 1 h. The solution was filtered through a filter paper.

Weigert solution A and B

100 ml Weigert A + 100 ml Weigert B

Tris-NaCl blocking (TNB) buffer

7.88g Tris-HCl was dissolved in 500ml water and pH adjusted to 7.5 using NaOH. NaCl (4.383g) and 2.5g Blocking reagent were added and the solution heated up to 55°C for about 30minutes.

Tris-NaCl Tween (TNT) buffer

This was prepared by adding 250µl of Tween 20 to Tris-NaCl solution.

2.5 Kits Used

High capacity cDNA reverse transcription kit (Applied Biosystems, Massachusetts, USA)

Taqman® microRNA reverse transcription kit (Applied Biosystems, Massachusetts, USA)

Nucleospin® miRNA kit (Macherey-Nagel, Düren, Germany)

In situ cell death detection kit TMR red (Roche, Basel, Switzerland)

GoTaq® qPCR mastermix (Promega, Wisconsin, USA)

*mirVana*TM miRNA Isolation kit (ThermoFisher Scientific, California, USA)

2.6 Mouse husbandry

All mice were housed in a barrier facility and were maintained on a 12 hour light-dark cycle within the animal laboratory facility of the University, the Zentrale Versuchstierhaltung (ZVH), Klinikum Universität München. Mice had free access to water and mouse chow. The animal experiments were reviewed and approved by the government of upper Bavaria (Regierung von Oberbayern) in accordance with the German animal protection law.

2.7 Mouse strains

Mir21^{-/-} mice (courtesy provided by Eric Olson, University of Texas Southwestern Medical Center, Department of Molecular Biology, Dallas, USA)¹⁴⁸ were obtained and crossed with *ApoE*^{-/-} mice to obtain *Mir21*^{-/-} *ApoE*^{-/-} mice. *Mir21*^{+/+} *ApoE*^{-/-} littermate mice served as control in this study.

2.8 Animal models of atherosclerosis

2.8.1 Atherosclerosis in whole body knock-out mice

Mir21^{-/-} *ApoE*^{-/-} and *Mir21*^{+/+} *ApoE*^{-/-} mice (6-8 weeks old), were fed a high fat diet (HFD) (21.2% crude fat, 0.15% cholesterol and 17.3% crude protein, ssniff-Spezialdiaeten GmbH; Soest, Germany) for 12 weeks to induce atherosclerosis. The mice were then anesthetized with ketamine hydrochloride (80 mg/kg, IP) and xylazine (5 mg/kg, IP) and blood was taken from the mice by the orbital vein for blood cell count and serum lipid measurements. The mice tissues were perfused with cold sterile PBS to remove any remaining blood cells. The aortic roots were then quickly dissected and fixed in PAXgene® tissue fix for 2 hours and then placed in PAXgene® tissue stabilizer both found in the PAXgene® tissue container. On the following day, the samples were dehydrated and paraffin embedded (see also section

2.10.1.1). The aortic roots were sectioned and in situ PCR performed on the sections to study the expression of *miR-21-3p* and *miR-21-5p* in atherosclerotic lesions.

2.8.2 Atherosclerosis in bone marrow transplanted mice

To study the effect of *Mir21* deficiency in bone marrow (BM) cells in atherosclerosis, BM cells from donor animals were transplanted into female recipient mice (8-10 weeks). The BM of *Mir21*^{+/+}*ApoE*^{-/-} mice was reconstituted with BM cells from either *Mir21*^{+/+}*ApoE*^{-/-} (*Mir21*^{+/+}/ BM *Mir21*^{+/+}) or *Mir21*^{-/-}*ApoE*^{-/-} (*Mir21*^{+/+}/ BM *Mir21*^{-/-}). The BM of *Mir21*^{-/-}*ApoE*^{-/-} mice was as well reconstituted with BM cells from *Mir21*^{-/-}*ApoE*^{-/-} (*Mir21*^{-/-}/ BM *Mir21*^{-/-}) mice. Recipient mice were first subjected to an ablative dose (5 Gy) of whole body irradiation (2 times, 5 Gy, 4 hours apart, Faxitron CP-160). After the irradiation, the mice were then transferred into fresh cages and placed on normal chow diet and antibiotic water (200ml water, 250µl Borgal Solution 24% diluted 1:10 with sterile water). The mice were kept on the normal chow and antibiotic water for a period of 3 weeks after the irradiation and BM transplantation. 24 hours following the irradiation, femurs and tibias were removed aseptically from donor mice and the marrow cavities were flushed with sterile PBS and a single cell suspension prepared by pipetting the cells up and down repeatedly followed by passing the cells through a cell strainer (40 µm, BD Falcon) to remove any large pieces of tissue or bone which may be present. BM cells (5 million cells/mouse) were injected via the tail vein into recipient mice, which were fixed in a mouse strainer.

After monitoring mice consistently for 3 weeks, they were then placed on HFD for 12 weeks to induce atherosclerosis, after which they were sacrificed and their tissues harvested. The mice were anesthetized with ketamine hydrochloride (80 mg/kg, IP) and xylazine (5 mg/kg, IP) and blood was taken from the mice orbital vein for blood cell count and serum lipid measurements. They were then perfused with sterile PBS to remove any remaining blood in the tissues. The thoraco-abdominal aorta and aortic root were harvested for processing, staining and atherosclerosis quantification. Aortic roots were fixed in PAXgene whiles thoraco-abdominal aorta fixed overnight in 4% PFA. Tissues from BM transplanted mice that were to be used for RNA isolation for microarray experiment were quickly perfused with RNAlater (Ambion) and the aortic root as well as thoraco-abdominal aorta were harvested and kept in RNAlater for RNA isolation.

2.8.3 Fixation of tissues

Mouse tissues were flushed always with sterile PBS to clear the blood and thereafter tissues harvested and fixed. Tissues to be used for RNA isolation and microarray were first perfused with RNA stabilization solution, RNAlater before harvesting. After anesthetizing the mice and drawing blood, the abdominal and chest cavities were then opened and PBS (5ml) or RNAlater (1 ml) perfused slowly using a syringe (30G x ½", Omnican F, B. Braun) for 5-10

min through the left ventricle while the solution was allowed to flow out through an incision in the right atrium. The aortic roots and thoraco-abdominal aorta were harvested and kept in PAXgene Tissue Fix and stabilizer or 4% PFA respectively. The aortic root samples after fixation were dehydrated and embedded in paraffin whereas thoraco-abdominal aorta were fixed overnight after which en face preparation and Oil red O staining were performed.

PAXgene Tissue Fix fixes tissues without nucleic acid crosslinking and degradation and therefore, preserves morphology as well as nucleic acids. It includes 2 components: the PAXgene® Tissue Fix solution which rapidly penetrates and fixes the tissue, and PAXgene® Tissue stabilizer in which nucleic acids and morphology of the tissue are stable for up to 7 days at room temperature and for longer periods at 2-8°C or -20°C. After 2 hours of fixation, tissues were removed from the PAXgene Tissue Fix solution and transferred to the PAXgene Tissue Stabilizer solution. Stabilized samples were embedded in paraffin for histological studies. To stabilize RNA, the vascular tree was flushed with 0.5-1 ml RNAlater solution. After this perfusion, tissues were dissected and placed in RNAlater solution. Samples were stored in RNAlater solution for 1-21 days at 4°C before the RNA was isolated for qRT-PCR analysis. All instruments used during organ dissection were first treated with RNaseZap® (Ambion, Austin, TX, USA) to remove RNases according to the manufacturer's instructions.

2.8.4 Serum analysis and blood cell count

After anesthetizing the animals, approximately 500-700 µl of blood from the orbital veins was collected in serum separating tubes (SST, Sarstedt) and allowed to clot at room temperature for 2 h. Subsequently, the tubes were centrifuged at 2000 x g for 20 min and the serum in the supernatant was collected and stored at -20°C.

About 100-200 µl of blood was also collected in EDTA tubes (SST, Sarstedt, Nümbrecht, Germany) and kept on ice. The different blood cells were counted using animal blood counter.

2.9 Laser capture microdissection (LCM)

Aortic root tissues from *Mir21^{+/+}Apoe^{-/-}* mice lethally irradiated (see section 2.8.2) and transplanted with BM cells from either *Mir21^{+/+}Apoe^{-/-}* (BM *Mir21^{+/+}*) mice or *Mir21^{-/-}Apoe^{-/-}* (BM *Mir21^{-/-}*) mice, were used for this experiment. All equipments used for sectioning, such as microtome and knife, forceps, and water bath were first treated with RNaseZap® (Ambion, Austin, TX, USA). Serial sections (10 µm thick) of the aortic roots were mounted on membrane-mounted metal frame slides (POL frameslides, Leica Microsystems). Sections were deparaffinized under RNase-free conditions according to the following procedure:

1. Xylene for 3 minutes.
2. 100% ethanol for 3 minutes.

After deparaffinization, the sections were left standing to completely dry up. Laser capture microdissection was performed using a laser microdissection system (CTR6000, Leica Microsystems) attached to an inverted microscope (LMD7000, Leica Microsystems). At least 20-30 sections of plaque tissue without the endothelial cells or medial cells were collected from each mouse into a buffer (TM1) belonging to the RNA isolation kit. RNA was isolated using the PAXgene Tissue miRNA kit (PreAnalytix, Switzerland) according to the manufacturer's instructions. The lesion area without the endothelial cells and medial cells to be cut from the section is first demarcated with a selection tool from the software interface (Figure 3), after which the command is entered for the cut to be made.

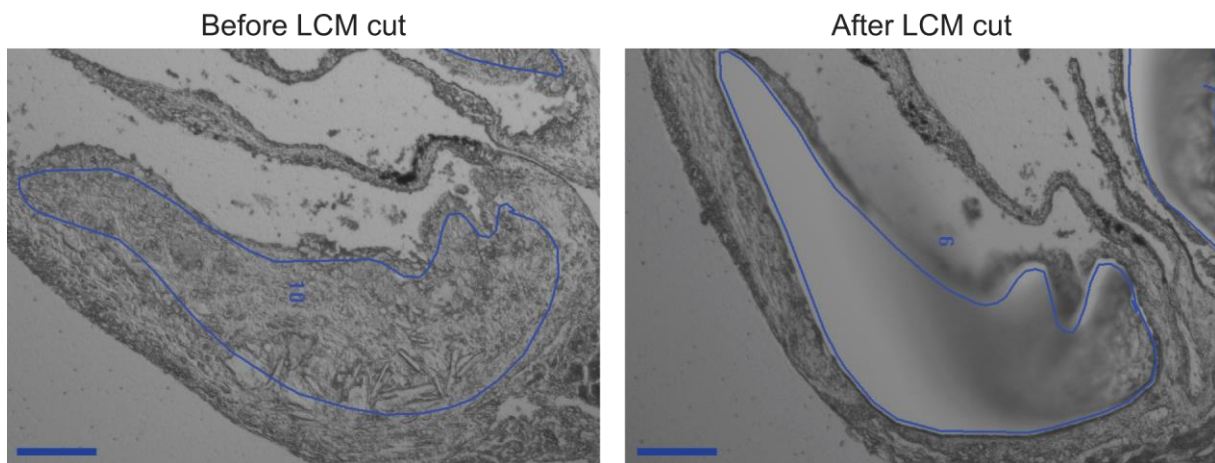


Figure 3: Laser capture-microdissection of aortic root lesions. Sections of aortic root with lesions on membrane-mounted metal frame slides were deparaffinized and left to dry under RNase-free environment. Lesion area excluding the endothelial and medial cells are marked with a selection tool and then cut with the laser. The lesions were then collected in TM1 buffer and RNA isolated later.

2.10 Lesion characterization

2.10.1 Histology

2.10.1.1 Paraffin embedding, sectioning, and deparaffinization

To quantify the lesion size, aortic roots were harvested from mice after they were sacrificed and fixed in PAXgene. Next, tissues were dehydrated using tissue processor and embedded in liquid paraffin (approximate temperature 60°C) according to the following protocol:

1. 70% Ethanol, 30 min, 20°C

2. 70% Ethanol, 30 min, 20°C
3. 96% Ethanol, 30 min, 20°C
4. 96% Ethanol, 30 min, 20°C
5. 100% Ethanol, 30 min, 20°C
6. 100% Ethanol, 30 min, 20°C
7. 100% Ethanol, 30 min, 20°C
8. Xylene, 30 min, 45°C
9. Xylene, 30 min, 45°C
10. Xylene, 30 min 45°C
11. Paraffin, 30 min, 62°C
12. Paraffin, 30 min, 62°C
13. Paraffin, overnight, 62°C

The tissues were then blocked in paraffin and allowed to harden at 0°C (Leica EG1160) before sectioning using a microtome. Serial sections (5 µm thick) from the aortic root were collected on glass slides (Superfrost plus glass slides, ThermoFisher Scientific, California, USA) within from the point that the 3 aortic valves appear until the valves disappear. After sectioning, the slides were incubated in a 37°C incubator for 5-6 h or at room temperature overnight to reduce detachment of the tissue during staining. To measure lesion size, 3-5 serial sections containing all three aortic valves and 50-100µm apart were selected and EVG (Elastic Van Gieson) staining was performed. Deparaffinization and rehydration of the sections was performed according to the following protocol before staining:

1. Xylene, 10 min.
2. Xylene, 10 min.
3. 100% ethanol, 5 min
4. 100% ethanol, 5 min
5. 96% ethanol, 5 min
6. 70% ethanol, 5 min

2.10.1.2 EVG staining

1. Resorcin-fuchsin solution (Roth, X877.1), 20 min
2. Tap water (bath in fluent water), 1 min.
3. 80% ethanol
4. Weigert Solution A+B [100 ml solution A and 100 ml solution B, freshly prepared (see also section 2.4)], 15 min
5. 1% HCl-alcohol, 5 seconds (quick dive in solution)
6. Bath in fluent tap water, 10 min
7. Millipore water, 5 seconds (quick dive in solution)
8. Van Gieson Picrofuchsin (Merck, 1.15974/4) for 30 seconds

9. Tap water
10. 96% ethanol, 4 min
11. Isopropanol, 2 min
12. Xylene, 5 min
13. Xylene, 5 min
14. Sections were mounted in Vitro clud

2.10.1.3 Image acquisition and lesion area quantification

Images were taken using a bright-field microscope (Leica DM6000B, Leica microsystems) connected to a camera (Leica DFC295, Leica Microsystems). The lesion area was quantified using the java based image processing software Image J (1.46r National Institutes of Health, Maryland, USA).

2.11 *En face* preparation and oil red o staining

The lipid deposition area in the thoraco-abdominal aorta was detected and quantified using Oil red O staining of *en face* prepared tissues. The entire aorta including the aortic arch and the abdominal aorta were dissected using a dissection microscope and pinned with needles onto a rubber slide for fixation in 4% PFA over night at 4°C. The aortas were then cut open longitudinally and the adventitia removed carefully. The cut aortas were then pinned down with the luminal surface upside on the rubber slides. The pinned aortas were dipped in 60% isopropanol for 15 to 20 seconds followed by incubation in Oil red working solution for 15 min. The aortas were then immersed in 60% isopropanol for 10 to 15 seconds, rinsed with tap water and afterwards mounted in glycerol gelatin (diluted 3:7 with tap water, Sigma).

To mount the stained *en face* prepared tissue, the pins were removed and the tissue moved onto a glass slide and covered using a cover slip and mounting gelatin. The images were taken with a bright-field microscope (Leica DM6000B, Leica microsystems) connected to a camera (Leica DFC295, Leica Microsystems) and using LAS software (Leica Microsystems). The area of lipid deposition in the stained aortic wall were quantified using Adobe Photoshop CS6 (Adobe Systems, California, USA) and ImageJ (1.46r, NIH, USA). The percentage area of lesion was calculated using the area of lipid deposition and total area of the thoraco-abdominal aorta.

2.12 Immunofluorescence staining

To study the cellular composition of the lesions, immunostaining was performed in deparaffinized sections (5 µm thick) using antibodies against SMA, MAC2, CD3, and

collagen type I. In addition, double immunofluorescence stainings for XAF1 and PLIN2 were performed. Aortic root sections from *Mir21^{+/+}Apoe^{-/-}* mice whose BM were reconstituted with BM cells from either *Mir21^{+/+}Apoe^{-/-}* (BM *Mir21^{+/+}*) or *Mir21^{-/-}Apoe^{-/-}* (BM *Mir21^{-/-}*) were selected for the immunostaining. 2–3 sections/mouse with 50 – 100 μ m distances between sections were selected and deparaffinised using graded Xylene and alcohol and antigen retrieval performed by cooking the sections in citrate buffer (see section 2.4) for 20 minutes. The tissues were then blocked with Blocking Solution A for 30 minutes and then incubated over night with the primary antibody at 4°C. The sections were then washed several times and incubated with the specific secondary antibody for 30 minutes, washed and mounted with Vectashield mounting medium with DAPI (4',6-diamidino-2-phenylindole) (Table 1). Double staining was performed by making a cocktail of the antibodies and incubating them together on the tissues.

The percentage of the positively stained area or cell number was quantified using image analysis software (ImageJ). The background of negative control staining was used to adjust the threshold. In addition, the number of immunostained cells in the plaques was determined by counting DAPI positive nuclei within the immunostained area. The number of the immunostained cells was expressed as the absolute cell number in the plaques or as the percentage of total plaque cells.

Antigen	Antigen retrieval	Blocking	Primary Ab	Detection system
SMA	none	Blocking solution A*, 30 min	1:200, 4°C, ON	donkey-anti-mouse IgG, FITC-conjugated, 1:100, 30 min
MAC2	none	Blocking solution A*, 30 min	1:400, 4°C, ON	donkey-anti-rat IgG-FITC-conjugated, 1:100, 30 min
Collagen type I	CB*, 20 min at 100°C	Blocking solution A*, 30 min	1:400, 4°C, ON	anti-rabbit Cy3-conjugated, 1:300, 30 min
CD3	CB*, 20 min at 100°C	10% goat serum, 30 min	1:100, 4°C, ON	goat-anti-rabbit IgG-Dylight549-conjugated, 1:400, 30 min

Table 1: Immunostaining protocols: CB = Citrate buffer; Ab = antibody details are provided in sections 2.3; * see section 2.4 for more details.

2.12.1 TUNEL and MAC2 staining

Combined TUNEL (terminal deoxynucleotidyl transferase dUTP nick end labelling) assay and MAC2 staining was performed in some of the aortic root sections to quantify macrophage apoptosis. TUNEL staining was done according to the kit protocol (In situ cell death detection kit, TMR red, Roche). The TUNEL assay detects and quantifies the apoptosis at the single cell level, based on non-radioactive labeling of DNA strand breaks. The sections were first

deparaffinized and permeabilized by cooking in 0.1 M citrate buffer (pH 6) for 20 min. Then, the sections were incubated with the freshly prepared TUNEL reaction mixture (containing label and enzyme solution) in a humidified chamber in the dark at 37°C for 15 min. Following TUNEL staining, the sections were used for Mac 2 immunostaining. The percentage of TUNEL positive macrophages were analyzed by counting TUNEL positive and MAC2 positive cells (DAPI) and expressing as a percentage of total number of macrophages (MAC2 positive cells).

2.13 In situ PCR

In situ PCR for mature microRNAs was performed on aortic root sections to show expression of *miR-21-3p* and *miR-21-5p* strands in the different cells in aortic root lesions of mice maintained on HFD for 12 weeks. 4µm thick aortic root sections obtained from *Mir21*^{-/-} *ApoE*^{-/-} and *Mir21*^{+/+} *ApoE*^{-/-} mice fed HFD for 12 weeks were fixed in Paxgene and used for this experiment. The processes included removing of paraffin wax from the sections, protease digestion, DNase digestion, ultramer extension, stringency wash, microRNA cDNA labelling and detection. The experiment was done under a hood to minimize as much as possible any RNase contamination. All containers were autoclaved and others wiped with RNase zap.

Deparaffinization: The sections were bathed in xylene and graded alcohol to remove the paraffin wax from the sections.

Protease Digestion: The sections were then treated with 60 µl of pepsin solution (13mg of Dako pepsin powder, S3002 dissolved in 9.5ml DEPC water and 0.5ml of 0.2M HCl) for 10 - 20 minutes at room temperature. Protease digestion was then stopped by washing sections shortly with DEPC water and followed by washing three times in RNase-free 100% ethanol. Sections were then left to dry.

DNase digestion: Tissue chambers (SecureSeal™ hybridization chamber, Applied Biosystems, Massachusetts, USA) were then placed on each tissue to ensure the DNase does not evaporate or flow away during the overnight incubation period. RNase-free DNase (Roche, Switzerland) was diluted 1:10 with the buffer. 50µl of the DNase was added to each section and the chambers covered. The slides were then incubated at 37°C overnight. DNase was removed the next day by first removing the tissue chambers from the sections and washing 3 times with DEPC water and finally RNase free 100% ethanol and allowed to dry.

Ultramer extension with amplification: GeneAmp® EZ rTth RNA PCR Kit (Applied Biosystems, Massachusetts, USA) was used for this step. Reaction mix (50µl per section) containing 25µl of 2x Reaction mix buffer, 1.6 µl of 2% BSA solution, 0.6µl of 1mM digoxigenin dUTP (Roche, Switzerland), 1.4µl RNase inhibitor (Roche), 1 µl of rTth DNA polymerase, 3 µl of the Taq-insitu-Primers(100 µM)(RT primer 1.2ul, Forward primer 0.9ul,

Reverse primer 0.9 μ l) and 17.4 μ l RNase free water. There were 2 sections on each slide. One section was always used as a negative control. The reaction mix for the control therefore had only negative control primers and no *miR-21* primers.

The tissues were covered with SecureSeal™ hybridization chamber and 50 μ l reaction mixture pipetted onto each section via the holes of the chamber. The slides were then placed in a thermal cycler (Eppendorf Master Cycler Nexus) and reverse transcription and amplification was performed with the following cycle:

50°C – 30 minutes

94°C – 3 minutes

94°C – 15 seconds

56°C – 30 seconds

72°C – 20 seconds

72°C – 5 minutes

Number of cycles for amplification was 25. Slides were afterwards rinsed in xylene and 100% ethanol 3 minutes each and air-dried.

Stringency wash: 1x SSC (Saline-sodium citrate) with 2% BSA and 0.2x SSC with 2% BSA were used for the stringency washing steps. The solutions were pre-heated at 60°C in an oven. Washing in 1x SSC with 2% BSA was for 5 minutes and 0.2x SSC with 2% BSA was for 10 minutes.

Labelling of digoxigenin labelled microRNA cDNA with secondary antibody: This step included blocking of the tissues with Tris-NaCl blocking (TNB) buffer (section 2.4) for 30 minutes, followed by Avidin for 10 minutes and then with Biotin for another 10 minutes all at room temperature. HRP labelled secondary anti-body; DIG-anti-POD was diluted 1:150 with TNB buffer and incubated with the tissues at room temperature for 1 hour. The tissues were then washed 3 times for 5 minutes in Tris-NaCl Tween (TNT) buffer. Finally the tissues were incubated for 5 minutes with TSA (Tyramide Signal Amplification) Plus Biotin amplification reagent (Diluted stock solution 1:50 with 1x Plus Amplification Diluent). They were then washed three times in TNT (5 minutes) and incubated for 30 minutes with Dylight 549 labeled Streptavidin (dilute with PBS 1:200).

2.13.1 MAC2 immunostaining after in situ PCR

In order to detect the expression of *miR-21-3p* and *miR-21-5p* in lesional macrophages, the sections were then immunostained with MAC2 antibody after in situ PCR. One drop of 1% BSA blocking solution was added to each section and incubated for 30 minutes. After which the blocking solution was removed from the sections and 50µl of the primary antibody MAC2 (supernatant of cultured M3/38.1.2.8 HL2 cells) was added to each of the sections. Negative control sections on each slide however were incubated with 50µl of Isotyp normal rat IgG (diluted with antibody solution 1:160). After an overnight incubation period, the sections were washed 3 times with PBS and a secondary antibody anti-rat FITC (diluted 1:100 in PBS) was added on each section and incubated again for 30 minutes. The sections were washed gently with PBS three times and then were then mounted with coverslips using Vectashield fluorescent mounting medium with DAPI. Micrographs were taken using a Leica DM 6000B microscope.

2.14 Global gene expression analysis by microarray

To determine the targets of *miR-21-3p* and *miR-21-5p* as well study effect of *Mir21* knockout in BM cells on mRNA expression in atherosclerotic lesions, a global gene expression analysis was performed with samples isolated from aortic arch containing atherosclerotic lesions. Recipient mice *Mir21*^{+/+}*ApoE*^{-/-} were irradiated twice with a lethal dose of X-ray (5 Gy) 4 hours apart and their BM reconstituted with BM cells from either *Mir21*^{+/+}*ApoE*^{-/-} (BM *Mir21*^{+/+}) or *Mir21*^{-/-}*ApoE*^{-/-} (BM *Mir21*^{-/-}). After monitoring the the health and well-being of the mice for 3 weeks, they were then placed on HFD for 12 weeks to induce atherosclerosis, after which they were sacrificed and their tissues harvested. The mice were sacrificed as previously described in section 2.8.2 and then perfused with RNAlater. The aortic arch containing atherosclerotic lesions, were then carefully dissected out and kept in RNAlater until RNA isolation at -80°C.

Tissues were lysed and RNA isolation was performed using a *mirVana*TM miRNA Isolation kit according to the manufacturer's instructions. The samples were then sent to a private company IMG Laboratory (Martinsried, Germany) where RNA purity, integrity and concentration were determined and microarray performed. RNA samples were spiked with in vitro synthesized polyadenylated transcripts (One-Color RNA Spike-In Mix, Agilent Technologies, Carlifornia, USA), which serve as an internal labeling control for linearity, sensitivity and accuracy. The spiked total RNA was reverse transcribed into cDNA and then converted into Cyanine-3 labeled cRNA (Low Input Quick-Amp Labeling Kit One-Color, Agilent Technologies). All steps were carried out according to the manufacturer's instructions.

cRNA concentration (ng/μl), RNA absorbance ratio (A260nm/A280nm) and Cyanine-3 dye concentration (pmol/μl) were recorded for all cRNA samples using NanoDrop ND-1000 UV/VIS spectrophotometer. Yield and specific activity of each reaction were determined and samples with a yield of cRNA above 825 ng and a specific activity above 6.0 pmol Cyanine-3 per μg cRNA were processed to the hybridization step. However, samples with a cRNA yield less than 825 ng and a specific activity higher than 6.0 pmol Cyanine-3 per μg cRNA were considered still sufficient for microarray analysis as long as the amount of cRNA was sufficient for hybridization. Following cRNA clean-up and quantification 550 to 600 ng of each Cyanine-3-labeled cRNA sample was fragmented and prepared for one-color-based hybridization (Gene Expression Hybridization Kit, Agilent Technologies). Labeled cRNA samples were hybridized at 65°C for 17 hrs on separate Agilent SurePrint G3 Mouse Gene Expression 8x60K Microarrays (AMADID 028005). Afterwards, microarrays were washed with increasing stringency using Gene Expression Wash Buffers (Agilent Technologies) followed by drying with acetonitrile (Sigma). Fluorescent signal intensities were detected with Scan Control A.8.4.1 software (Agilent Technologies) on the Agilent DNA Microarray Scanner and extracted from the images using Feature Extraction 10.7.3.1 software (Agilent Technologies). Feature Extraction 10.7.3.1 (Agilent Technologies), GeneSpring GX 12.6 (Agilent Technologies) and Marfin 1.9 (IMGM Laboratories) were used for quality control, statistical data analysis, RNA annotation and visualization.

2.15 In vitro experiments

2.15.1 Cell culture of BM-derived macrophages (BMDMs)

To study the specific targets of the different strands of *Mir21* in macrophages, as well as the role *Mir21* plays in the circadian rhythm in macrophages, bone marrow-derived macrophages (BMDMs) were cultured by seeding and incubating BM cells in a macrophage differentiation medium for 6 – 7 days and used for various experiments. To isolate BM cells, the mice (*Mir21*^{+/+}*Apoe*^{-/-} mice or *Mir21*^{-/-}*Apoe*^{-/-} mice) were sacrificed by cervical dislocation and their blood drawn from the left ventricle of the heart. The femur and tibia were then harvested and kept in cold PBS and moved to a sterile chamber for the isolation of the BM cells. The BM is then flushed out of the bones with sterile Gibco® DMEM/F12 medium (ThermoFisher Scientific, California, USA) using a syringe.

The cell suspension was then pipetted up and down several times to achieve a single cell suspension which was then passed through a 40μm cell strainer (Becton, Dickinson and Company, NJ, USA) to remove foreign tissues like bones. The cells were then washed by centrifuging and resuspending in new amount of medium. The cells were then counted and seeded at a density of 5 x 10⁵/ml in macrophage cell differentiation medium. The components of the macrophage cell differentiation medium were as follows:

DMEM/F12 medium (ThermoFisher Scientific, California, USA)

10% Fetal bovine serum (Sigma-Aldrich, Steinheim, Germany)

10% L929 cell medium

1‰ Gentamicin (ThermoFisher Scientific, California, USA)

BM cells are kept in CO₂ incubator at 37°C for 7 days with the medium changed on the 3rd day.

2.15.2 Synchronisation of BMDMs

In order to study the role of *Mir21* in the circadian rhythm of macrophages, BMDMs are synchronised by incubating the cells with horse serum medium for 2 hours and then replaced with serum-free medium. After synchronising the cells, the expression of clock genes was assessed using qRT-PCR after every 4 hours over a 24 hour period. The horse serum medium constituted DMEM/F12 medium, 50% horse serum, heat inactivated (ThermoFisher Scientific, California, USA) and 10% L929 cell medium.

2.15.3 Treatment of BMDMs with mimics

In order to study the role of *miR-21-3p* and *miR-21-5p* strands on circadian rhythm in macrophages and to study the targets of each specific strand, BMDMs were cultured from BM cells isolated from *Mir21*^{-/-}*Apoe*^{-/-} mice and transfected with either *miR-21-3p* mimic or *miR-21-5p* mimic. The cells were then synchronised 24 hours after transfection and cells harvested 8 hours after synchronisation and the expression of clock genes, *Mbl2* and *Xaf1* assessed using qRT-PCR.

2.15.4 Stimulation of BMDMs to M1 and M2 macrophages

To examine the role of *Mir21* in the polarization of macrophages to either M1 (pro-inflammatory) or M2 (anti-inflammatory) macrophages, BM cells isolated from *Mir21*^{+/+}*Apoe*^{-/-} mice or *Mir21*^{-/-}*Apoe*^{-/-} mice and cultured in macrophage differentiation medium were stimulated to generate M1 and M2 macrophages. The expressions of mRNA in these cells were then quantified using qRT-PCR. M1 stimulation was performed by treating the cells with 50 ng/ml lipopolysaccharide (LPS) for 8 hours and afterwards treating the cells

with 20 ng/ml interferon gamma (IFN- γ) for 6 hours. The cells were then lysed and RNA isolated using the mirVana miRNA isolation kit (Applied Biosystems). M2 stimulated was done by treating the cells with 20 ng/ml interleukin 4 (IL-4) for 6 hours.

2.16 Quantitative real time polymerase chain reaction (qRT-PCR)

Total RNA was either isolated using the mirVana miRNA isolation kit (Applied Biosystems) or Nucleospin miRNA kit (Macherey-Nagel). The RNA concentration was determined by measuring the absorbance at 260 nm (A260) in a spectrophotometer. The absorbance at 280 nm was also measured to determine the RNA purity. RNA with an A260/A280 ratio of 1.8-2.0 was used for qRT-PCR. Total RNA was reverse transcribed to cDNA using Taqman microRNA RT kit or high capacity cDNA reverse transcription kit both from Applied Biosystems with 2 ng RNA and 300 – 500 ng RNA for the microRNA and high capacity cDNA reverse transcription respectively.

MiR expression levels were quantified using Taqman universal PCR master mix (Applied Biosystems) whereas qRT-PCR for mRNAs was performed using Taqman universal PCR master mix (Applied Biosystems) or gene specific primers and SYBR Green master mix (Promega). All real-time PCR experiments were run on a 7900HT thermocycler (Applied Biosystems). Relative expression levels were normalized to a single or to multiple reference genes (*snoRNA135* and *U6* for miR; *Gapdh* and *B2m*, mRNA), scaled to the sample with the lowest expression (qbase+ software; Biogazelle), and logarithmically transformed (Log_2 or Log_{10}).

2.17 Statistical analysis

The differences between two groups were compared using unpaired, 2-tailed Student's t-test. More than two groups were compared using one-way or two-way analysis of variance (ANOVA) followed by a Newman-Keuls post-test (Prism 5.0; GraphPad). All data except the microarray data represent mean \pm s.e.m. *P* value < 0.05 was always considered significant.

3 Results

3.1 Role of *Mir21* in macrophages during atherogenesis

3.1.1 *miR-21-3p* and *miR-21-5p* expression in atherosclerotic lesions

To study the expression of both *miR-21-5p* and *miR-21-3p* strands in atherosclerotic lesions, in situ PCR combined with MAC2 double staining was performed on aortic root lesions of *Mir21*^{+/+}*ApoE*^{-/-} mice fed on a high fat diet (HFD) for 12 weeks. The expression of *miR-21-5p* was detected in lesional macrophages as well as luminal cells of the lesion, most likely endothelial cells (Figure 4A). The expression of *miR-21-3p* was detectable only in lesional macrophages but not in luminal cells (Figure 4B). Neither *miR-21-5p* nor *miR-21-3p* was detected in lesions from *Mir21*^{-/-}*ApoE*^{-/-} mice after performing in situ PCR.

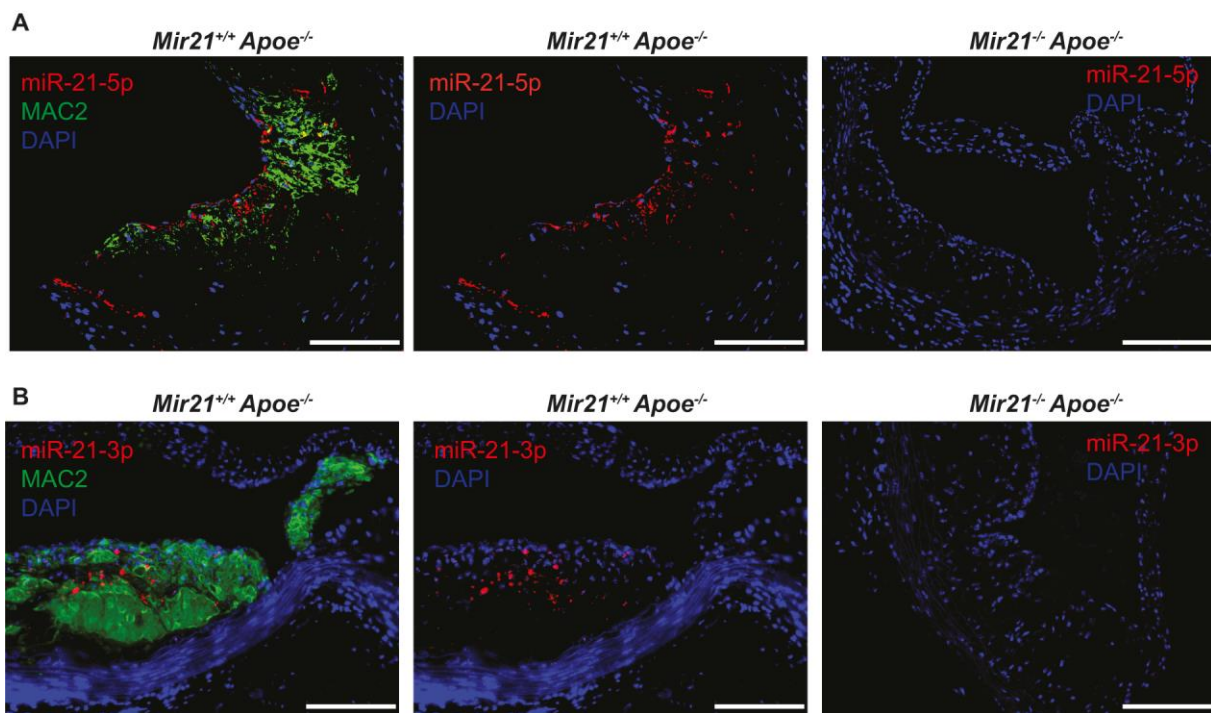


Figure 4: Expression of *miR-21-5p* and *miR-21-3p* strands in mouse atherosclerotic lesions. Expression and localization of *miR-21-5p* (A) and *miR-21-3p* (B) in aortic root lesions of *Mir21*^{+/+}*ApoE*^{-/-} mice fed HFD for 12 weeks using in situ PCR. Expression of *miR-21-5p* and *miR-21-3p* (red) by lesional macrophages is shown by MAC2 immunostaining (green). The expression of *miR-21-5p* was detected also in luminal cells but *miR-21-3p* expression was localized with only lesional macrophages. Negative control staining was performed in sections obtained from *Mir21*^{-/-}*ApoE*^{-/-} mice fed HFD for 12 weeks. Nuclei were counterstained with DAPI (blue). Scale bars: 100µm.

3.1.2 Role of *Mir21* in macrophage polarization

3.1.2.1 Regulation of *Mir21* during macrophage polarization

To determine the role of *Mir21* expression in macrophage polarization and function during atherosclerosis, the expression and regulation of *miR-21-3p* and *miR-21-5p* strands in different macrophage phenotypes were assessed. BMDMs were cultured and stimulated with either LPS and IFN- γ (M1 stimulation, see also section 2.15.4) or IL-4 (M2 stimulation). M0 macrophages were not stimulated. The expression level of *miR-21-3p* and *miR-21-5p* in M0, M1 and M2 macrophages was quantified using qRT-PCR.

There were no significant differences in the expressions of *miR-21-3p* (Figure 5A) and *miR-21-5p* (Figure 5B) between M0, M1 and M2 macrophages. These results indicate that *Mir21* expression may not be involved in macrophage polarization and that both pro-inflammatory and anti-inflammatory stimulation of macrophages do not differentially regulate *miR-21-3p* and *miR-21-5p*.

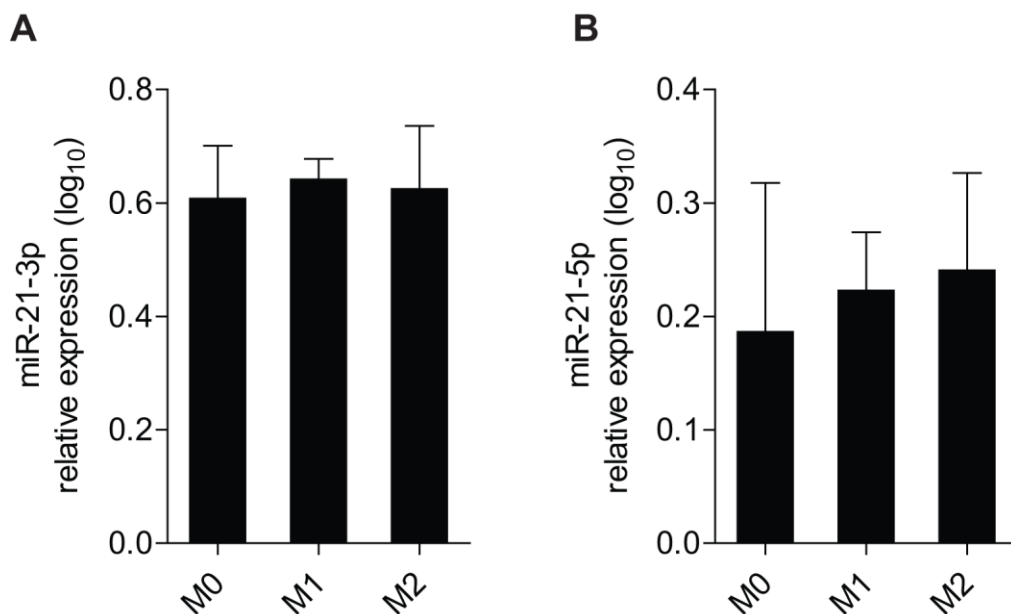


Figure 5: Expression of *miR-21-3p* and *miR-21-5p* in M0, M1 and M2 macrophages. BMDMs were treated with LPS and IFN- γ (M1 stimulation), IL-4 (M2 stimulation) or not stimulated at all (M0) and afterwards the expression of *miR-21-3p* and *miR-21-5p* in these cells quantified using qRT-PCR. The expression of *miR-21-3p* (A) and *miR-21-5p* (B) between M0, M1 and M2 showed no significant difference. $n = 3$ samples per group. Results were analysed using two-way ANOVA. The means \pm s.e.m. are shown.

3.1.2.2 Effect of oxLDL on *Mir21* expression in macrophages

To further examine the regulation of *miR-21-3p* and *miR-21-5p* expression, the effect of oxLDL on their expression was assessed. BMDMs were treated with oxLDL (200 μ g/ml) for 24 hours and 72 hours. The expressions of *miR-21-3p* and *miR-21-5p* were measured using qRT-PCR. Stimulation with oxLDL significantly increased the expressions of *miR-21-3p* and *miR-21-5p* after 72 hours compared to cells treated with 200 μ g/ml of native LDL (nLDL) (Figure 6). There were no significant differences in the expressions of both strands at 24 hours between oxLDL and nLDL.

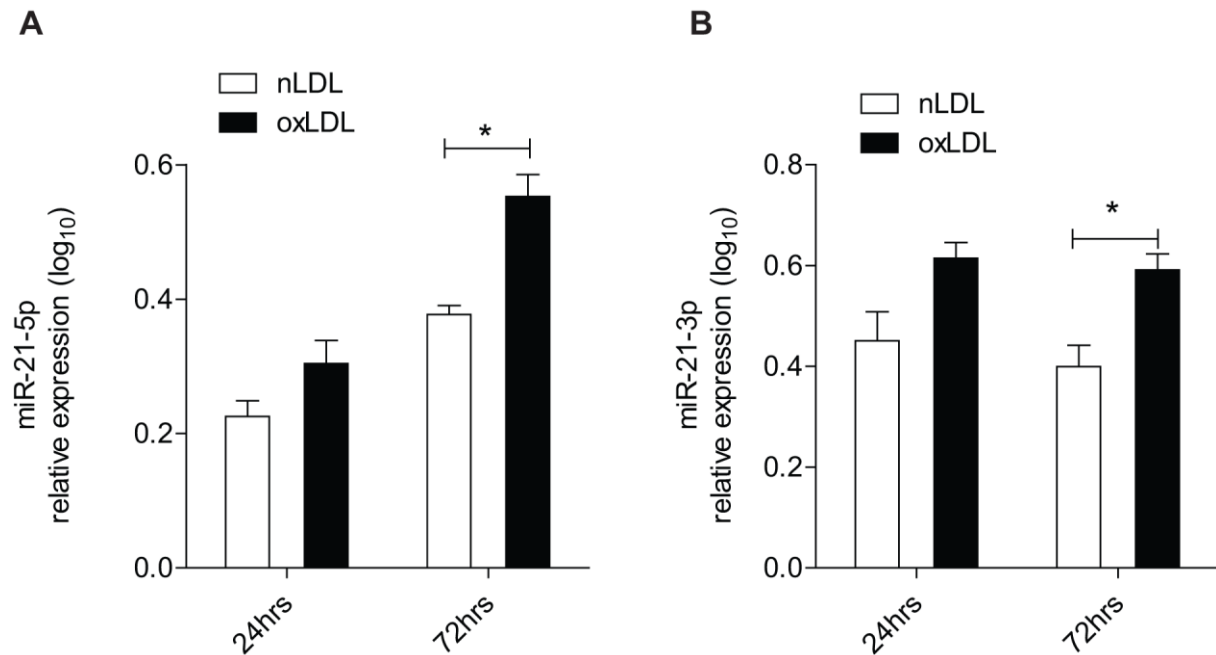


Figure 6: Differential expression of *miR-21-5p* and *miR-21-3p* after oxLDL. BMDMs were treated with either 200 μ g/ml oxLDL or nLDL for 24 and 72 hours. Cells were then lysed and expression of *miR-21-5p* (A) and *miR-21-3p* (B) were assessed by qRT-PCR. n = 3-4 samples per group. Results were analysed using two-way ANOVA. The means \pm s.e.m. are shown.

3.1.2.3 Effect of *Mir21* on cytokine expression in M0, M1 and M2 macrophages

To investigate the role of *Mir21* expression in the different macrophage phenotypes, the effect of *Mir21* deficiency in BMDMs on the expression of cytokines was assessed after M1 and M2 stimulation. Pro-inflammatory (M1) and anti-inflammatory (M2) markers were quantified in M0, M1 and M2 macrophages using qRT-PCR. BM cells were isolated from *Mir21*^{+/+}*ApoE*^{-/-} mice and *Mir21*^{-/-}*ApoE*^{-/-} mice and cultured for 7 days without any stimulation (M0) and the relative expression levels of M1 markers; *Ccl2*, *Il-6*, *iNos*, *Tnf- α* , *Il-1 β* and M2 markers; *Arg1* and *Mrc1* were quantified in the cells using qRT-PCR. There were no significant differences in M1 and M2 markers in unstimulated BMDMs from *Mir21*^{+/+}*ApoE*^{-/-} mice and *Mir21*^{-/-}

Apoe^{-/-} mice (Figure 7). This result indicates that in unstimulated macrophages *Mir21* deficiency may not affect the production of M1 and M2 cytokines.

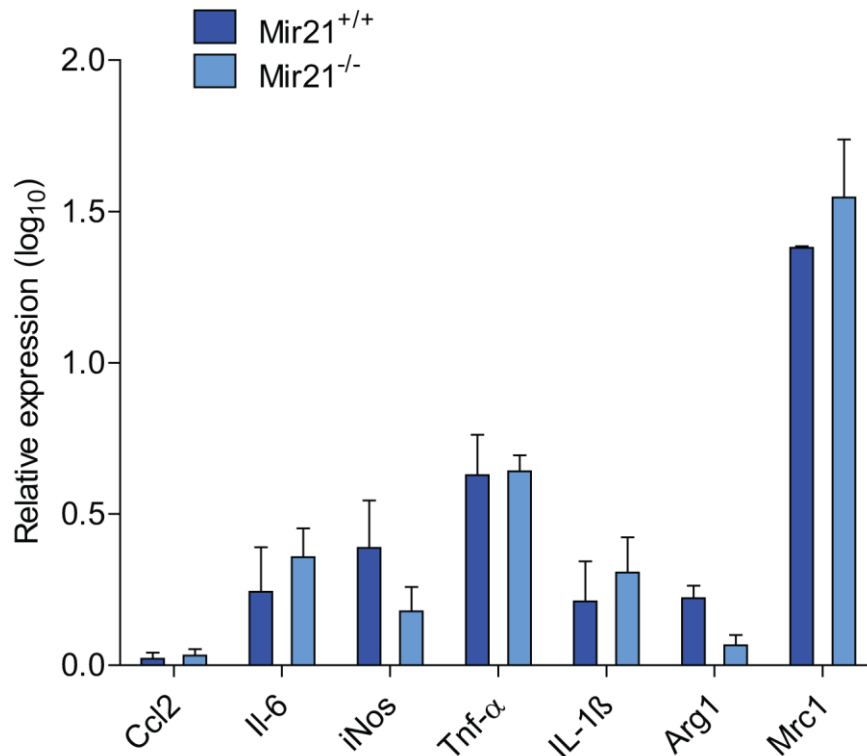


Figure 7. Effect of *Mir21* on the expression of M1 and M2 markers. BM cells were isolated from *Mir21*^{+/+}*Apoe*^{-/-} mice and *Mir21*^{-/-}*Apoe*^{-/-} mice and cultured in macrophage differentiation medium for 7 days and RNA from unstimulated cells were isolated. Expression levels of M1 and M2 markers were quantified in *Mir21*^{+/+}*Apoe*^{-/-} and *Mir21*^{-/-}*Apoe*^{-/-} BMDMs using qRT-PCR. n = 3 samples per group. Results were analysed using two-way ANOVA. The means ± s.e.m. are shown.

To determine the effect of *Mir21* deficiency on the expression of M1 and M2 cytokines after stimulation, BMDMs from *Mir21*^{+/+}*Apoe*^{-/-} mice and *Mir21*^{-/-}*Apoe*^{-/-} mice were either stimulated with LPS and IFN- γ (M1 stimulation) or IL-4 (M2 stimulation) after 6 days of culturing the cells. The relative expression levels of M1 and M2 markers were quantified in the stimulated cells using qRT-PCR. IL-4 treatment increased the expression of *Il-6* in *Mir21*^{-/-}*Apoe*^{-/-} BMDMs compared to *Mir21*^{+/+}*Apoe*^{-/-} BMDMs (Figure 8A). *Il-1 β* expression was increased in *Mir21*^{-/-}*Apoe*^{-/-} BMDMs after M1 stimulation compared to BMDMs isolated from *Mir21*^{+/+}*Apoe*^{-/-} mice (Figure 8B). This suggests that under pro-inflammatory conditions, *Mir21* deficiency may lead to the increased production of *Il-1 β* in macrophages. In addition, *Mir21* deficiency in BMDMs may increase *Il-6* production upon anti-inflammatory stimulation.

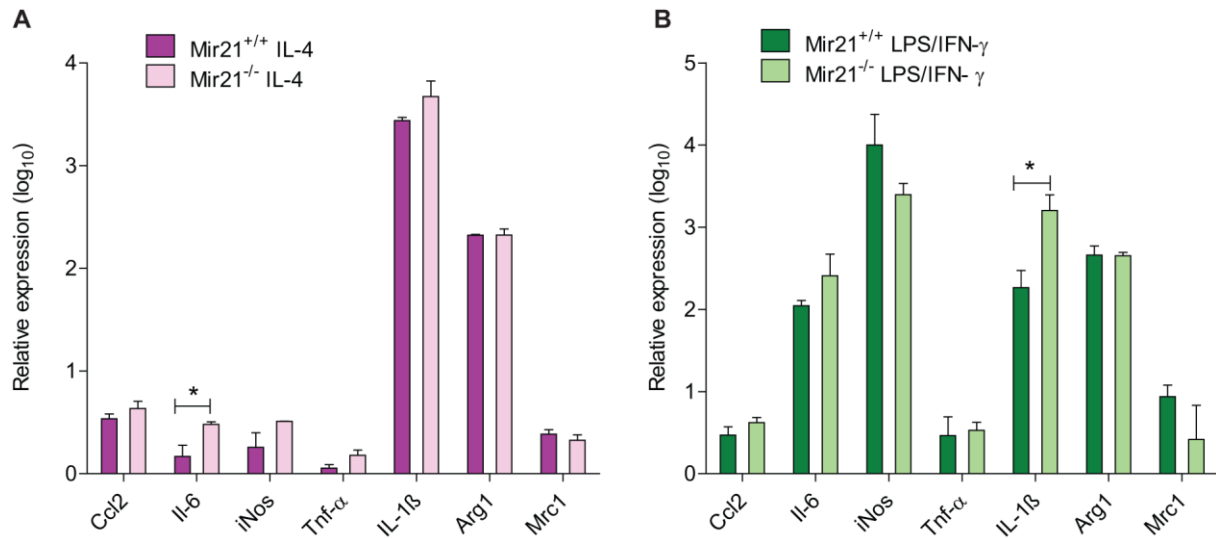


Figure 8: Expression of M1 and M2 markers in stimulated BMDMs. BM cells were isolated from *Mir21*^{+/+}*Apoe*^{-/-} mice and *Mir21*^{-/-}*Apoe*^{-/-} mice and cultured. Expression levels of M1 and M2 markers were quantified in *Mir21*^{+/+}*Apoe*^{-/-} and *Mir21*^{-/-}*Apoe*^{-/-} BMDMs after stimulation with IL-4 (A) or LPS and IFN-γ (B) using qRT-PCR. n = 3 samples per group. * $P < 0.05$. P values were obtained using a two-way ANOVA. The means \pm s.e.m. are shown.

3.1.3 The effect of hematopoietic deficiency of *Mir21* on lesion formation

To assess the role of *Mir21* expression in macrophages during atherogenesis, the BM of *Mir21*^{+/+}*Apoe*^{-/-} mice was reconstituted with BM cells from either *Mir21*^{+/+}*Apoe*^{-/-} mice (*Mir21*^{+/+}/ BM *Mir21*^{+/+}) or *Mir21*^{-/-}*Apoe*^{-/-} mice (*Mir21*^{+/+}/ BM *Mir21*^{-/-}). In addition, the BM of *Mir21*^{-/-}*Apoe*^{-/-} mice was also reconstituted with BM cells from *Mir21*^{-/-}*Apoe*^{-/-} mice (*Mir21*^{-/-}/ BM *Mir21*^{-/-}) mice. The mice were then fed HFD for 12 weeks and afterwards sacrificed, tissues harvested and atherosclerosis quantified.

3.1.3.1 Blood cell data of BM transplanted mice

After 12 weeks of HFD, the mice were sacrificed and blood samples were collected for blood cell count and serum cholesterol levels analysis. In addition, the aortic root and thoraco-abdominal aorta were perfused and harvested for the quantification of atherosclerosis. Serum cholesterol levels were measured using the Cayman's Cholesterol Fluorometric Assay kit according to the manufacturer's instructions. There was no significant difference in serum cholesterol levels in all three groups of mice after 12 weeks of HFD (Figure 9), indicating that the genotype of the BM cells transplanted into the mice did not affect serum cholesterol levels.

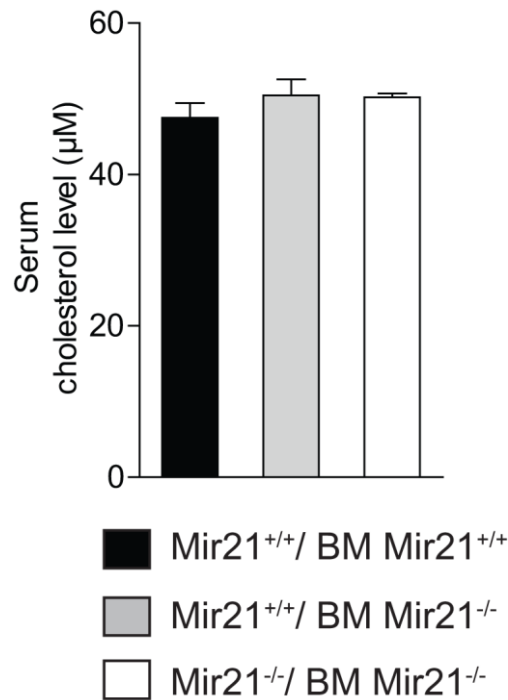


Figure 9: Serum cholesterol levels of BM transplanted mice. Mice were anaesthetized and blood from the orbital vein collected after 12 weeks of HFD. The blood was allowed to clot at room temperature and centrifuged at 2000 x g. The supernatant (serum) was collected and the level of cholesterol measured for each mouse using a Cholesterol Fluorometric Assay kit (Cayman Chemical, MI, USA) according to the manufacturer's instructions. One-way ANOVA and Newman-Keuls multiple comparison test were performed to determine any difference between the groups. The means \pm s.e.m. are shown.

Whole blood was also collected from each mouse via the orbital vein after the mouse had been anesthetized in EDTA tubes (Sarstedt, Nümbrecht, Germany). The different blood cells were then quantified using an automated veterinary Animal Blood Counter. The white blood cell (WBC) count, red blood cell (RBC) count, haemoglobin levels (Hgb), haematocrit (HCT), platelet count (PLT) and the percentages of lymphocytes, monocytes and granulocytes were all quantified and analysed to determine any differences between the groups (Figure 10). There were no significant differences among the groups for all of the cellular components of the blood. This data indicates that the bone marrow transplantation was successful and also the observed differences in atherosclerosis were not due to difference in circulating blood cells.

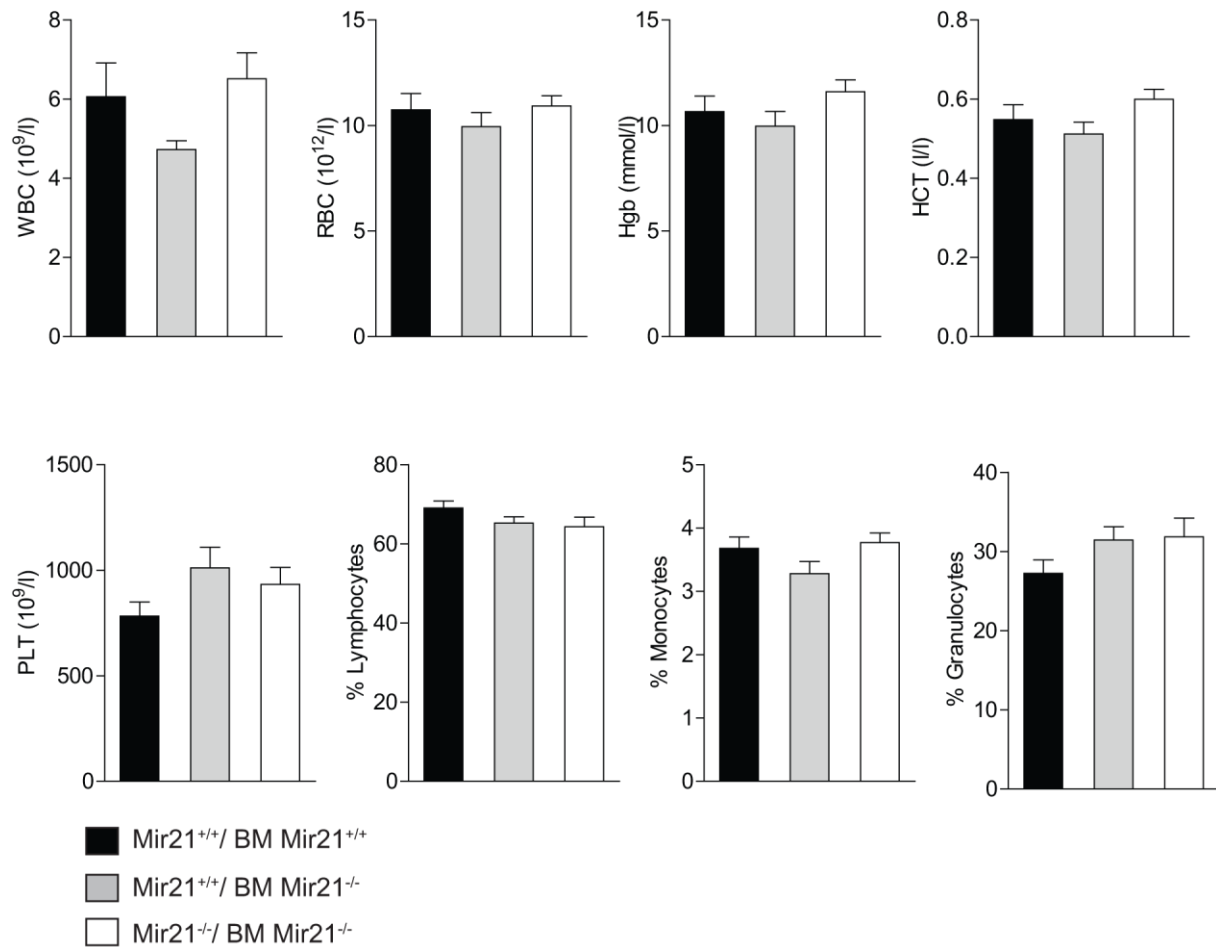


Figure 10: Blood composition and cell count of BM transplant recipient mice. Blood samples from each mouse were collected from the orbital vein into EDTA tubes and gently agitated to mix the blood and EDTA well so as to prevent the blood from clotting. The blood cell count was then performed with an automated veterinary animal blood counter. The white blood cell (WBC), red blood cell (RBC), haemoglobin levels (Hgb), haematocrit (HCT), platelet count (PLT) and the percentages of lymphocytes, monocytes and granulocytes were analysed. One-way ANOVA and Newman-Keuls multiple comparison test were performed to determine any difference between the groups. The means \pm s.e.m. are shown.

3.1.3.2 Quantification of atherosclerosis in BM transplanted mice

Atherosclerosis in BM transplanted mice was assessed after 12 weeks of HFD by Oil red O staining of *en face* prepared thoraco-abdominal aortas and in EVG stained sections of aortic roots by morphometry. Lesion formation was significantly reduced in thoraco-abdominal aortas of Mir21^{+/+} BM Mir21^{-/-} mice and Mir21^{-/-} BM Mir21^{-/-} mice compared to Mir21^{+/+} BM Mir21^{+/+} mice after 12 weeks HFD (Figure 11). The difference in lesion area of Mir21^{+/+} BM Mir21^{-/-} mice and Mir21^{-/-} BM Mir21^{-/-} mice was not statistically significant. These results suggest that *Mir21* knock-out in BM cells reduces atherosclerosis.

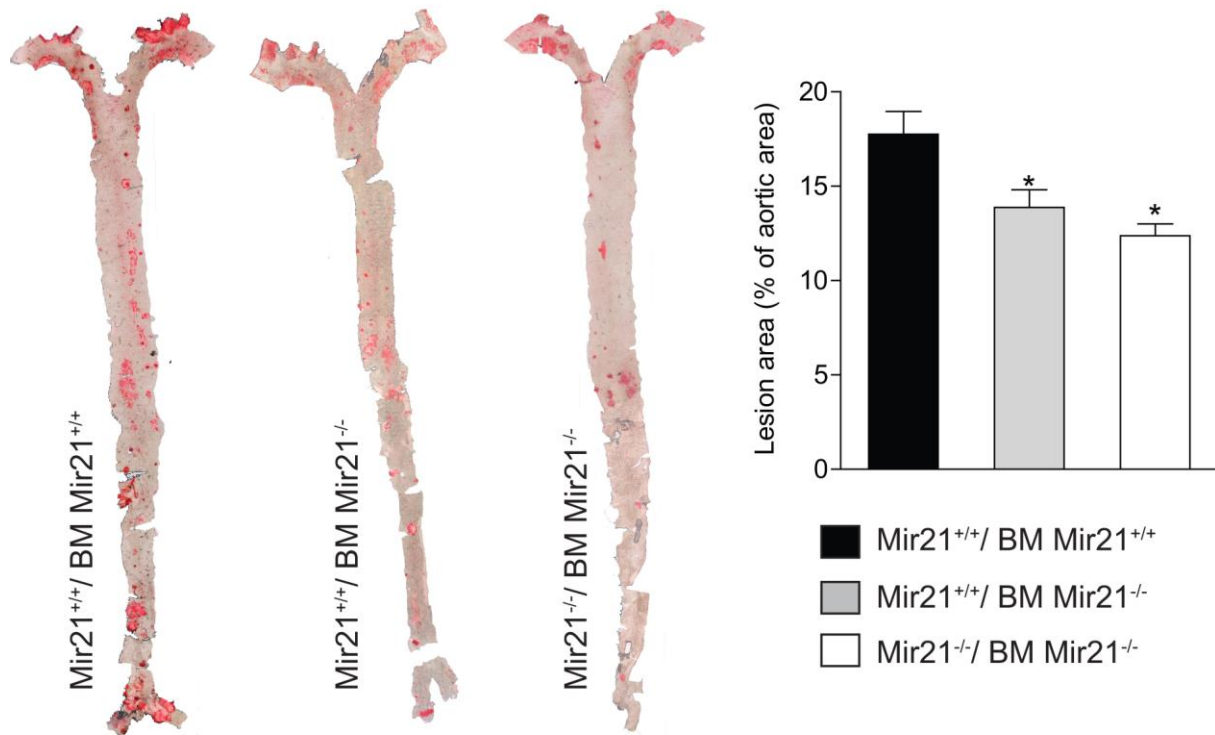


Figure 11: BM deficiency of *Mir21* and atherosclerosis in thoraco-abdominal aorta. Atherosclerotic lesions were analysed in *Mir21*^{+/+}*Apoe*^{-/-} mice transplanted with *Mir21*^{+/+}*Apoe*^{-/-} (*Mir21*^{+/+}/ BM *Mir21*^{+/+}) or *Mir21*^{-/-}*Apoe*^{-/-} (*Mir21*^{+/+}/ BM *Mir21*^{-/-}) BM cells as well as *Mir21*^{-/-}*Apoe*^{-/-} transplanted with *Mir21*^{-/-}*Apoe*^{-/-} BM cells (*Mir21*^{-/-}/ BM *Mir21*^{-/-}) after 12 weeks of HFD. Lesions were quantified in Oil red O stained *en face* prepared aortas (n = 7-8 mice per group). * $P < 0.05$. P values were obtained using One-way ANOVA and Newman-Keuls multiple comparison test. The means \pm s.e.m. are shown.

Atherosclerotic lesion area and necrotic core area were quantified in aortic root sections from *Mir21*^{+/+}/ BM *Mir21*^{+/+} mice, *Mir21*^{+/+}/ BM *Mir21*^{-/-} mice and *Mir21*^{-/-}/ BM *Mir21*^{-/-} mice. Lesion area and necrotic core area were significantly reduced in *Mir21*^{+/+}/ BM *Mir21*^{-/-} mice compared to *Mir21*^{+/+}/ BM *Mir21*^{+/+} mice (Figure 12B and C). There was however no change in aortic root lesion area and necrotic core area of *Mir21*^{-/-}/ BM *Mir21*^{-/-} mice compared to *Mir21*^{+/+}/ BM *Mir21*^{+/+} mice (Figure 12B and C). Put together, these data indicate that *Mir21* deficiency in BM-derived cells reduces atherosclerotic lesion area and necrotic core area in mice. However, *Mir21* knock-out in BM cells as well as other vascular cells resulted in reversal of the beneficial effect of the knock-out in only BM cells. *Mir21* expression may therefore have different roles in different cells during atherogenesis and in other vascular cells *Mir21* expression could have an opposing effect as compared to *Mir21* in BM cells.

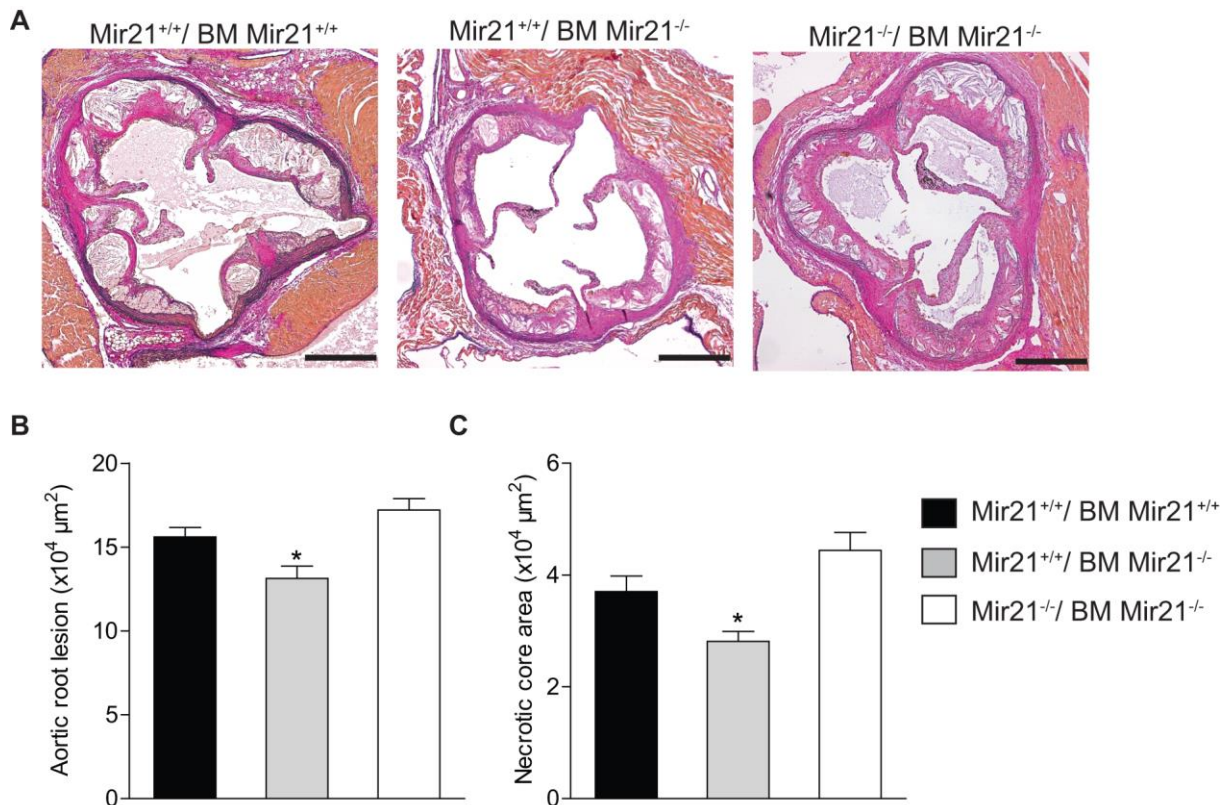


Figure 12: BM deficiency of *Mir21* and atherosclerosis in the aortic root. Atherosclerotic lesions were quantified in *Mir21*^{+/+}*Apoe*^{-/-} mice transplanted with *Mir21*^{+/+}*Apoe*^{-/-} (Mir21^{+/+}/ BM Mir21^{+/+}) or *Mir21*^{-/-}*Apoe*^{-/-} (Mir21^{+/+}/ BM Mir21^{-/-}) BM cells and *Mir21*^{-/-}*Apoe*^{-/-} mice transplanted with *Mir21*^{-/-}*Apoe*^{-/-} BM cells (Mir21^{-/-}/ BM Mir21^{-/-}) after 12 weeks of HFD. Lesion area and necrotic core area were analysed in cross-sections of aortic root stained with EVG stain (n = 7-8 mice per group). * *P* < 0.05. *P* values were obtained using One-way ANOVA and Newman-Keuls multiple comparison test. The means ± s.e.m. are shown. Scale bars; 250 μm.

3.1.4 The effect of *Mir21* deficiency on cellular content of atherosclerotic lesions

To study the effect of *Mir21* knockout in BM cells on the cellular content of atherosclerotic lesions, the smooth muscle, macrophage, collagen type I and T-cell contents were assessed using immunostaining performed on aortic root sections from *Mir21*^{+/+}*Apoe*^{-/-} mice transplanted with *Mir21*^{+/+}*Apoe*^{-/-} (BM Mir21^{+/+}) or *Mir21*^{-/-}*Apoe*^{-/-} (BM Mir21^{-/-}) BM cells. To quantify macrophage accumulation in atherosclerotic lesions, MAC2 immunostaining was performed and the nuclei counter stained with DAPI. The number of MAC2 positive cells in atherosclerotic lesions from BM Mir21^{-/-} mice was significantly lower than that of BM Mir21^{+/+} mice (Figure 13A). SMA and Collagen type I immunostaining were also performed and analysis of the SMA area or Collagen area showed no significant difference between BM Mir21^{+/+} mice and BM Mir21^{-/-} mice (Figure 13B and C). This result suggests that *Mir21*

knockout in BM cells reduces macrophage cell content in atherosclerotic lesions but may not have any effect on smooth muscle content and collagen type I content.

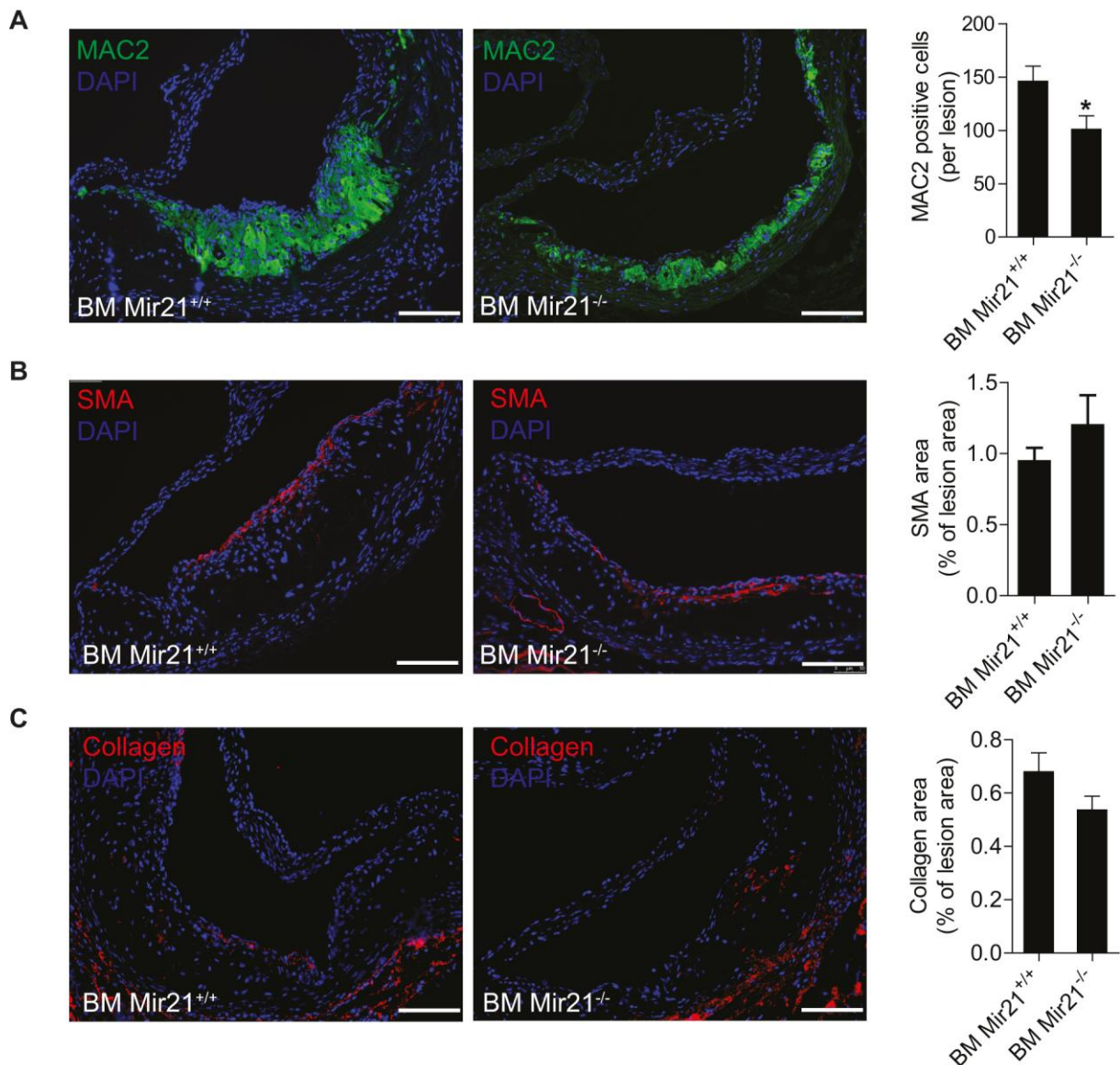


Figure 13: Effect of BM deficiency of *Mir21* on lesional cellular content. Aortic root sections from BM Mir21^{+/+} mice and BM Mir21^{-/-} mice fed HFD for 12 weeks were stained with MAC2, SMA and Collagen type I antibodies. MAC2 positive cell number in atherosclerotic lesions was determined by counting MAC2 positive and DAPI positive cells (A). SMA (B) and Collagen (C) area were analysed and expressed as a percentage of the whole lesion area. * $P < 0.05$. P values were obtained using two-tailed student's t-test. The means \pm s.e.m. are shown. Scale bars: 100 μ m.

The T-cell content of atherosclerotic lesions in their aortic root was assessed by performing CD3 immunostaining and analysis done by counting CD3 positive cells and normalizing to the total lesional cells. The percentage of CD3 positive cells in aortic root lesions of BM

$Mir21^{-/-}$ mice was significantly higher than that of BM $Mir21^{+/+}$ mice (Figure 14). This suggests that *Mir21* deficiency in BM cells increases recruitment of T-cells in atherosclerotic lesions.

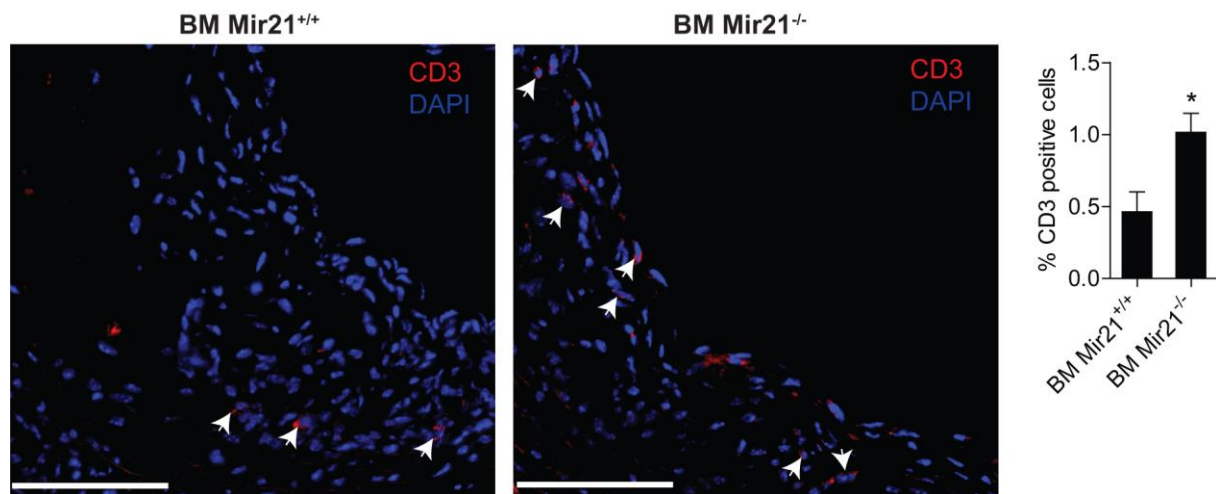


Figure 14: Effect of BM deficiency of *Mir21* on T-cell content in atherosclerotic lesions. CD3 immunostaining was performed on atherosclerotic lesions in aortic root sections from BM $Mir21^{+/+}$ and BM $Mir21^{-/-}$ mice fed HFD for 12 weeks. CD3 cell count was analysed using DAPI nuclei counter stained images. * $P < 0.05$. P values were obtained using two-tailed student's t-test. The means \pm s.e.m. are shown. Scale bars: 50 μ m.

3.1.5 The effect of *Mir21* deficiency on lipid content in macrophages

To study the role of *Mir21* expression on the accumulation of lipid droplets in lesional macrophages, aortic root sections were double stained with MAC2 and Perilipin 2 antibodies. Perilipin positive area normalised to total MAC2 area was analysed in sections obtained from BM $Mir21^{+/+}$ and BM $Mir21^{-/-}$ mice after 12 weeks of HFD. Even though perilipin area in atherosclerotic lesions of mice transplanted with $Mir21^{-/-}Apoe^{-/-}$ BM cells (BM $Mir21^{-/-}$) tended to increase compared to mice transplanted with $Mir21^{+/+}Apoe^{-/-}$ BM cells (BM $Mir21^{+/+}$), the difference between the two groups was not statistically significant (Figure 15). This data suggests that *Mir21* deficiency in BM cells may not play a significant role in lipid accumulation in macrophages during atherogenesis.

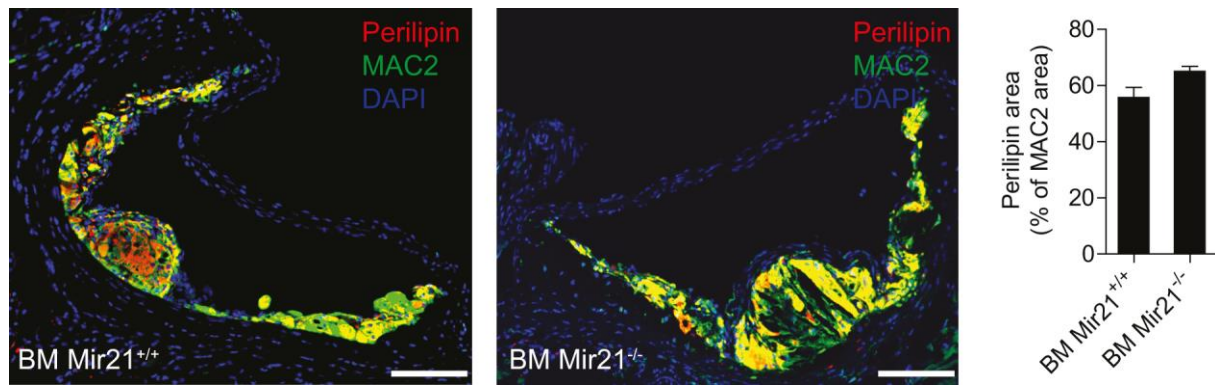


Figure 15: Effect of BM deficiency of *Mir21* on lipid accumulation in macrophages. Perilipin 2 and MAC2 double staining were performed on aortic root sections from BM Mir21^{+/+} and BM Mir21^{-/-} mice fed HFD for 12 weeks. There was no significant difference between BM Mir21^{-/-} mice and BM Mir21^{+/+} mice after a two-tailed student's t-test analysis was performed. The means \pm s.e.m. are shown. Scale bars: 100 μ m.

3.1.6 The effect of *Mir21* deficiency on macrophage apoptosis in atherosclerosis

To determine the mechanism leading to the reduction in macrophage cell number, necrotic core area and atherosclerotic lesion area of BM Mir21^{-/-} mice after 12 weeks HFD, TUNEL assay was performed using aortic root sections and double stained with MAC2 to determine the number of apoptotic macrophages in the lesions in BM Mir21^{+/+} mice and BM Mir21^{-/-} mice. TUNEL positive macrophages were analysed and the percentage of TUNEL positive macrophages to the total number of macrophages in each section was determined. The percentage of apoptotic macrophages (TUNEL positive MAC2 cells) in the atherosclerotic lesions of BM Mir21^{-/-} mice after 12 weeks HFD when compared with that of BM Mir21^{+/+} mice was significantly higher (Figure 16). This effect on macrophage apoptosis suggests that *Mir21* deficiency in BM cells may lead to increased macrophage apoptosis during atherosclerosis and this may reduce macrophage accumulation and hence atherosclerotic lesion formation.

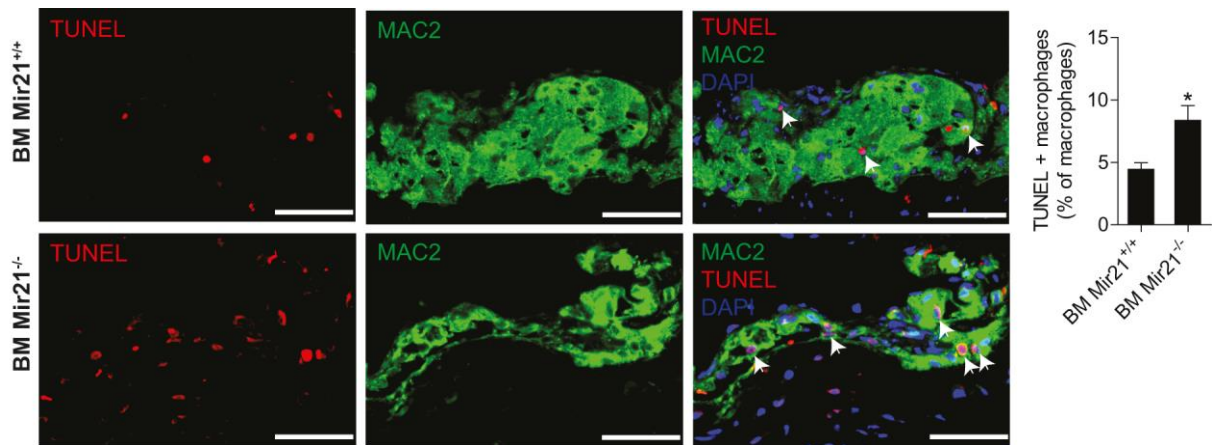


Figure 16: Effect of *Mir21* deficiency on lesional macrophage apoptosis. TUNEL staining was performed on aortic root sections from BM *Mir21*^{+/+} and BM *Mir21*^{-/-} mice fed HFD for 12 weeks. Sections were then counter stained with MAC2 antibody and TUNEL positive MAC2 positive cells were counted and expressed as a percentage of total MAC2 positive cells. * $P < 0.05$. P values were obtained using two-tailed student's t-test. The means \pm s.e.m. are shown. Scale bars: 50 μ m.

3.2 Targets of *Mir21* in macrophages during atherogenesis

3.2.1 Effect of *Mir21* deficiency on mRNA expression in atherosclerotic lesions

To study the molecular mechanisms through which *Mir21* deficiency in BM cells leads to reduced atherosclerosis, as well as to determine possible targets of the different strands (*miR-21-3p* and *miR-21-5p*), a global gene expression analysis was performed with samples isolated from the aortic arch of *Mir21*^{+/+} *ApoE*^{-/-} mice transplanted with either *Mir21*^{+/+} *ApoE*^{-/-} (BM *Mir21*^{+/+}) or *Mir21*^{-/-} *ApoE*^{-/-} (BM *Mir21*^{-/-}) BM cells and fed a HFD for 12 weeks. The global gene expression analysis revealed a total number of 500 upregulated and 585 downregulated gene transcripts (fold change ≥ 1.5 ; $P \leq 0.05$, $n = 3$ mice per group) in the aortic arch atherosclerotic lesions of BM *Mir21*^{-/-} versus BM *Mir21*^{+/+} mice (Figure 17).

The most significantly upregulated genes in atherosclerotic lesions from BM *Mir21*^{-/-} (KO) mice compared to BM *Mir21*^{+/+} (WT) mice were *Xaf1*, *Arntl*, *Npas2*, *Nfil3*, *Foxs1*, *Adamts4*, *Ier5* and *Tmem82*. In addition, *Mbl2* (highlighted in red in Figure 17) which is expressed in lesions and plays a role in atherosclerosis¹⁴⁶ was also highly upregulated in the microarray. Some of the most significantly downregulated genes included *Chrono*, *Dbp*, *Tef*, *Dec1*, *Bpifa1*, *Scgb3a1*, *Elovl3*, *Nr1d2*, *Olf734* and *Stox1*. Notable among the differentially regulated genes is that, several differentially regulated genes are involved in the circadian rhythm pathway. The circadian rhythm pathway genes are highlighted in orange and the most highly upregulated gene *Xaf1* as well as *Mbl2* are highlighted in red (Figure 17).

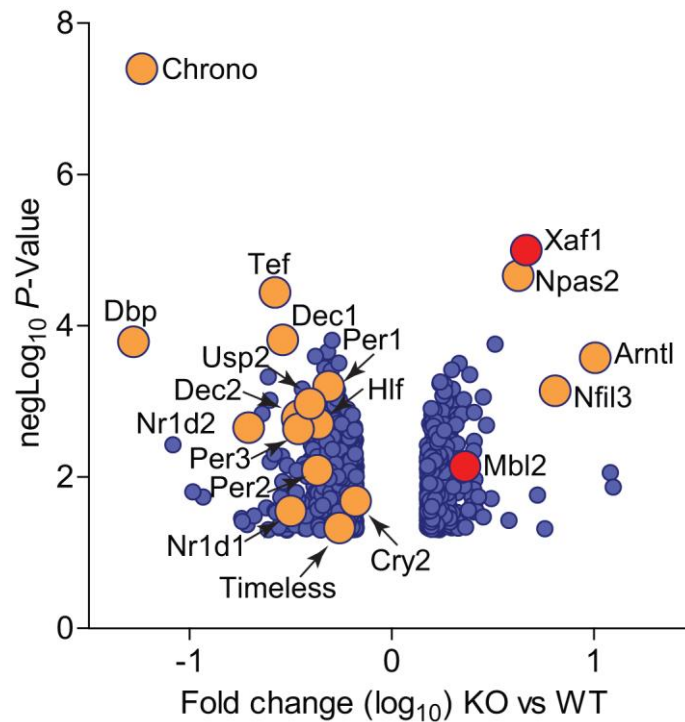


Figure 17: Differentially regulated genes in aortic arch atherosclerotic lesion. Genome wide expression profiling (Agilent SurePrint G3 Mouse Gene Expression Microarray) was performed with RNA samples isolated from the aortic arch of BM Mir21^{+/+} and BM Mir21^{-/-} mice after 12 weeks HFD. The plot shows Log₁₀ of fold change and in blue dots upregulated and downregulated gene transcripts (fold change ≥ 1.5 ; $P \leq 0.05$, $n = 3$ mice per group) in atherosclerotic lesions from BM Mir21^{-/-} mice (KO) compared to BM Mir21^{+/+} mice (WT). The most highly upregulated gene *Xaf1* is shown in red as well as *Mbl2* which plays a role in atherosclerosis. Some of the highly upregulated and downregulated genes which are involved in the circadian rhythm are highlighted in orange.

To identify the pathways that the differentially regulated genes may be involved in during atherosclerosis, a pathway analysis using Ingenuity Pathway Analysis (IPA, Qiagen) was performed using the results of the microarray analysis. IPA was used to determine the molecular pathway which was highly upregulated in atherosclerotic lesions of BM Mir21^{-/-} mice compared to BM Mir21^{+/+} mice. The circadian rhythm signalling pathway was the most significantly upregulated pathway (Table 2). Genes that positively regulate the circadian pathway were significantly upregulated, whereas negative regulators that modulate circadian rhythm through a negative feedback mechanism were downregulated in the microarray. For example a main regulator of the circadian rhythm *Arntl1* was upregulated, whereas downstream genes *Per1*, *Per2*, *Per3*, *Cry2* and *Nr1d2* were downregulated in atherosclerotic lesions in the aortic arch of BM Mir21^{-/-} mice compared to BM Mir21^{+/+} mice (Table 2).

The pathway analysis (Table 2) also showed several pathways and their genes that were highly upregulated in the microarray. Pathways including axonal guidance signalling, Calcium transport, Wnt/ β -catenin, basal cell carcinoma signalling, sonic hedgehog signalling

Results

and mTOR signalling are involved in cell growth, proliferation and cell motility and they may contribute to macrophage survival and removal of apoptotic cells during atherogenesis. Moreover, TR/LXR activation, Stearate biosynthesis I and Triacylglycerol biosynthesis are known to be involved in metabolism. These pathways may also contribute important roles in vascular cells during atherosclerosis.

Pathway	<i>p</i> -value	Genes
Circadian rhythm signalling	5.83109E-06	Arntl, Cry2, Vipr2, Per1, Per2, Bhlhe41, Per3, Nr1d1, Bhlhe40
Stearate biosynthesis I (animals)	0.0026	Acs13, Acot2, Fasn, Dbt, Acot4, Elovl6
Axonal guidance signalling	0.0031	Enpeo, Rnd1, Rgs3, Sema6a, Plxna2, Adams2, Ntn1, Nfat5, Sufu, Adam24, Ntrk1, Adam23, Adams5, Adams4, Gng4, Itgb1, Sema3g, Pappa, Stk36, Wnt9b, Kalrn, Arhgef15, Ptch1, Vegfc, Fzd9, Adam20, Hhip, Gnao1, Fzd5, Sema4b
Calcium transport I	0.0064	Atp2a2, Atp2b4, Atp2b2
Basal cell carcinoma signalling	0.0091	Stk36, Wnt9b, Sufu, Ptch1, Fzd5, Fzd9, Hhip, Tcf7
Wnt/ β -catenin signalling	0.0098	Axin2, Tgfr1, Wnt9b, Lrp6, Fzd9, Kremen1, Tcf7, Sox17, Wif1, Gnao1, Rarb, Cd44, Fzd5, Ppp2r1b
Eicosanoid signaling	0.0134	Pla2g16, Ltb4r2, Tbx2r, Pla2g3, PnpLa3, Alox12, Hpgds
TR/RXR activation	0.0215	F10, Mtor, Adrb1, Fasn, Dio1, Thra, ME1, Nr1g
Aryl hydrocarbon receptor signalling	0.0269	Ctsd, Aldh1l1, Nfix, Mgst2, Tp73, Rarb, Cdkn1a, Hsp90aa1, Nrip1, Nfkb1, Esr1
Sonic hedgehog signalling	0.0316	Stk36, Sufu, Ptch1, Hhip
Thyroid hormone metabolism II	0.0389	Ugt3a2, Ugt2b7, Dio1, Sult1b1
mTOR signalling	0.0470	Mtor, Vegfc, Ppp2r1b
Triacylglycerol biosynthesis	0.0471	Mogat1, Lpin1, Dbt, Elovl6

Table 2: Most significantly upregulated pathways in atherosclerosis after *Mir21* knockout in BM cells. Using the data generated from microarray results performed in atherosclerotic lesions of BM *Mir21*^{-/-} mice and BM *Mir21*^{+/+} mice, pathway analysis was performed with the Ingenuity Pathway Analysis (IPA, Qiagen) software and this generated a list of most upregulated molecular pathways based on the highly upregulated genes and downregulated genes involved in a pathway.

3.2.2 Differentially regulated circadian clock genes in aortic root lesions

To investigate the role of the circadian rhythm in atherosclerosis, the expression levels of *Arntl1*, *Nfil3*, *Npas2*, *Per1*, *Per2*, *Per3*, *Nr1d2* and *Dbp* were quantified in atherosclerotic lesion isolated from the aortic root of BM *Mir21*^{+/+} mice and BM *Mir21*^{-/-} mice after 12 weeks HFD using qRT-PCR. *Arntl1*, *Nfil3* and *Npas2* were upregulated in atherosclerotic lesions of BM *Mir21*^{-/-} mice compared to BM *Mir21*^{+/+} mice. *Per2*, and *Nr1d2* in atherosclerotic lesions of BM *Mir21*^{-/-} mice were downregulated compared to BM *Mir21*^{+/+} mice (Figure 18). Even though *Per1* was downregulated in BM *Mir21*^{-/-} mice, the difference was not statistically significant. This data indicate that *Mir21* deficiency in BM cells may upregulate the circadian pathway and this may play an important role in reducing atherosclerotic lesion formation.

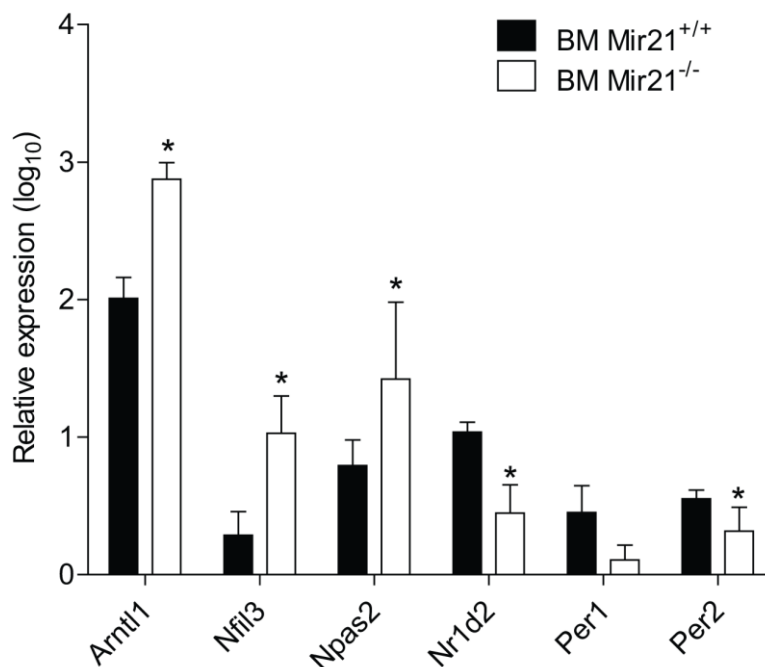


Figure 18: Differentially regulated circadian clock genes in atherosclerotic lesions. Expression level of circadian clock genes were quantified in atherosclerotic lesions isolated from the aortic root of *Mir21*^{+/+} *Apoe*^{-/-} transplanted with either *Mir21*^{+/+} *Apoe*^{-/-} (BM *Mir21*^{+/+}) or *Mir21*^{-/-} *Apoe*^{-/-} (BM *Mir21*^{-/-}) BM cells and fed HFD for 12 weeks. n = 3-4 per group. * $P < 0.05$. P values were obtained using two-tailed student's t-test. The means \pm s.e.m. are shown.

3.2.3 Effect of BM deficiency of *Mir21* on circadian clock genes in lesional macrophages

To further study the effect of BM deficiency of *Mir21* on the circadian clock genes in lesional macrophages, atherosclerotic lesional cells without endothelial cells were isolated from sections of the aortic root using laser capture microdissection. qRT-PCR was performed in laser-microdissected samples from BM *Mir21*^{+/+} mice and BM *Mir21*^{-/-} mice after 12 weeks of HFD. *Arntl1* and *Nfil3* were significantly upregulated in BM *Mir21*^{-/-} mice compared with BM *Mir21*^{+/+} mice in laser-microdissected lesional macrophages (Figure 19). *Npas2* was upregulated in BM *Mir21*^{-/-} mice compared to BM *Mir21*^{+/+} mice samples but the difference was not statistically significant. There was also a significant downregulation of *Per2* in lesional macrophages of BM *Mir21*^{-/-} mice compared to BM *Mir21*^{+/+} mice. The cells isolated from the atherosclerotic lesions were microdissected without the endothelial cells and medial cells and therefore consisted predominantly of lesional macrophages and the data suggest that *Mir21* deficiency in BM cells may lead to upregulation of the circadian pathway in lesional macrophages and this may play a role in reducing atherosclerosis.

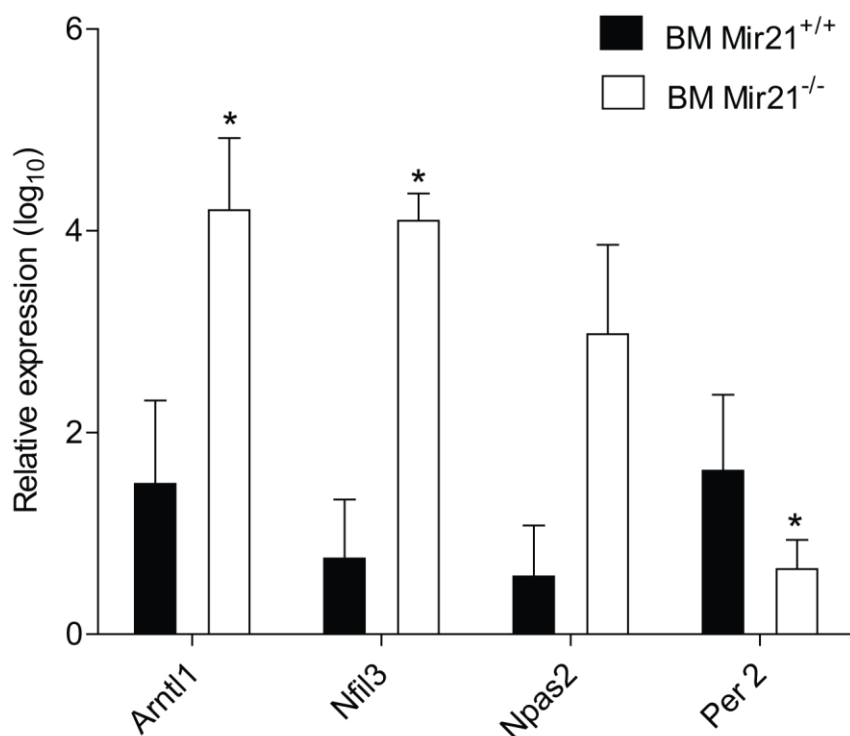


Figure 19: Expression of circadian clock genes in lesional macrophages. The relative expression levels of circadian clock genes were quantified in laser-microdissected lesional cells from aortic root sections of BM *Mir21*^{+/+} mice and BM *Mir21*^{-/-} mice after 12 weeks of HFD using qRT-PCR (n = 3-4 mice per group). * P < 0.05. P values were obtained using two-tailed student's t-test. The means ± s.e.m. are shown.

3.2.4 Effect of bone marrow deficiency of *Mir21* on *Xaf1* and *Mbl2* expression in lesional macrophages

In order to study the mechanism behind the increased macrophage apoptosis, decreased macrophage cell number and necrotic core area in atherosclerotic lesions in BM *Mir21*^{-/-} mice compared to BM *Mir21*^{+/+} mice after 12 weeks HFD, qRT-PCR using laser-microdissected lesional cells was performed to quantify the expression of *Xaf1* and *Mbl2*. The lesional cells were dissected without the endothelial and medial cells and must be mainly consisting of macrophages. Both *Xaf1* and *Mbl2* were upregulated in BM *Mir21*^{-/-} mice compared to BM *Mir21*^{+/+} mice (Figure 20). *Xaf1* was the most highly upregulated gene in the microarray analysis. The upregulation of *Xaf1* and *Mbl2* in lesional macrophages may play a role in increasing apoptosis and efferocytosis of dead cells thereby leading to reduced necrotic core area and atherosclerotic lesion sizes in mice transplanted with BM cells deficient of *Mir21* (BM *Mir21*^{-/-}) compared to mice transplanted with wildtype BM cells (BM *Mir21*^{+/+}).

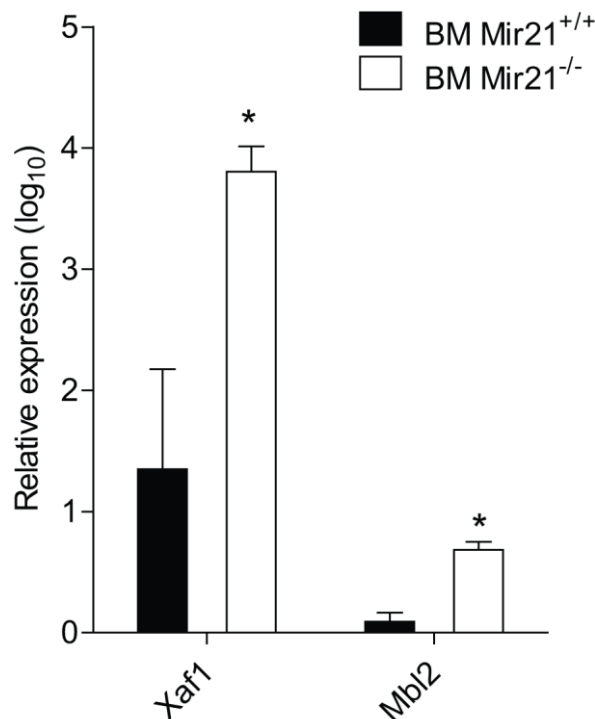


Figure 20: Expression of *Xaf1* and *Mbl2* in lesional macrophages. The relative expression levels of *Xaf1* and *Mbl2* were assessed in laser-microdissected lesional cells isolated from aortic root sections of BM *Mir21*^{+/+} mice and BM *Mir21*^{-/-} mice after 12 weeks of HFD using qRT-PCR (n = 3-4 mice per group). * $P < 0.05$. P values were obtained using two-tailed student's t-test. The means \pm s.e.m. are shown.

To study the functional relevance of the upregulation of *Xaf1* gene in lesional macrophages, XAF1 immunostaining was performed in aortic root sections. The sections were counter stained with MAC2 antibody and XAF1 positive, MAC2 positive cells were analysed. The percentage of macrophages expressing XAF1 was significantly higher in BM *Mir21*^{-/-} mice as compared to BM *Mir21*^{+/+} (Figure 21). This result indicates that *Mir21* knockout in BM cells leads to the increased expression of XAF1 protein in lesional macrophages.

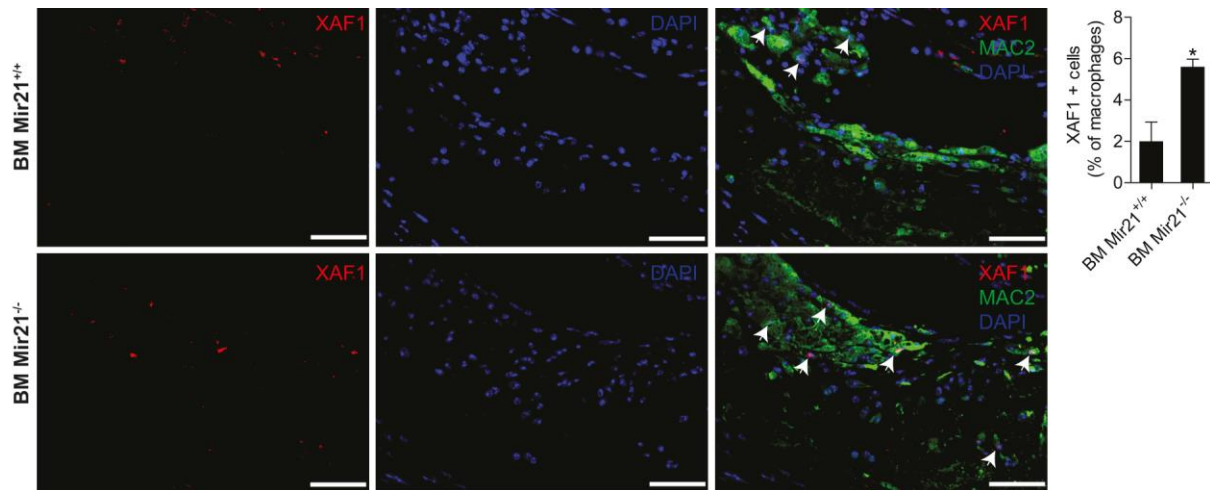


Figure 21: XAF1 expression in lesional macrophages. XAF1 and MAC2 immunostaining were performed on aortic root sections from BM *Mir21*^{+/+} mice and BM *Mir21*^{-/-} mice after 12 weeks of HFD. XAF1 expressing macrophages were counted and expressed as a percentage of the total lesional macrophages. n = 4 mice per group * $P < 0.05$. P values were obtained using two-tailed student's t-test. The means \pm s.e.m. are shown.

3.3 Effect of *Mir21* on circadian clock in macrophages

3.3.1 Circadian rhythmic expression of *miR-21-3p* and *miR-21-5p*

To study the individual roles of the different strands of *Mir21*, the 24-hour circadian expression pattern of both *miR-21-3p* and *miR-21-5p* in BMDMs were examined after the cells were synchronised. BM cells isolated from *Mir21*^{+/+} *Apoe*^{-/-} mice were cultured and incubated for seven days and RNA isolated every 4 hours after synchronisation over a 24-hour period. The relative expression for each time point was quantified by qRT-PCR. There was no rhythmic expression of the *miR-21-5p* strand observed in BMDM within the 24-hour period; however, *miR-21-3p* showed a rhythmic expression over the 24-hour period shown (Figure 22). The expression level of *miR-21-3p* differed at different time points within the 24-hour circadian period. This observation indicates that at different time points in a circadian period, the effect and function *miR-21-3p* strand changes and may have more significant role

to play in the circadian rhythm of macrophages. The results also suggests that *miR-21-5p* may have a longer half-life and more stable than *miR-21-3p*.

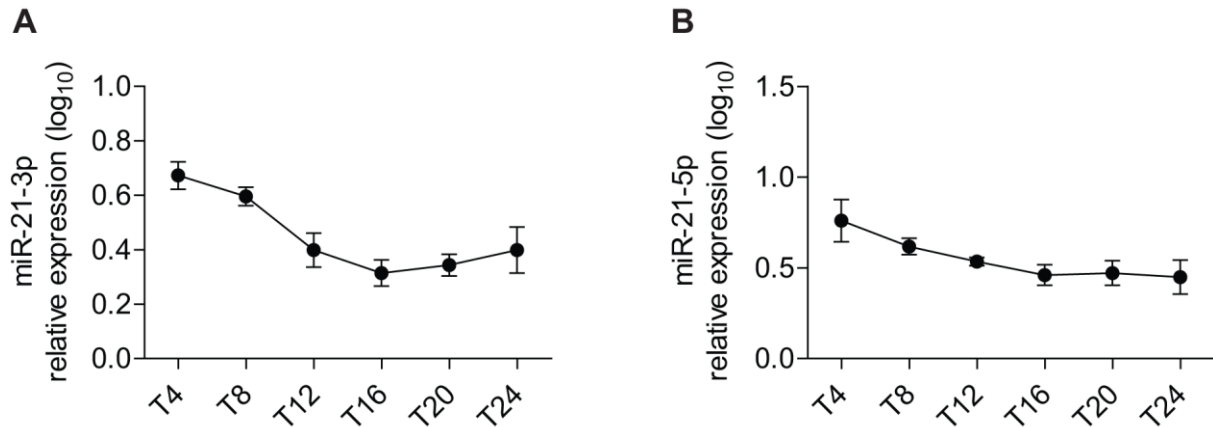


Figure 22: Circadian expression of *miR-21-3p* and *miR-21-5p* in BMDMs. Relative expression levels of *miR-21-3p* and *miR-21-5p* strands were quantified in BMDMs over a 24-hour period after synchronisation using qRT-PCR. BM cells isolated from *Mir21*^{+/+}*Apoe*^{-/-} mice were cultured for 7 days and synchronised. qRT-PCR was performed by harvesting samples every 4 hours over a period of 24 hours. *miR-21-3p* (A) strand showed a rhythmic expression over a 24-hour period but the 24-hour expression pattern of *miR-21-5p* (B) did not show a rhythmic pattern.

3.3.2 Effect of *Mir21* deficiency on circadian clock genes in BMDMs

To study the role of *Mir21* expression in the regulation of circadian clock genes, we quantified the expression of circadian clock genes in BMDMs isolated from *Mir21*^{+/+}*Apoe*^{-/-} mice and *Mir21*^{-/-}*Apoe*^{-/-} mice after synchronisation. The cells were cultured for 7 days and afterwards synchronised and then samples were harvested every 4 hours over 24 hours. The relative expression levels of *Arntl1*, *Nfil3*, *Npas2*, *Per2* and *Per3* in *Mir21*^{-/-}*Apoe*^{-/-} BMDMs were quantified using qRT-PCR and compared with the expression of *Mir21*^{+/+}*Apoe*^{-/-} BMDMs. The expression levels of *Arntl1* in *Mir21*^{-/-}*Apoe*^{-/-} cells as compared to *Mir21*^{+/+}*Apoe*^{-/-} cells over the 24-hour period were significantly higher for all time points (Figure 23A). This shows that *Mir21* deficiency in macrophages results in increased amplitude of *Arntl1* expression and hence an upregulation of the circadian rhythm. Similarly, *Nfil3* expression was increased in *Mir21*^{-/-}*Apoe*^{-/-} BMDMs compared to *Mir21*^{+/+}*Apoe*^{-/-} BMDMs, however the differences were only significant at T8 and T24 (Figure 23B). The expression levels of *Npas2* were also increased in *Mir21*^{-/-}*Apoe*^{-/-} BMDMs at certain time points (T4, T8 and T12) compared to the expression in *Mir21*^{+/+}*Apoe*^{-/-} BMDMs (Figure 23C) but reduced from T16 to T24. This indicates a shift in the phase and also amplitude of *Npas2*

expression. These results put together suggest that in BMDMs the Knock-out of *Mir21* leads to the upregulation of genes that positively regulate the circadian rhythm.

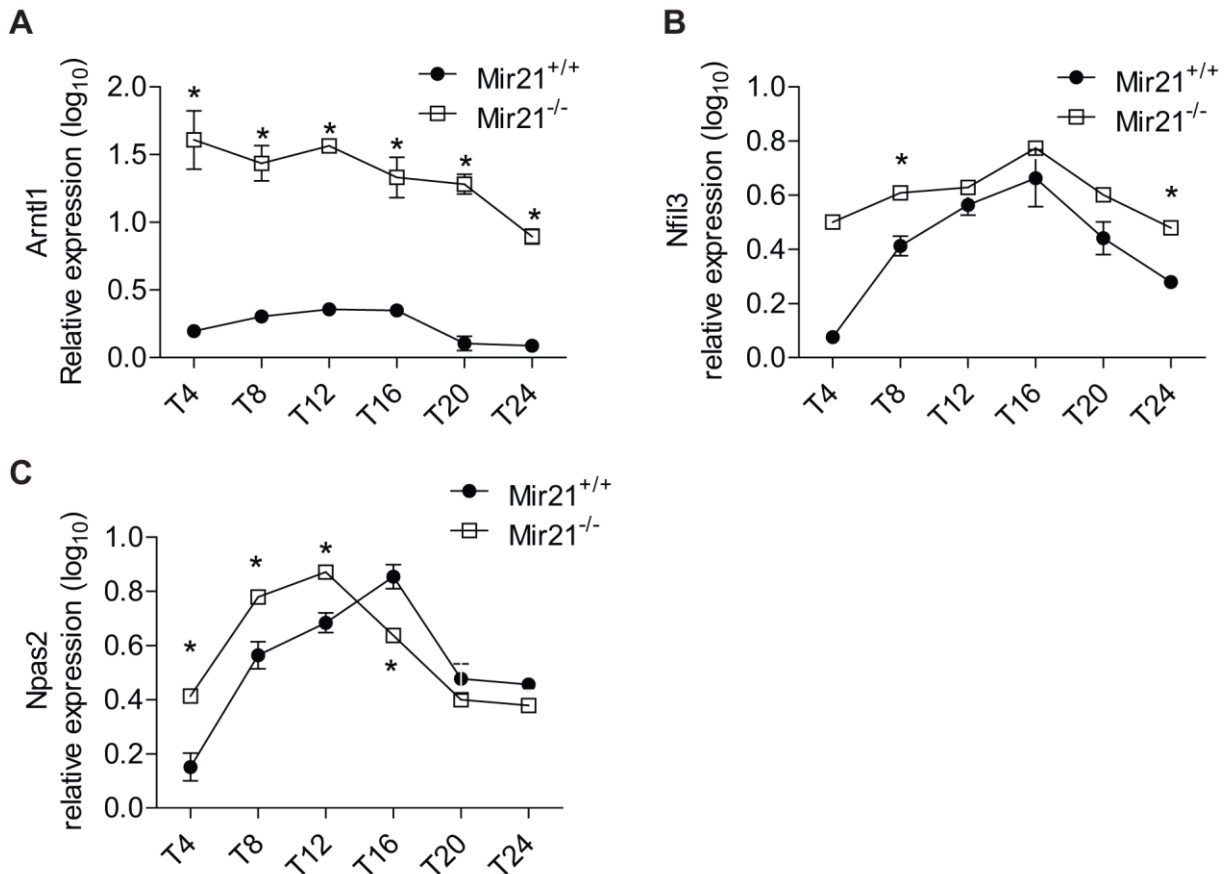


Figure 23: Expression of upstream circadian clock genes in BMDMs. Relative expression levels of *Arntl1*, *Nfil3* and *Npas2* in synchronised BMDMs isolated from *Mir21*^{+/+}*Apoe*^{-/-} mice and *Mir21*^{-/-}*Apoe*^{-/-} mice were quantified over a 24-hour period using qRT-PCR after synchronisation. The expression of *Arntl1* in *Mir21*^{-/-}*Apoe*^{-/-} as compared to *Mir21*^{+/+}*Apoe*^{-/-} BMDMs is shown in **A**. The expression pattern of *Nfil3* and *Npas2* in *Mir21*^{-/-}*Apoe*^{-/-} BMDMs and *Mir21*^{+/+}*Apoe*^{-/-} BMDMs are shown in **B** and **C**. n = 2-4 samples per group. * $P < 0.05$. P values were obtained using a two-way ANOVA. The means \pm s.e.m. are shown.

To further examine the effect of *Mir21* knock-out on the downstream circadian clock genes, the expression levels of *Per 2* and *Per 3* were quantified in synchronised BMDMs isolated from *Mir21*^{+/+}*Apoe*^{-/-} and *Mir21*^{-/-}*Apoe*^{-/-} mice over 24 hours. The expression of *Per 2* was significantly higher in *Mir21*^{-/-}*Apoe*^{-/-} compared to *Mir21*^{+/+}*Apoe*^{-/-} BMDMs at T4 but also lower at T12 (Figure 24A), indicating a shift in the phase of its expression. *Per3* expression in *Mir21*^{-/-}*Apoe*^{-/-} BMDMs were significantly lower at T8 and T12 but higher at T4 compared to *Mir21*^{+/+}*Apoe*^{-/-} BMDMs (Figure 24B). This shows a shift in the phase of *Per3* and lowered amplitude from T8 to T24. These results suggest that BM deficiency of *Mir21* leads to changes and shifts in the expression of *Per2* and *Per3* genes.

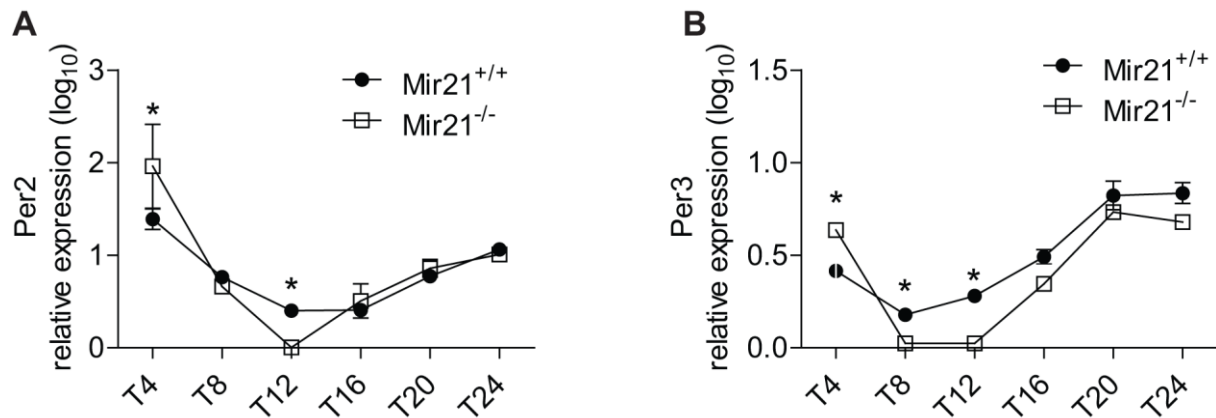


Figure 24: Expression of downstream circadian genes in BMDMs. Relative expression level of *Per2*, and *Per3* in synchronised BMDMs isolated from *Mir21*^{+/+}*ApoE*^{-/-} mice and *Mir21*^{-/-}*ApoE*^{-/-} mice were quantified using qRT-PCR. The expression level of *Per 2* in *Mir21*^{-/-}*ApoE*^{-/-} BMDMs and *Mir21*^{+/+}*ApoE*^{-/-} BMDMs over 24 hours is shown in **A**. *Per 3* (**B**) expression shows reduced amplitude from T4 in *Mir21*^{-/-}*ApoE*^{-/-} compared to *Mir21*^{+/+}*ApoE*^{-/-} BMDMs. n = 2-4 samples per group for each time point. * $P < 0.05$. P values were obtained using a two-way ANOVA. The means \pm s.e.m. are shown.

3.3.3 Circadian expression of *Xaf1* and *Mbl2*

To study the circadian role of *Mir21* expression in the regulation of *Xaf1* and *Mbl2* and in macrophage apoptosis during atherosclerosis, the expression of *Xaf1* and *Mbl2* in BMDM over 24 hours after synchronisation were assessed in BMDMs obtained from *Mir21*^{+/+}*ApoE*^{-/-} mice. *Xaf1* showed a circadian rhythmic expression in contrast to *Mbl2* expression (Figure 25).

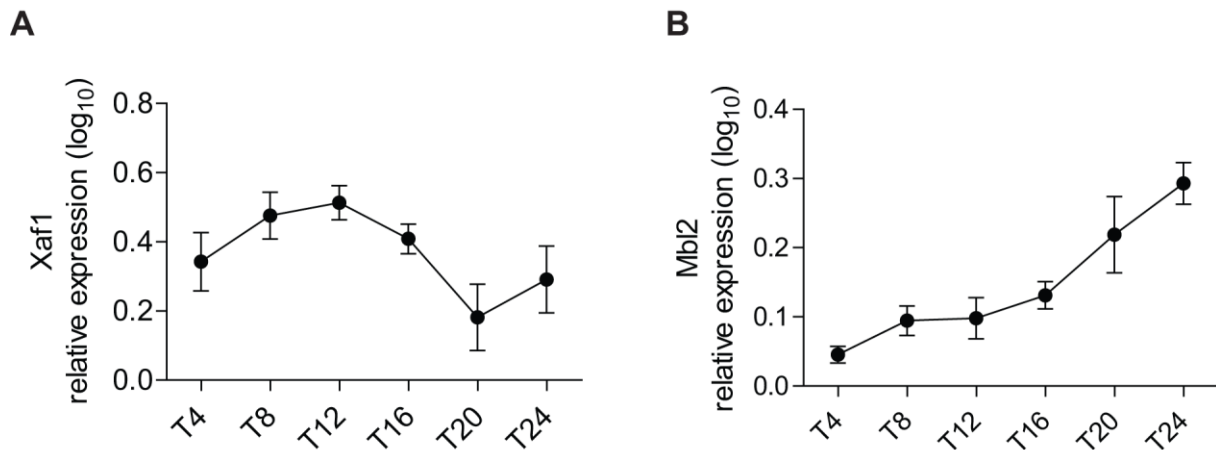


Figure 25: Circadian expression of *Xaf1* and *Mbl2* in BMDMs. Relative expression level of *Xaf1* and *Mbl2* were quantified in BMDMs over a 24-hour period after synchronisation using qRT-PCR. BM cells isolated from *Mir21*^{+/+}*Apoe*^{-/-} mice were cultured for 7 days and synchronised and qRT-PCR was performed by harvesting samples every 4 hours over a period of 24 hours. The circadian expression of *Xaf1* (A) and *Mbl2* (B) are shown.

3.3.4 Effect of *miR-21-3p* and *miR-21-5p* on circadian clock genes in macrophages

To study the individual roles played by the different strands of *Mir21* in the circadian rhythm signalling, apoptosis and efferocytosis, experiments to determine which specific strand targets or regulates circadian clock genes, *Xaf1* and *Mbl2* were conducted. The relative expression levels of *Arntl1*, *Nfil3*, *Npas2*, *Xaf1* and *Mbl2* were quantified in *Mir21*^{-/-}*Apoe*^{-/-} BMDMs after synchronising and transfecting the cells with either *miR-21-3p* or *miR-21-5p* mimic. BMDMs were isolated from *Mir21*^{-/-}*Apoe*^{-/-} mice and cultured for 6 days and transfected with the mimic, the cells were then synchronised 24 hours after transfection and qRT-PCR performed 8 hours after synchronisation. Increasing the expression of *miR-21-5p* by transfecting *Mir21*^{-/-}*Apoe*^{-/-} BMDMs with mimic led to the downregulation of *Mbl2* but not *Arntl1*, *Nfil3*, *Npas2* and *Xaf1* compared to cells transfected with control mimic (Figure 26). The down regulation of *Mbl2* upon increased expression of *miR-21-5p* indicates that *miR-21-5p* may regulate *Mbl2* expression in macrophages but not the clock genes *Arntl1*, *Nfil3* and *Npas2* as well as *Xaf1*.

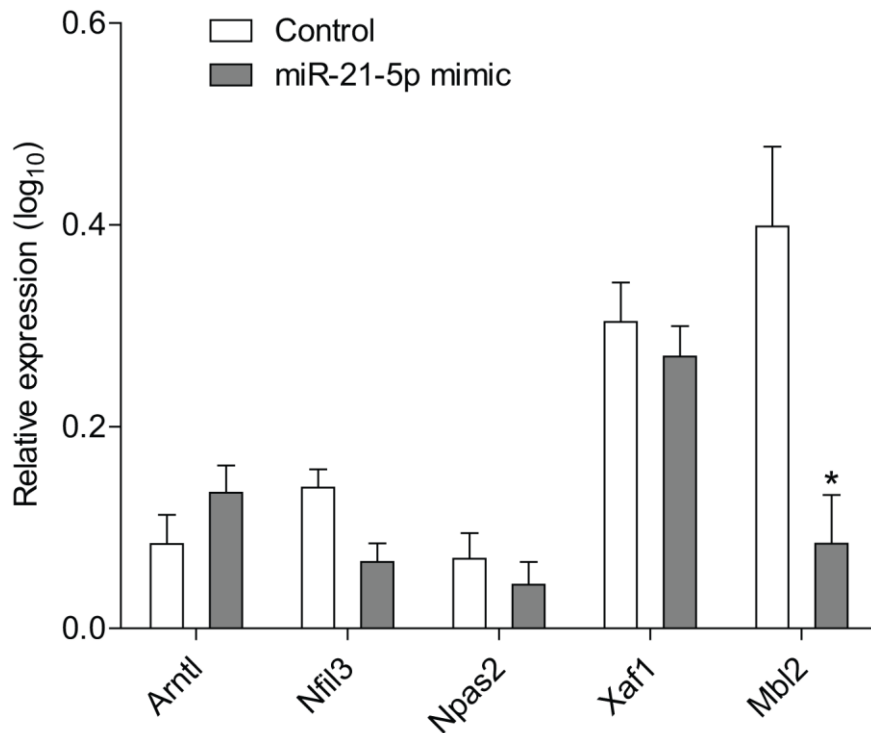


Figure 26: Expression of circadian clock genes, *Xaf1* and *Mbl2* in *Mir21*^{-/-} *ApoE*^{-/-} BMDMs after *miR-21-5p* mimic transfection. BMDMs from *Mir21*^{-/-} *ApoE*^{-/-} mice were cultured till confluent at day 6 in macrophage differentiation medium and then transfected with either *miR-21-5p* mimic or control mimic. The cells were then synchronised 24 hours after transfection and samples harvested 8 hours after synchronisation. The expression of clock genes, *Xaf1* and *Mbl2* were quantified by qRT-PCR. n = 3-4 samples per group. * $P < 0.05$. P values were obtained using a two-way ANOVA. The means \pm s.e.m. are shown.

The upregulation of *miR-21-3p* in *Mir21*^{-/-} *ApoE*^{-/-} BMDMs downregulated *Nfil3*, *Npas2* and *Xaf1* after transfection with the mimic compared to BMDMs transfected with control mimic (Figure 27). There were no significant differences in expression level of *Arntl1* and *Mbl2* in *Mir21*^{-/-} *ApoE*^{-/-} BMDMs transfected with *miR-21-3p* mimic compared to control mimic, suggesting that increased expression of *miR-21-3p* in macrophages may lead to downregulation of circadian clock genes *Nfil3* and *Npas2* as well as the downregulation of pro-apoptotic gene *Xaf1*. Taken together, these results suggest that *miR-21-3p* may regulate the clock genes as well as *Xaf1* in macrophages whereas *miR-21-5p* regulates *Mbl2* expression.

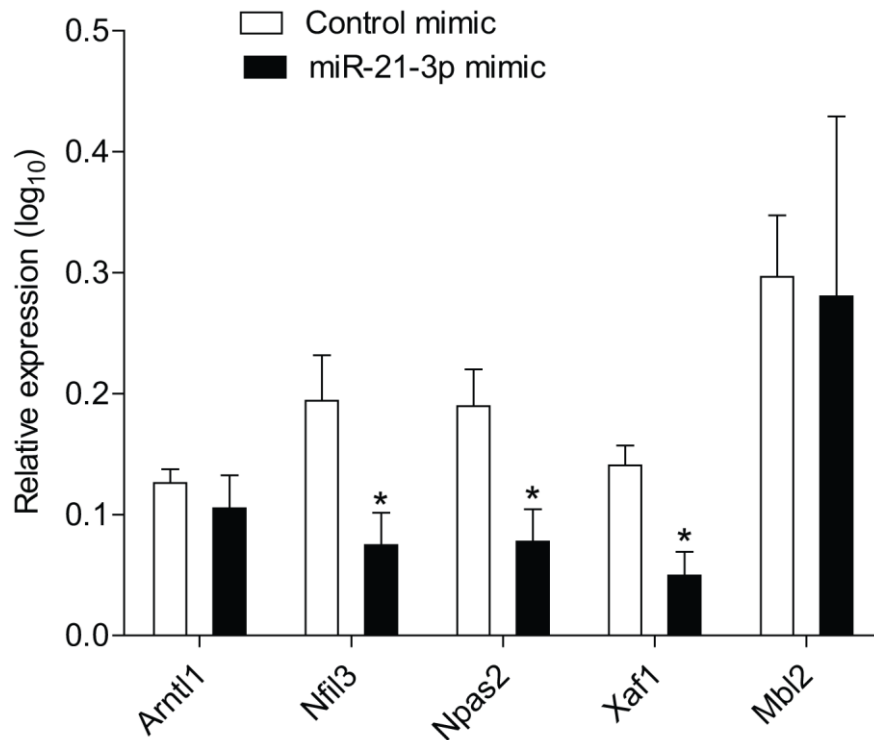


Figure 27: Expression of circadian clock genes, *Xaf1* and *Mbl2* in *Mir21*^{-/-} *ApoE*^{-/-} BMDMs after *miR-21-3p* mimic transfection. BM cells were isolated from *Mir21*^{-/-} *ApoE*^{-/-} mice and cultured in macrophage differentiation medium for 6 days and then transfected with either *miR-21-3p* mimic or control mimic. The cells were then synchronised 24 hours after transfection and samples harvested 8 hours after synchronisation and the expression of genes quantified by qRT-PCR. n = 3-4 samples per group. * $P < 0.05$. P values were obtained using a two-way ANOVA. The means \pm s.e.m. are shown.

To determine whether the regulation of the clock genes by *miR-21-3p*, occurs through direct targeting, microRNA target prediction tool RNAhybrid was used to predict possible binding sites for *miR-21-3p* in the 3' UTR of clock genes *Arntl1*, *Nfil3* and *Npas2*¹⁴⁹. The target prediction analysis showed binding sites for *miR-21-3p* seed sequence in the 3' UTR of *Arntl1*, *Nfil3* and *Npas2* in mice and in humans (Figure 28), but no possible binding sites for *Xaf1* was predicted by the tool. The presence of possible binding sites suggests that *miR-21-3p* may directly target *Arntl1*, *Nfil3* and *Npas2* but may regulate the expression of *Xaf1* indirectly.

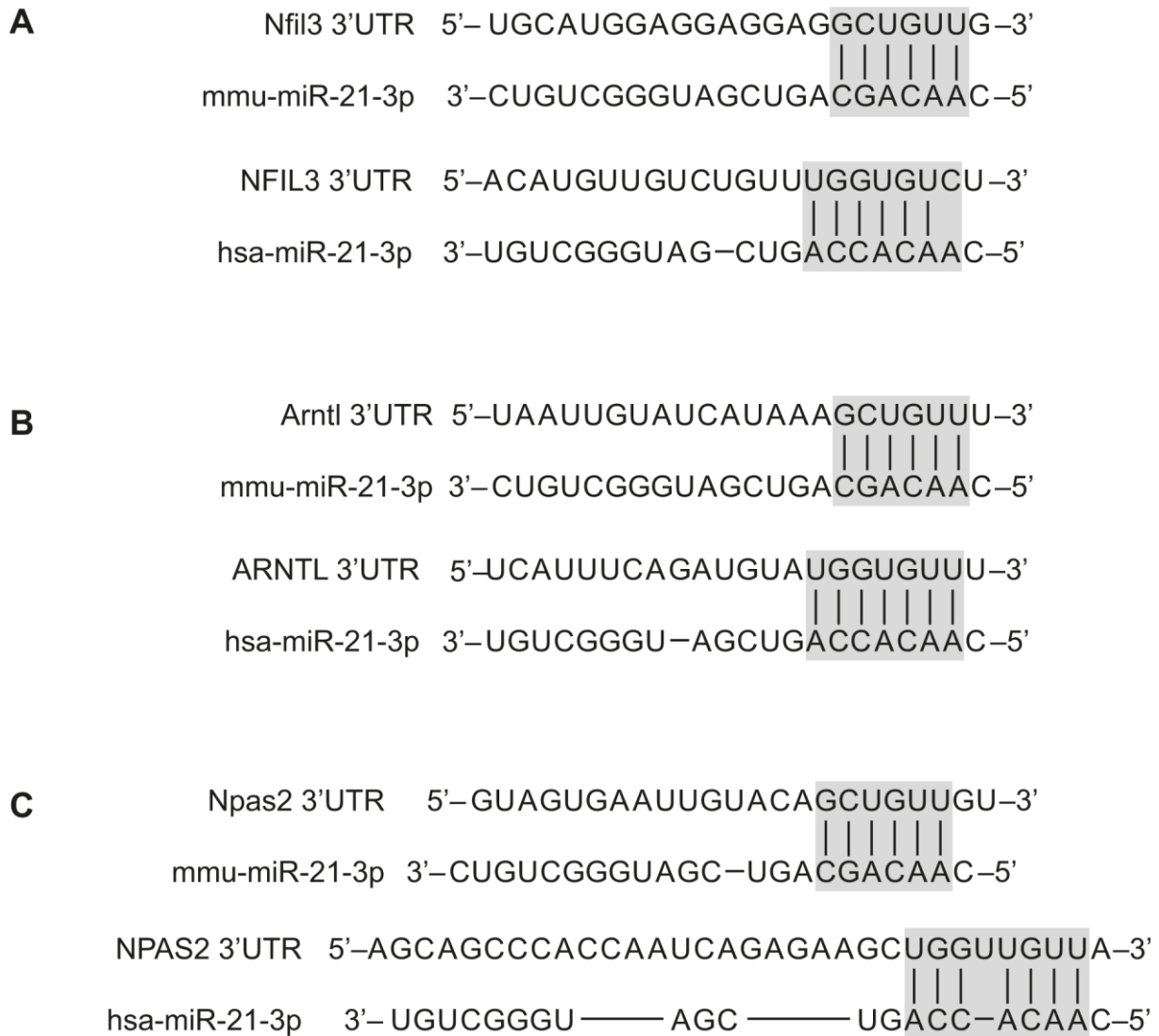


Figure 28: Predicted binding sites for *miR-21-3p*. Predicted binding sites for *miR-21-3p* analysis were performed for human and mouse *Arntl1*, *Nfil3* and *Npas2* using RNAhybrid (<http://bibiserv.techfak.uni-bielefeld.de/rnahybrid/>), ref # 142.

RNAhybrid target sites prediction tool was also used to search for possible binding sites for *miR-21-5p* in the 3'UTR of *Mbl2*. A possible binding site was predicted in mice but not in humans (Figure 29).

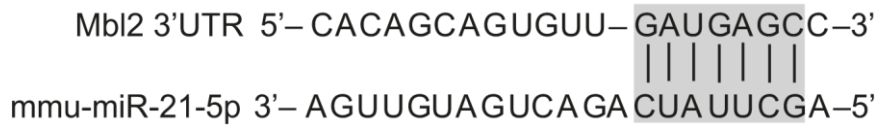


Figure 29: Predicted binding sites for miR-21-5p. Prediction of binding sites in the 3'UTR of human and mouse *Mbl2* for *miR-21-5p* was performed using RNAhybrid (<http://bibiserv.techfak.uni-bielefeld.de/rnahybrid/>), ref # 142.

To further study the regulation of *Arntl*, *Nfil3*, *Npas2* and *Xaf1* by *miR-21-3p*, an immunoprecipitation assay was performed using BMDMs isolated from *ApoE*^{-/-} mice that has its Argonaute protein (AGO2) epitope tagged with MYC. After culturing the cells, they were transfected with *miR-21-3p* mimic using lipofectamin and the cells lysed 24 hours after transfection. The tagged AGO2 protein was then precipitated using antibody anti-C-MYC conjugated to magnetic beads as previously shown by He *et al* (2012)¹⁵⁰. The enrichment of *Arntl*, *Nfil3*, *Npas2* and *Xaf1* was then assessed by qRT-PCR. *Nfil3* and *Xaf1* were enriched in the immunoprecipitated samples (Figure 29), suggesting that *miR-21-3p* may directly target *Nfil3* and *Xaf1* in macrophages.

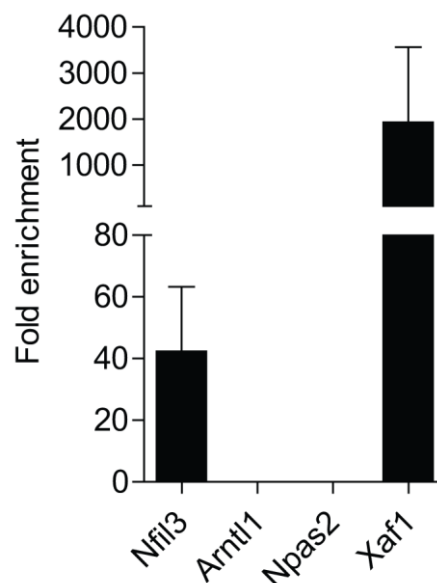


Figure 30: Enrichment of miR-21-3p and its targets. BMDMs were cultured from *ApoE*^{-/-} mice with Argonaute protein (AGO2) epitope tagged with MYC and GFP. The cells were then transfected with *miR-21-3p* mimic using lipofectamin. After 24 hours, cells were lysed and incubated with magnetic beads conjugated with C-MYC antibody. The immunoprecipitated RNA-protein complex was dissociated from the beads and the enrichment of targets assessed using qRT-PCR.

4 Discussion

4.1 Role of *Mir21* in macrophages and atherosclerosis

4.1.1 *miR-21* and macrophage polarization

MicroRNAs play crucial roles in the innate immune response and are dysfunctionally regulated in unresolved inflammation¹⁵¹. In M1 macrophages, microRNAs such as *miR-155-5p* and *miR-147-5p*, *miR-181a*, *miR-204-5p* and *miR-451* are significantly upregulated, whereas *let-7c*, *miR-27a* and *miR-222* are upregulated in M2 macrophages^{74, 152-154}, suggesting a functional role for different microRNAs in macrophage polarization. Moreover, colony-stimulating factor 1 receptor (CSF-1R) suppresses M1 polarization but enhances M2 polarization by inducing the expression of *miR-21-5p*¹⁵⁵. However, the expression level of both *miR-21-5p* and *miR-21-3p* was not differentially regulated in macrophages after stimulation with either LPS/IFN- γ (M1) or IL-4 (M2), suggesting that both strands of *Mir21* may not play roles in the polarization of macrophages. In previous reports, LPS stimulation upregulated *miR-21-5p* expression in mouse macrophages, but not in human macrophages⁹³. The difference in the results could be due to the fact that macrophages in the current study were stimulated with LPS and IFN- γ as compared to using only LPS. Another reason may be because different cells were used in this study as compared to the earlier report.

To study the role of *miR-21-3p* and *miR-21-5p* in macrophage polarization, the effect of *Mir21* gene knockout on M1 and M2 marker gene expression was determined. In contrast to previous studies, which showed that *miR-21-5p* expression skewed the macrophage phenotype towards the M1 subtype^{93, 156}, in the current study deletion of the *Mir21* gene slightly increased the mRNA expression of IL-1 β and IL-6 after LPS/IFN-g and IL-4 treatment respectively. The difference between the results of the current study and the previous reports, which mainly studied the role of *miR-21-5p*, may be partly explained by the use of *Mir21* knock-out macrophages which lack the expression of both *miR-21-5p* and *miR-21-3p* in the current study⁹³. Moreover, *Mir21* expression also suppressed *Il-6* and enhanced *Il-10* expression in other studies^{93, 157}, whereas in yet another study *Mir21* expression inhibited both *Il-10* and *Il-6*¹⁵⁶. The different effects on *Il-6* in the various studies can be attributed to the cell types used; while the current study used mouse BMDMs, Wang *et al*¹⁵⁶ used thioglycollate induced peritoneal macrophages. *Il-6* is a pro-inflammatory cytokine expressed in human plaques¹⁵⁸ and promotes atherosclerosis in aged mice but prevents atherosclerosis progression in young mice¹⁵⁹⁻¹⁶¹. In the current study, however, the role of *Il-6* in atherosclerosis *in vivo* could not be determined, because it was not significantly upregulated in the microarray performed with aortic arch lesions of mice. Overall, *Mir21* gene expression did not play a role in macrophage polarization, even though there was a mild effect of *Mir21* gene expression on the level of the two cytokines.

Mir-33a and *Mir-33b* are upregulated in response to hypercholesterolemia¹⁶² suggesting that the expression of microRNAs could be regulated by the production of oxLDL which is a

feature of dyslipidemia¹⁶³. *Mir-21-3p* and *miR-21-5p* were significantly upregulated in BMDMs after being exposed to oxLDL and this is in line with a previous study that *miR-21-5p* is upregulated in human mammary epithelial cells in response to oxLDL¹⁶³.

4.1.2 The role of *Mir21* on atherosclerosis

Mir-21 is significantly upregulated in disease states like cancer^{164, 165} and atherosclerotic lesions¹⁶⁶ and together with *miR-155* are among a small number of selectively upregulated microRNAs in atherosclerotic lesions¹⁶⁷. *Mir-155* enhances atherosclerosis by enhancing pro-inflammatory responses in leukocytes¹⁶⁷ and the upregulation of *miR-21* in several cells, enhances atherosclerosis related processes^{88, 89} indicating that microRNAs may contribute to atherosclerotic related processes in a cell specific manner. *Mir21* expression in hematopoietic cells increased atherosclerotic lesion size in the aortic sinus as well as in the thoraco-abdominal aorta in *Apoe*^{-/-} mice, suggesting that *Mir21* expression in hematopoietic cells may be pro-atherogenic. In situ PCR combined with MAC2 immunostaining showed *miR-21-5p* was expressed by lesional macrophages as well as luminal cells that may likely be endothelial cells and *miR-21-3p* expression was localized only with MAC2 positive cells. This indicates that *miR-21-5p* may be upregulated in macrophages and possibly endothelial cells during atherosclerosis, whereas *miR-21-3p* may be expressed only in macrophages. The expression of both strands of *Mir21* in lesional macrophages suggests that the effect of *Mir21* gene expression in hematopoietic cells on lesion formation maybe attributable to the role played by the two strands in macrophages as against other cells of hematopoietic origin. The differential expression pattern also suggests that the role each strand plays during atherogenesis may be different. The *miR-21-5p* strand may modulate pathways in macrophages as well as in endothelial cells, whereas *miR-21-3p* may modulate pathways only in lesional macrophages. Moreover, these results taken together suggest that both strands may occur as a functional *miR-21-5p/miR-21-3p* pair in macrophages during atherogenesis.

Deleting *Mir21* from hematopoietic cells as well from other vascular cells reduced lesion area in thoraco-abdominal aorta but not in the aortic sinus. The reduction of lesion formation in thoraco-abdominal aorta and increased lesion area in the aortic sinus may be because lesions in the aortic sinus are more advanced^{172, 173} and also suggest that *Mir21* gene expression may have different effect in macrophages and other vascular cells like endothelial and smooth muscle cells. *Mir21* expression in macrophages maybe detrimental in atherosclerosis but in endothelial cells, it may be beneficial depending on the part of the vasculature and the stage of the lesions. Advanced lesion formation occurs through enhanced macrophage number and altered function whereas early lesions may develop due to changes in smooth muscle and endothelial cells¹⁷⁴. The pathogenic conditions that exist in the aortic root may be different from the whole aorta¹⁷⁵ and therefore the stage and extent of lesion development may be different. The results from this study suggest that the role of *Mir21* gene expression in endothelial and smooth muscle cells during atherosclerosis may depend on the part of the aorta, pathogenic factors that exist at that part and possibly the stage of atherosclerosis. The

effect of gene expression and cellular contributions to the different stages of lesion development in the aortic root compared to the whole aorta may require further studies. The differential expression of *Mir21* strands in macrophages and endothelial cells during atherosclerosis may also explain the different effect of *Mir21* gene expression in the different cells. In endothelial cells In situ PCR showed only the *miR-21-5p* expression, whereas *miR-21-5p* and *miR-21-3p* were both expressed in lesional macrophages. Taking these results together, the expression of both strands in macrophages may enhance atherosclerosis whereas the expression of *miR-21-5p* in endothelial cells may be beneficial and this is in line with a previous report in which the expression of *Mir21* in endothelial cells reduced endothelial dysfunction, an atherosclerosis related process in vitro⁹².

4.1.3 The mechanism of *Mir21* in macrophages on atherosclerosis

4.1.3.1 Effect on lesion composition

Although macrophages play a central role in atherosclerosis, other myeloid cells including neutrophils and dendritic cells are found in lesions and contribute to specific processes during atherogenesis¹⁸⁴. Neutrophils are detected in human and murine atherosclerotic lesions suggesting a functional role during lesion formation¹⁸⁵. Circulating neutrophils are associated with the occurrence of cardiovascular events in humans¹⁸⁶ and lesion size in mice¹⁸⁷. Neutrophil recruitment precedes the infiltration of monocytes into lesions and depletion of circulating neutrophils lead to reduced diet-induced lesion formation and advancement^{188, 189}. Neutrophils are recruited in response to endothelial dysfunction and in turn secrete granule proteins that aggravate endothelial dysfunction and recruit monocytes as well as enhance inflammatory polarization of macrophages¹⁸⁵. Neutrophils respond transiently to inflammation and therefore apoptosis play a crucial role in the regulation of their function during immune response^{188, 190}. The anti-apoptotic role of *miR-21* expression¹⁹¹ could suppress apoptosis and depletion of neutrophils thereby enhancing macrophage accumulation and lesion development. Even though the contribution of neutrophils and other hematopoietic cells to atherogenesis is possible, in situ PCR showed the expression of *miR-21* strands co-localized mainly in lesional macrophages suggesting that the observed effects may be due to the effect of *miR-21* in macrophages. Atherosclerosis was enhanced due to reduced apoptosis of lesional macrophages and increased necrotic core formation in the aortic sinus. Reduced macrophage apoptosis also led to increased lesional macrophage accumulation thereby contributing to increased lesion sizes¹⁷⁶⁻¹⁷⁸. In the early atherosclerosis, monocytes derived from BM progenitor cells infiltrate the lesion and differentiate into macrophages through the function of macrophage colony-stimulating factor (M-CSF)^{39, 179, 180}. Evidence on the sources of increased lesional macrophage number has been a contested subject. Though earlier studies suggested that this was mainly due to infiltration of circulating monocytes^{181, 182}, it is now known that increased lesional macrophage number occurs largely due to increased proliferation of recruited cells³⁸ and this study supports this finding that reduced apoptosis

and removal of lesional macrophages contributes to increased lesion formation. This also suggests that *Mir21* expression in hematopoietic cells may regulate macrophage accumulation in lesions by reducing apoptosis. The anti-apoptotic function of *Mir21* expression in macrophages during atherosclerosis in the current study is in line with previous studies and occurs in vascular smooth muscle cells, endothelial cells and in cancer cells as well^{89, 90, 183}.

The normal arterial intima is principally composed of endothelial cells and smooth muscle cells with collagen playing a role in the attachment of the endothelial cells to the subendothelial matrix¹⁹². During atherosclerosis, the morphology and cellular component of the intima is significantly altered and each stage is distinctively characterised by specific cellular content¹⁹³. In early stages of atherosclerosis, smooth muscle cells migrate from the media into the intima and change from their contractile phenotype and begin proliferating¹⁹⁴ resulting in increased deposition of smooth muscle cells¹⁹⁵. In the advanced stage, smooth muscle cells secrete and deposit collagen^{196, 197}. *Mir21* gene expression in hematopoietic cells did not have any significant effect on the smooth muscle and collagen content of aortic root lesions. The *Mir21* gene was knocked out only in BM cells and hence was expressed in other vascular cells as smooth muscle cells, this may account for the similar levels of smooth muscle cell content suggesting that processes regulated by *Mir21* expression were not differentially regulated.

T lymphocytes are present in human atherosclerotic lesions¹⁹⁸⁻²⁰⁰ as well as in murine atherosclerotic lesions²⁰¹, pointing to a role of the adaptive immune cells in atherogenesis. In the current study, T cell population in lesions was assessed by quantifying CD3 positive cells. The CD3 complex consists of cell surface molecules that are associated with the T cell receptor (TCR) and involved in the assembly of TCR and activation of T cells²⁰². Generally, T cell population in the lesions was very low with the average cell percentage below 1%. In contrast to previous reports, in which increased T cell number in lesions was associated with increased lesion formation, *Mir21* expression in hematopoietic cells was associated with decreased T cell population but increased atherosclerosis^{200, 203}. Moreover, in both reports by Hansson *et al*²⁰³ and Emeson *et al*²⁰⁰, T cells and macrophage accumulation were associated but in the current study, reduced macrophage accumulation was associated with increased T cell number. Different T cell subsets may play opposing roles in atherosclerosis and during atherogenesis a dynamic equilibrium may exist between the various subsets¹⁸⁹, with subtypes like CD4⁺, CD8⁺ and T_H1 driving the progression of atherosclerosis by increasing, whereas T_{reg} cells and T_H2 cells suppress atherosclerosis^{32, 177, 189, 204, 205}. The current study did not examine the specific subtype of T cell located within the lesions, but the data taken together indicates the T cell subtype maybe different from the previous reports discussed. *Mir21* expression in hematopoietic cells may inhibit recruitment of T_{reg} cells and T_H2 cells. *Mir21* expression level in T cells is highly upregulated upon activation of CD4⁺ cells and suppresses apoptosis of activated T cells thereby enhancing inflammation²⁰⁶. Moreover, *miR-21* is differentially expressed between memory cells compared to naive cells in a microRNA expression profile between naive and central memory CD4⁺ and CD8⁺ cells²⁰⁷ suggesting that

Mir21 expression may either have resulted in the increased CD4⁺, CD8⁺ and T_H1 subtypes or suppressed T_{reg} and T_H2 subtypes.

The uptake of lipids by macrophage receptor CD36 leads to the formation of foam cells, a characteristic feature in early atherosclerosis²⁰⁸⁻²¹⁰. The formation of foam cells is due to the dysregulation of lipid metabolism and defective cholesterol efflux²¹¹ indicating that factors that affect lipid accumulation and metabolism could increase the development of atherosclerosis. *Mir21* gene expression in macrophages had no effect on the expression of Adipose differentiation-related protein (ADFP) or Perilipin 2 (PLIN2) a lipid droplet-associated protein that regulates lipid turnover and is expressed in macrophages²¹²⁻²¹⁴, in contrast to previous report that ADFP is highly expressed in advanced lesions²¹⁵. The result of the current study suggests that *Mir21* expression in macrophages does not affect lipid uptake.

4.1.3.2 Macrophage *Mir21* expression and apoptosis

Even though atherosclerosis has been looked at as a condition arising from chronic inflammatory response, emerging evidence points more to the problem of failed resolution of inflammation and inability of immune cells to switch from pro-inflammatory to a resolution state¹¹. Resolution of inflammation involves the reduction of immune cell recruitment, removal of inflammatory cells through apoptosis and phagocytic clearance and a switch from M1 to M2 macrophage phenotype²¹⁶. Macrophage apoptosis is critical in clearance and resolution of inflammation²¹⁷ and occurs in both early and advanced lesions²¹⁸. However, the effects of macrophage apoptosis are different at each stage¹⁷¹. In early lesions when a necrotic core has not yet developed, increased macrophage apoptosis is beneficial and inhibits lesion development^{44, 45}. In accordance with previous studies that showed anti-apoptotic role of *Mir21* expression^{219, 220}, apoptosis of lesional macrophages was inhibited by the expression of *Mir21*.

In accordance with these observations, *Xaf1* was upregulated in microarray analysis of lesions from mice in which *Mir21* gene was knocked out in hematopoietic cells, suggesting that *Mir21* expression in macrophages reduced *Xaf1* expression. X-linked inhibitor of apoptosis (XIAP) associated factor 1 (XAF1) is a pro-apoptotic nuclear protein that interacts and sequesters XIAP thereby inhibiting the anti-caspase activity of XIAP¹³⁴ and is downregulated in several cancer cell lines²²¹⁻²²⁴. Interestingly, *Mir21* is the single gene that is upregulated in all solid cancer tumours¹⁶⁵ suggesting that the increased expression of *Mir21* downregulates *Xaf1* and hence decreases apoptosis. Put together, these data suggest that *Mir21* expression may regulate macrophage apoptosis through targeting of *Xaf1*. Immunohistochemistry showed decreased expression of XAF1 in lesional macrophages of mice expressing *Mir21* gene in hematopoietic cells, suggesting that downregulation of the mRNA also reduced protein expression. Reduced macrophage apoptosis resulted in increased macrophage accumulation in the aortic root and lesion formation in accordance with previous report, that prolonged survival of macrophages lead to enhanced lesion development²²⁵.

Taken together, these data suggest that *Mir21* mediated regulation of *Xaf1* and apoptosis, increases macrophage survival and is pro-atherogenic.

4.1.3.3 Macrophage *Mir21* expression and efferocytosis

The *Mir21* mediated suppression of macrophage apoptosis, coupled with increased lesional macrophage number and increased necrotic core formation, suggest a defective efferocytosis in lesions. Apoptotic lesional macrophages, must be quickly removed by efferocytosis else will trigger secondary necrosis and the development of a necrotic core which is characteristic of advanced lesions²²⁶. Even though previous studies show that efferocytosis declines during later stages of atherosclerosis, leading to increased necrotic core formation and making macrophage apoptosis detrimental in atherosclerosis^{42, 227-229}, in the current study where lesions were examined after 12 weeks of HFD, efferocytosis may have been defective resulting in increased necrotic core area. Efferocytosis occurs through the recognition of phagocytic receptors and molecules such as tyrosine kinase *Mertk*, *Fas*, transglutaminase-2, complement protein *C1q*, and *lactadherin*²³⁰⁻²³². *MiR-155* inhibits efferocytosis in advanced lesions by targeting B-cell lymphoma 6 (*Bcl6*) and the deficiency of *miR-155* reduces necrotic core formation and deposition of apoptotic cell bodies²³³ and this supports the results from the current study that *Mir21* expression may target pathways involving the expression or signaling of phagocytic receptors and reduce efferocytosis.

Interestingly, results from microarray analysis also showed significant upregulation of *Mbl2* in atherosclerotic lesions when *Mir21* gene was knocked out in hematopoietic cells. Mannose binding lectin (MBL) is a Ca^{2+} -dependent lectin that is known to opsonize pathogens and activate the complement system by recognizing specific carbohydrate molecules and binding to them²³⁴ as well as promotes the phagocytosis and clearance of pathogens during an inflammatory response¹⁴⁵. In line with the current study, decreased expression of MBL which is associated with early onset and progression of atherosclerosis in humans^{143-145, 235-237} was associated with increased necrotic core area and lesion size. Expression of MBL in early atherogenesis may be beneficial by increasing the rapid phagocytosis and clearance of apoptotic cells thereby limiting necrotic core formation as well as inflammation^{142, 238}. Taken together, these data suggest that *Mir21* deficiency in hematopoietic cells may reduce atherosclerosis by increasing apoptosis of lesional macrophages through elevated *Xaf1* and efferocytosis through upregulation of *Mbl2* in lesions. Targeting macrophage apoptosis, and efferocytosis therefore may present a therapeutic potential for suppressing atherosclerosis^{225, 239-245}.

MicroRNAs exhibit tissue-specific and cell-specific expression pattern²⁴⁸, and this pattern can be differentially regulated by inflammation, laminar shear stress, hypoxia and cardiovascular risk factors⁵⁹. The tissue and cell-specific expression leads to microRNAs regulating different molecular pathways in different cells leading to varying functions and contributions to disease states in different cells⁷. In human plaques *miR-21-3p* and *miR-21-5p* are differentially expressed in different artery beds during atherosclerosis⁷⁰. Even though recent studies suggest

that relative miR-5p/miR-3p (microRNA/microRNA*) expression between various tissues are conserved²⁴⁹, *miR-21-3p* is selectively upregulated in macrophages in response to oxidative stress⁹⁹, whereas *miR-21-5p* is upregulated in response to LPS stimulation⁹³. This indicates that *miR-21-3p* and *miR-21-5p* may be regulated by different stimuli in different cells and hence play different roles in certain pathways.

4.2 Regulation of the macrophage clock by *Mir21* in atherosclerosis

4.2.1 *Mir-21* expression and circadian rhythm

In *ApoE*^{-/-} mice, hyperlipidemia disrupts the circadian rhythm and affects apoptosis-related genes thereby contributing to the process of lesion development^{255, 256} and in the current study, both strands of the *Mir21* gene were upregulated in response to oxLDL suggesting that uptake of oxLDL disrupts the circadian rhythm in macrophages by upregulating *Mir21*. The mRNA expression profile showed differential regulation of key circadian clock genes in atherosclerotic lesions after knock-out of *Mir21* gene from BM cells. The upregulation of upstream regulators of the circadian rhythm *Arntl*, *Npas2* and *Nfil3* and downregulation of *Per1*, *Per2*, *Per3*, *Nr1d1*, *Nr1d2*, *Chrono* and *Dbp* suggests that *Mir21* expression regulates the circadian rhythm of BM-derived cells and this plays a critical role in atherosclerosis. In wildtype hematopoietic cells, *Mir21* targets *Arntl*, *Nfil3* and *Npas2* and hence dampening or inhibiting the circadian pathways. The downregulation of the circadian rhythm may lead to dysregulation of pathways like the metabolism, inflammation, apoptosis and survival of hematopoietic cells and thereby enhancing atherosclerosis. Also, a possible mechanism may be the loss of circadian control of other downstream genes and thus enhance atherosclerosis. In knock-out mice, the circadian rhythm is then restored and therefore reduces the risk of lesion development. The result of the current study is in line with previous report that knock-down of *Rev-erba* (*Nr1d1*) in BM cells of *Ldlr*^{-/-} mice increases atherosclerotic lesions in the aorta with associated increase in M1 macrophages suggesting that disrupted circadian rhythm in macrophages leads to increased inflammation and atherosclerosis¹³¹. Moreover, human plaque-derived VSMCs exhibit different circadian oscillation from that of normal carotid VSMCs¹²⁹, suggesting that dysregulation of the circadian rhythm in cells enhances atherosclerosis.

Moreover, a pathway analysis using the IPA software showed that the circadian pathway was the most highly upregulated pathway in lesions from mice with BM knock-out of *Mir21*. Several other molecular pathways also upregulated are known to be associated with metabolism (TR/LXR activation, Stearate biosynthesis I, Triacylglycerol biosynthesis and Thyroid hormone metabolism II), cell proliferation and growth (Wnt/ β -catenin, basal cell carcinoma signalling, sonic hedgehog signalling and mTOR signalling) as well as with cell motility (axonal guidance signalling and Calcium transport). These pathways may play a

synergistic role with the circadian rhythm signalling in atherosclerosis or they may either be regulated by the circadian pathway or vice versa. Functional circadian pathway exists in splenic and peritoneal macrophages and play important roles in regulating various functions such as cytokine expression and phagocytosis in the macrophage^{132, 257, 258}. Immune response to LPS involves the targeting of *Bmal1* via *miR-155* upregulation and increased production of inflammatory cytokines and in mice lacking *Bmal1* in their myeloid cells, there is increased risk of sepsis upon LPS treatment²⁵⁹. The *Mir21* regulation of the circadian rhythm in myeloid cells may therefore enhance atherosclerosis by reducing apoptosis of macrophages.

More recent studies have shown that the rhythmic oscillations of certain microRNAs play crucial roles in certain disease conditions. One such study showed that rhythmic expression of *miR-96-5p* in mouse midbrain is involved in the regulation of Gluthathione, which plays a role in neurodegenerative diseases²⁶⁰. Studies that identified direct targeting of circadian clock genes show a direct interaction and regulation of the circadian rhythm by microRNAs. For example, *miR-124* and *Clock* has been identified as a microRNA-mRNA target pair that exist in human glioma cell lines and is involved in the regulation of NF- κ B activity and proliferation²⁶¹. Furthermore, *miR-185* controls the expression of *Cry1*, providing evidence for the involvement of microRNAs in fine tuning the circadian rhythm of cells²⁶².

4.2.2 Role of the clock genes in *miR-21-3p* and *5p* –regulated *Mbl2* and *Xaf1* expression

Mir-291 and *miR-132* exhibit circadian rhythm of expression in the SCN and act as down stream effectors of the pacemaker activity via post-transcriptional regulation of targets, indicating a possible role of microRNAs in modulating the circadian rhythm^{263, 264}. In retinal cells also, microRNAs play crucial roles in the circadian rhythm of the retina suggesting that an important aspect of entrainment and circadian control involves microRNAs²⁶⁵. In line with the previous reports, *miR-21-3p* in the current study showed a rhythmic expression over 24 hours whereas *miR-21-5p* did not. This suggests a role of *miR-21-3p* in regulating the circadian rhythm in macrophages but *miR-21-5p* may not be involved in circadian rhythm regulation. It is not clear in this study how the circadian pattern of *miR-21-3p* is regulated or controlled and although this could possibly be through rhythmic expression of regulators of *Mir21* transcription, further study is required to understand it better. The circadian expression *miR-21-3p* but not *miR-21-5p* suggests that this regulation may not be at the level of transcription but post-transcriptional. The expression of the clock genes in BMDMs isolated from *Mir21*^{-/-} mice (KO) was compared with that of *Mir21*^{+/+} mice (WT). The amplitude of *Bmal1* (*Arntl1*) was significantly higher at all time points in KO macrophages. *Nfil3* and *Npas2* expression level showed higher amplitude at certain time points as well as shift. The difference in amplitude and phase of *Arntl1*, *Nfil3* and *Npas2* expression suggest that *Mir21* expression regulates the circadian rhythm in macrophages. In the absence of *Mir21* gene in

macrophages, increased expression of clock genes leads to a more robust circadian pathway and this may affect down stream regulation of various cellular functions. Consequently, the expression level of downstream and negative regulator of the circadian pathway *Per2*, was reduced when the *Mir21* gene was knocked out. Moreover, the expression pattern of *Per2* had an opposite pattern to that of *Nfil3*, suggesting the regulation of *Per2* transcription by *Nfil3* and this result is in line with previous reports that *Per2* is regulated by *Nfil3*^{266, 267}.

Xaf1 and *Mbl2* which respectively enhance apoptosis and efferocytosis were highly expressed in atherosclerotic lesions after *Mir21* knock-out in hematopoietic cells along with the upregulation of clock genes. *Xaf1* showed a circadian expression over the 24-hour period in macrophages and a comparison with the expression pattern of *miR-21-3p* shows they both have opposite circadian patterns, suggesting that *miR-21-3p* and *Xaf1* may be a microRNA-mRNA target pair. The circadian oscillation of *Xaf1* may be regulated by the passenger strand thereby reducing apoptosis of macrophages during atherogenesis. *Mbl2* on the other hand did not show an oscillating pattern in macrophages. The expression level was continually increasing over the 24-hour period and that also coincided with the non-oscillatory expression pattern of *miR-21-5p* which was also consistently decreasing. Put together, these data suggest that both strands of *Mir21* contribute to atherosclerosis by reducing apoptosis via the circadian regulation of *Xaf1* by *miR-21-3p* and inhibiting phagocytic clearance by *miR-21-5p* targeting of *Mbl2*. A circadian microRNA-mRNA target pair is defined as one in which both elements show rhythmic expression and a sequence-based target relationship can be established²⁶⁸. Putative target binding sites of *miR-21-3p* and *miR-21-5p* in the 3'UTR of the circadian clock genes *Arntl1*, *Nfil3*, *Npas2* as well as *Xaf1* and *Mbl2* using the target prediction tool RNAhybrid showed no predicted binding sites for the *miR-21-5p* seed sequence for any of the clock genes in both mice and humans. Binding sites were predicted for the *miR-21-3p* seed sequence in the 3'UTR of *Arntl*, *Nfil3* and *Npas2* in both humans and mice suggesting that *miR-21-3p* may regulate the circadian rhythm pathway by targeting and inhibiting the expression of clock genes in macrophages during atherosclerosis.

Further in vitro studies showed that *miR-21-3p* expression led to decreased expression of *Nfil3* and *Npas2* but not *Arntl1*. MicroRNA targeting of mRNA has been shown not only to be dependent on the presence of binding sites but also varies based on the concentrations of the targets²⁶⁹. This may explain why even though binding sites were predicted for three mRNA, *miR-21-3p* upregulation in macrophages showed reduction of *Nfil3* and *Npas2* but not *Arntl1* expression compared to control samples. Taken together, these results suggest that *miR-21-3p* may regulate the expression of *Xaf1* through the circadian pathway in macrophages and hence apoptosis. Moreover, *miR-21-5p* expression in macrophages reduced the expression level of *Mbl2* and in accordance with this result, binding sites for the seed sequence were predicted for *Mbl2* in mice but not in humans. *Mbl2* expression in lesional macrophages may therefore be directly regulated by *miR-21-5p* during atherosclerosis and this may inhibit efferocytosis and lead to the formation of a necrotic core. The results of the current study suggest that the two strands of *Mir21* gene in macrophages may regulate apoptosis and efferocytosis during atherosclerosis. It is unclear from the current study how the

regulation of the circadian rhythm interacts with the regulation of *Xaf1* and hence apoptosis. One possibility is that the circadian expression of *miR-21-3p* directly targets and regulates the expression of *Xaf1* in a circadian manner thereby regulating apoptosis and inhibiting *miR-21-3p* results in high expression of *Xaf1* and hence increased apoptosis and reduced accumulation of lesional macrophages. Another possibility is that the deregulation of the circadian rhythm through the targeting of *Nfil3* by *miR-21-3p* results in the cells being resistant or less sensitive to the apoptotic pathway. Cell cycle and apoptosis are controlled in part by the circadian rhythm and in tumours, the peripheral circadian rhythm is found to be deregulated²⁷⁰. In *Period* mutant (mPer) mice for example, cells are resistant to apoptosis and the expression of genes that control cell cycle like *Cyclin D1*, *Cyclin A*, *Mdm-2*, and *Gadd45a* are suppressed and these mice are prone to tumourigenesis^{271, 272}. The expression of circadian clock genes may therefore be associated to cell cycle regulation and sensitivity to apoptosis. Therefore, the deregulation of the circadian clock in macrophages may result in decreased response of macrophages to apoptotic pathways suggesting a combinatory effect of *Xaf1* regulation and the circadian rhythm. The mechanism through which the circadian rhythm regulates apoptosis however, needs to be further investigated.

4.3 Clinical relevance

MicroRNAs are involved in the development of several human diseases and the evidence supporting therapeutic potential has caused them to receive much attention. *Mir21* expression is known to contribute to myocardial disease by increasing growth and survival of cardiac fibroblasts, increase fibrosis during heart transplant, and enhance atherosclerosis and neointimal lesion formation after balloon injury in carotid arteries. However, *Mir21* expression also improves endothelial function by increasing nitric oxide production in response to shear stress suggesting that, *Mir21* may have different roles and effects in different cell types during atherosclerosis. The current study investigated the role of *Mir21* expression in macrophages during atherosclerosis and indicated a possible combinatory role of both the guide and passenger strands in enhancing atherosclerosis. The expression of the passenger strand (*miR-21-3p*) in macrophages regulated the circadian clock and apoptosis, whereas the guide strand (*miR-21-5p*) regulated efferocytosis of lesional macrophages. *Mir21* is highly conserved in humans and mouse and therefore, translating results in mice models of atherosclerosis to humans could present promising therapeutic measures.

Potentially, *miR-21-3p* and *miR-21-5p* can be inhibited using antisense oligonucleotides (anti-miRs), in order to increase apoptosis and phagocytic removal of macrophages and hence inhibit atherogenesis. However, because *Mir21* expression plays different roles in other cells, there could be off-target effects of using anti-miRs that can inhibit the function of both *miR-21-3p* and *miR-21-5p* strands in different cells. Thus identifying the functional role of *Mir21* strands and their targets in a cell specific manner provides therapeutic targets for more effective and specific therapies, for instance by blocking the interaction between the *Mir21*

strands and their targets in macrophages during atherosclerosis. This may be achieved by using antisense oligonucleotides that bind to the microRNA target site of an mRNA known as target site blockers, which will prevent the microRNAs loaded RISC from targeting and repressing the mRNA. Therefore the result of the current study can be used to develop novel therapeutic strategies for improving macrophage function and resolution of inflammation during atherosclerosis.

5 Summary

Macrophages play a central role in the progression of atherosclerosis through the formation of foam cells, necrotic core and enhancement of inflammation. On the other hand, lesional macrophages could also contribute to the resolution of inflammation and lesional regression through cholesterol efflux and efferocytosis. MicroRNAs are a family of small (~22 nucleotide) noncoding RNA molecules that are responsible for post-transcriptional regulation of gene expression and are involved in several physiological processes including development, differentiation, metabolism, growth, proliferation and apoptosis. In atherosclerosis, microRNAs are expressed in various cells and regulate inflammation, cell proliferation, apoptosis and lipid metabolism. *Mir21* expression is involved in apoptosis, proliferation and inflammation in various cells during disease progression. Moreover, both strands of the pre-miR-21, *miR-21-5p* and *miR-21-3p* are highly upregulated in human atherosclerotic plaques. *miR-21-3p* is selectively upregulated in macrophages in response to oxidative stress and *miR-21-5p* is upregulated upon LPS stimulation. However, the role of *miR-21-5p* and *miR-21-3p* strands in macrophages during atherosclerosis is not known.

The current study indicates that *miR-21-5p* and *miR-21-3p* strands were expressed in atherosclerotic lesional macrophages. Moreover, the expression of both *miR-21-3p* and *-5p* strands were upregulated upon oxLDL stimulation in BMDMs suggesting a regulatory role of both *miR-21* strands in macrophages during atherosclerosis. Notably, *Mir21* deficiency in hematopoietic cells reduced atherosclerosis due to reduced lesional macrophage content and necrotic core area albeit macrophage apoptosis was increased. These data suggest that *Mir21* deficiency in macrophages may improve efferocytosis during lesion formation. Therefore, the expression of *miR-21* strands in macrophages exacerbates atherosclerosis.

Hematopoietic deficiency of *Mir21* significantly altered circadian clock gene expression in atherosclerotic arteries. The current study suggests that *miR-21-3p* in macrophages suppressed the circadian clock by directly targeting *Nfil3* and this dysregulation of the circadian rhythm may in turn have reduced the sensitivity of macrophages to the apoptotic pathway and hence increased accumulation and inflammation (Figure 31). Interestingly, *miR-21-3p* may also directly target pro-apoptotic *Xaf1* in lesional macrophages. What is not clear from this data is how the circadian rhythm is interconnected with the reduction of *Xaf1* expression and apoptosis and hence further studies will be needed. *miR-21-5p* also regulated *Mbl2* expression in macrophages and this may have led to decreased efferocytosis and hence increased necrotic core area (Figure 31). Both strands may therefore regulate apoptosis and efferocytosis in macrophages during atherosclerosis. *Mir21* expression in other vascular cells may have different effects on atherosclerosis as compared to macrophages and hence the effect of *Mir21* in endothelial cells need further studies. The results from this study suggests that specifically targeting *Mir21* in macrophages may be beneficial in atherosclerosis. However, to prevent the off-target effects of chronic deficiency of *Mir21*, blocking the interaction between the microRNAs with *Xaf1* and *Nfil3* may give stronger beneficial effects.

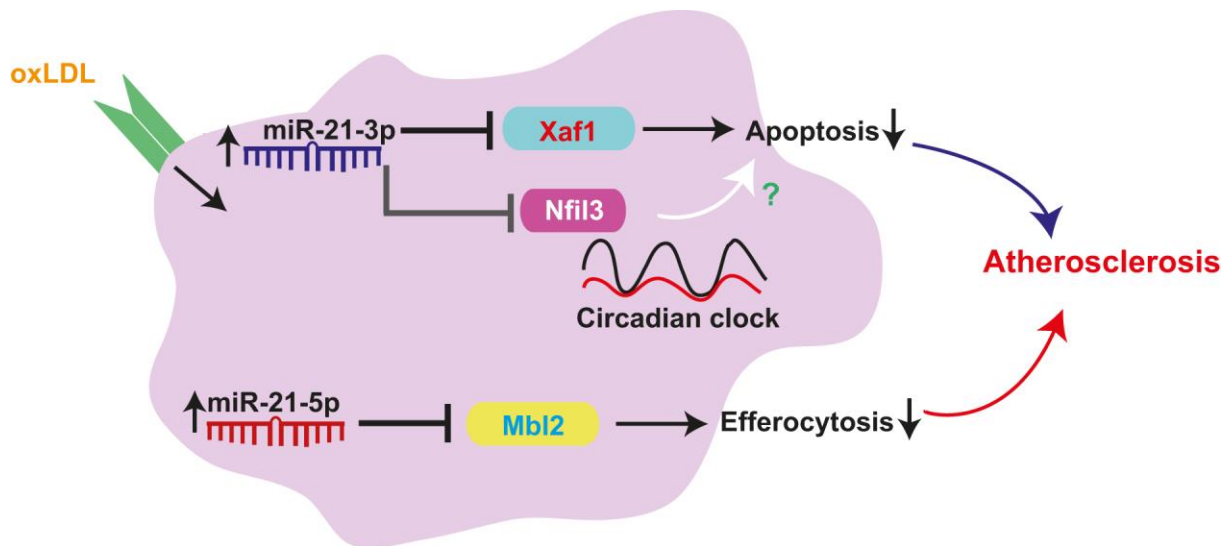


Figure 31: Mechanism by which *Mir21* in macrophages enhance atherosclerosis. Both *miR-21-5p* and *miR-21-3p* are upregulated by the uptake of oxLDL due to high fat diet intake. *miR-21-3p* targets *Nfil3* and *Xaf1* thereby suppressing the circadian rhythm and apoptosis respectively. This leads to increased accumulation of macrophages and atherosclerosis. *miR-21-5p* targets *Mbl2* and may inhibit efferocytosis which results in secondary necrosis and formation of necrotic core area.

6 References

1. Schober A, Nazari-Jahantigh M and Weber C. MicroRNA-mediated mechanisms of the cellular stress response in atherosclerosis. *Nature Reviews Cardiology*. 2015;12:361-374.
2. Schwenke DC and Carew TE. Initiation of atherosclerotic lesions in cholesterol-fed rabbits. II. Selective retention of LDL vs. selective increases in LDL permeability in susceptible sites of arteries. *Arteriosclerosis*. 1989;9:908-18.
3. Libby P. Inflammation in atherosclerosis. *Nature*. 2002;420:868-74.
4. Zeller I and Srivastava S. Macrophage functions in atherosclerosis. *Circ Res*. 2014;115:e83-5.
5. Tabas I, Garcia-Cardena G and Owens GK. Recent insights into the cellular biology of atherosclerosis. *The Journal of cell biology*. 2015;209:13-22.
6. Lopez AD, Mathers CD, Ezzati M, Jamison DT and Murray CJ. Global and regional burden of disease and risk factors, 2001: systematic analysis of population health data. *Lancet*. 2006;367:1747-57.
7. Bartel DP. MicroRNAs: genomics, biogenesis, mechanism, and function. *Cell*. 2004;116:281-97.
8. Ambros V. The functions of animal microRNAs. *Nature*. 2004;431:350-5.
9. Hosin AA, Prasad A, Viiri LE, Davies AH and Shalhoub J. MicroRNAs in Atherosclerosis. *Journal of vascular research*. 2014;51:338-49.
10. Insull W, Jr. The pathology of atherosclerosis: plaque development and plaque responses to medical treatment. *The American journal of medicine*. 2009;122:S3-S14.
11. Viola J and Soehnlein O. Atherosclerosis - A matter of unresolved inflammation. *Semin Immunol*. 2015;27:184-93.
12. Gautier EL, Huby T, Witztum JL, Ouzilleau B, Miller ER, Saint-Charles F, Aucouturier P, Chapman MJ and Lesnik P. Macrophage apoptosis exerts divergent effects on atherogenesis as a function of lesion stage. *Circulation*. 2009;119:1795-804.
13. Lusis AJ. Atherosclerosis. *Nature*. 2000;407:233-41.
14. World Health Organization. The top 10 causes of death. 2014;2015.
15. Alwan A. Global Atlas on cardiovascular disease prevention and control. 2011:8-14.
16. Yusuf S, Reddy S, Ounpuu S and Anand S. Global burden of cardiovascular diseases: part I: general considerations, the epidemiologic transition, risk factors, and impact of urbanization. *Circulation*. 2001;104:2746-53.
17. Yusuf S, Ounpuu S and Anand S. The global epidemic of atherosclerotic cardiovascular disease. *Medical principles and practice : international journal of the Kuwait University, Health Science Centre*. 2002;11 Suppl 2:3-8.
18. Grundy SM, Balady GJ, Criqui MH, Fletcher G, Greenland P, Hiratzka LF, Houston-Miller N, Kris-Etherton P, Krumholz HM, LaRosa J, Ockene IS, Pearson TA, Reed J, Smith SC, Jr. and Washington R. When to start cholesterol-lowering therapy in patients with coronary heart disease. A statement for healthcare professionals from the American Heart Association Task Force on Risk Reduction. *Circulation*. 1997;95:1683-5.

19. Libby P. The forgotten majority: unfinished business in cardiovascular risk reduction. *J Am Coll Cardiol.* 2005;46:1225-8.
20. Ross R. The pathogenesis of atherosclerosis: a perspective for the 1990s. *Nature.* 1993;362:801-9.
21. Chiu JJ and Chien S. Effects of disturbed flow on vascular endothelium: pathophysiological basis and clinical perspectives. *Physiol Rev.* 2011;91:327-87.
22. Schober A, Nazari-Jahantigh M, Wei Y, Bidzhekov K, Gremse F, Grommes J, Megens RTA, Heyll K, Noels H, Hristov M, Wang S, Kiessling F, Olson EN and Weber C. MicroRNA-126-5p promotes endothelial proliferation and limits atherosclerosis by suppressing Dlk1. *Nat Med.* 2014;20:368-+.
23. Warboys CM, Amini N, de Luca A and Evans PC. The role of blood flow in determining the sites of atherosclerotic plaques. *F1000 medicine reports.* 2011;3:5.
24. Williams KJ and Tabas I. The response-to-retention hypothesis of early atherogenesis. *Arterioscler Thromb Vasc Biol.* 1995;15:551-61.
25. Ross R, Glomset J and Harker L. Response to injury and atherogenesis. *The American journal of pathology.* 1977;86:675-84.
26. DiCorleto PE and Chisolm GM, 3rd. Participation of the endothelium in the development of the atherosclerotic plaque. *Progress in lipid research.* 1986;25:365-74.
27. Nievelstein PF, Fogelman AM, Mottino G and Frank JS. Lipid accumulation in rabbit aortic intima 2 hours after bolus infusion of low density lipoprotein. A deep-etch and immunolocalization study of ultrarapidly frozen tissue. *Arteriosclerosis and thrombosis : a journal of vascular biology / American Heart Association.* 1991;11:1795-805.
28. Goldstein JL, Ho YK, Basu SK and Brown MS. Binding site on macrophages that mediates uptake and degradation of acetylated low density lipoprotein, producing massive cholesterol deposition. *Proc Natl Acad Sci U S A.* 1979;76:333-7.
29. Boren J, Olin K, Lee I, Chait A, Wight TN and Innerarity TL. Identification of the principal proteoglycan-binding site in LDL. A single-point mutation in apo-B100 severely affects proteoglycan interaction without affecting LDL receptor binding. *The Journal of clinical investigation.* 1998;101:2658-64.
30. Haberland ME, Fogelman AM and Edwards PA. Specificity of receptor-mediated recognition of malondialdehyde-modified low density lipoproteins. *Proc Natl Acad Sci U S A.* 1982;79:1712-6.
31. Haberland ME, Olch CL and Fogelman AM. Role of lysines in mediating interaction of modified low density lipoproteins with the scavenger receptor of human monocyte macrophages. *The Journal of biological chemistry.* 1984;259:11305-11.
32. Hansson GK and Hermansson A. The immune system in atherosclerosis. *Nature immunology.* 2011;12:204-212.
33. Shah PK, Chyu KY, Dimayuga PC and Nilsson J. Vaccine for atherosclerosis. *J Am Coll Cardiol.* 2014;64:2779-91.
34. Moore KJ, Sheedy FJ and Fisher EA. Macrophages in atherosclerosis: a dynamic balance. *Nat Rev Immunol.* 2013;13:709-21.

35. Maskrey BH, Megson IL, Whitfield PD and Rossi AG. Mechanisms of resolution of inflammation: a focus on cardiovascular disease. *Arterioscler Thromb Vasc Biol.* 2011;31:1001-6.
36. Ross R. The Pathogenesis of Atherosclerosis — An Update. *New England Journal of Medicine.* 1986;314:488-500.
37. Randolph GJ. Emigration of monocyte-derived cells to lymph nodes during resolution of inflammation and its failure in atherosclerosis. *Current opinion in lipidology.* 2008;19:462-8.
38. Robbins CS, Hilgendorf I, Weber GF, Theurl I, Iwamoto Y, Figueiredo JL, Gorbatov R, Sukhova GK, Gerhardt LM, Smyth D, Zavitz CC, Shikatani EA, Parsons M, Rooijen NV, Lin HY, Husain M, Libby P, Nahrendorf M, Weissleder R and Swirski FK. Local proliferation dominates lesional macrophage accumulation in atherosclerosis. *Nat Med.* 2013.
39. Moore KJ and Tabas I. Macrophages in the pathogenesis of atherosclerosis. *Cell.* 2011;145:341-55.
40. Seimon TA, Nadolski MJ, Liao X, Magallon J, Nguyen M, Feric NT, Koschinsky ML, Harkewicz R, Witztum JL, Tsimikas S, Golenbock D, Moore KJ and Tabas I. Atherogenic lipids and lipoproteins trigger CD36-TLR2-dependent apoptosis in macrophages undergoing endoplasmic reticulum stress. *Cell metabolism.* 2010;12:467-82.
41. Tabas I. The role of endoplasmic reticulum stress in the progression of atherosclerosis. *Circulation research.* 2010;107:839-50.
42. Tabas I. Consequences and therapeutic implications of macrophage apoptosis in atherosclerosis: the importance of lesion stage and phagocytic efficiency. *Arteriosclerosis, thrombosis, and vascular biology.* 2005;25:2255-64.
43. Kockx MM and Herman AG. Apoptosis in atherosclerosis: beneficial or detrimental? *Cardiovascular research.* 2000;45:736-46.
44. van Vlijmen BJ, Gerritsen G, Franken AL, Boesten LS, Kockx MM, Gijbels MJ, Vierboom MP, van Eck M, van De Water B, van Berkel TJ and Havekes LM. Macrophage p53 deficiency leads to enhanced atherosclerosis in APOE*3-Leiden transgenic mice. *Circulation research.* 2001;88:780-6.
45. Liu J, Thewke DP, Su YR, Linton MF, Fazio S and Sinensky MS. Reduced macrophage apoptosis is associated with accelerated atherosclerosis in low-density lipoprotein receptor-null mice. *Arterioscler Thromb Vasc Biol.* 2005;25:174-9.
46. Tabas I. Macrophage death and defective inflammation resolution in atherosclerosis. *Nat Rev Immunol.* 2010;10:36-46.
47. Virmani R, Burke AP, Kolodgie FD and Farb A. Vulnerable plaque: the pathology of unstable coronary lesions. *J Interv Cardiol.* 2002;15:439-46.
48. Savill J and Fadok V. Corpse clearance defines the meaning of cell death. *Nature.* 2000;407:784-8.
49. Bouchareychas L, Pirault J, Saint-Charles F, Deswaerte V, Le Roy T, Jessup W, Giral P, Le Goff W, Huby T, Gautier EL and Lesnik P. Promoting macrophage survival delays progression of pre-existing atherosclerotic lesions through macrophage-derived apoE. *Cardiovascular research.* 2015.

50. Thorp E and Tabas I. Mechanisms and consequences of efferocytosis in advanced atherosclerosis. *J Leukoc Biol.* 2009;86:1089-95.
51. Martin CJ, Peters KN and Behar SM. Macrophages clean up: efferocytosis and microbial control. *Current opinion in microbiology.* 2014;17:17-23.
52. Nagornev VA and Maltseva SV. The phenotype of macrophages which are not transformed into foam cells in atherogenesis. *Atherosclerosis.* 1996;121:245-251.
53. Mantovani A, Garlanda C and Locati M. Macrophage diversity and polarization in atherosclerosis: a question of balance. *Arterioscler Thromb Vasc Biol.* 2009;29:1419-1423.
54. Bouhrel MA, Derudas B, Rigamonti E, Dievart R, Brozek J, Haulon S, Zawadzki C, Jude B, Torpier G, Marx N, Staels B and Chinetti-Gbaguidi G. PPARgamma activation primes human monocytes into alternative M2 macrophages with anti-inflammatory properties. *Cell metabolism.* 2007;6:137-43.
55. Reinhart BJ, Slack FJ, Basson M, Pasquinelli AE, Bettinger JC, Rougvie AE, Horvitz HR and Ruvkun G. The 21-nucleotide let-7 RNA regulates developmental timing in *Caenorhabditis elegans*. *Nature.* 2000;403:901-6.
56. Brennecke J, Hipfner DR, Stark A, Russell RB and Cohen SM. bantam encodes a developmentally regulated microRNA that controls cell proliferation and regulates the proapoptotic gene hid in *Drosophila*. *Cell.* 2003;113:25-36.
57. Krutzfeldt J and Stoffel M. MicroRNAs: a new class of regulatory genes affecting metabolism. *Cell metabolism.* 2006;4:9-12.
58. Nazari-Jahantigh M, Wei Y and Schober A. The role of microRNAs in arterial remodelling. *Thrombosis and haemostasis.* 2012;107:611-8.
59. Urbich C, Kuehbacher A and Dimmeler S. Role of microRNAs in vascular diseases, inflammation, and angiogenesis. *Cardiovascular research.* 2008;79:581-8.
60. Davis BN and Hata A. Regulation of MicroRNA Biogenesis: A miRiad of mechanisms. *Cell communication and signaling : CCS.* 2009;7:18.
61. Lee Y, Kim M, Han J, Yeom KH, Lee S, Baek SH and Kim VN. MicroRNA genes are transcribed by RNA polymerase II. *EMBO J.* 2004;23:4051-60.
62. Lee Y, Ahn C, Han J, Choi H, Kim J, Yim J, Lee J, Provost P, Radmark O, Kim S and Kim VN. The nuclear RNase III Drosha initiates microRNA processing. *Nature.* 2003;425:415-9.
63. Lund JM, Alexopoulou L, Sato A, Karow M, Adams NC, Gale NW, Iwasaki A and Flavell RA. Recognition of single-stranded RNA viruses by Toll-like receptor 7. *Proc Natl Acad Sci U S A.* 2004;101:5598-603.
64. Bartel DP. MicroRNAs: target recognition and regulatory functions. *Cell.* 2009;136:215-233.
65. Gregory RI, Chendrimada TP, Cooch N and Shiekhattar R. Human RISC couples microRNA biogenesis and posttranscriptional gene silencing. *Cell.* 2005;123:631-40.
66. Ro S, Park C, Young D, Sanders KM and Yan W. Tissue-dependent paired expression of miRNAs. *Nucleic acids research.* 2007;35:5944-5953.
67. Marco A, Macpherson JI, Ronshaugen M and Griffiths-Jones S. MicroRNAs from the same precursor have different targeting properties. *Silence.* 2012;3:8.

68. Zhang Y, Yang P, Sun T, Li D, Xu X, Rui Y, Li C, Chong M, Ibrahim T, Mercatali L, Amadori D, Lu X, Xie D, Li QJ and Wang XF. miR-126 and miR-126* repress recruitment of mesenchymal stem cells and inflammatory monocytes to inhibit breast cancer metastasis. *Nature cell biology*. 2013;15:284-94.
69. Almeida MI, Nicoloso MS, Zeng L, Ivan C, Spizzo R, Gafa R, Xiao L, Zhang X, Vannini I, Fanini F, Fabbri M, Lanza G, Reis RM, Zweidler-McKay PA and Calin GA. Strand-specific miR-28-5p and miR-28-3p have distinct effects in colorectal cancer cells. *Gastroenterology*. 2012;142:886-896 e9.
70. Raitoharju E, Lyytikainen LP, Levula M, Oksala N, Mennander A, Tarkka M, Klopp N, Illig T, Kahonen M, Karhunen PJ, Laaksonen R and Lehtimaki T. miR-21, miR-210, miR-34a, and miR-146a/b are up-regulated in human atherosclerotic plaques in the Tampere Vascular Study. *Atherosclerosis*. 2011.
71. Qin X, Wang X, Wang Y, Tang Z, Cui Q, Xi J, Li YS, Chien S and Wang N. MicroRNA-19a mediates the suppressive effect of laminar flow on cyclin D1 expression in human umbilical vein endothelial cells. *Proc Natl Acad Sci U S A*. 2010;107:3240-4.
72. Fang Y, Shi C, Manduchi E, Civelek M and Davies PF. MicroRNA-10a regulation of proinflammatory phenotype in athero-susceptible endothelium in vivo and in vitro. *Proc Natl Acad Sci U S A*. 2010;107:13450-5.
73. Chen T, Huang Z, Wang L, Wang Y, Wu F, Meng S and Wang C. MicroRNA-125a-5p partly regulates the inflammatory response, lipid uptake, and ORP9 expression in oxLDL-stimulated monocyte/macrophages. *Cardiovascular research*. 2009;83:131-139.
74. Nazari-Jahantigh M, Wei Y, Noels H, Akhtar S, Zhou Z, Koenen RR, Heyll K, Gremse F, Kiessling F, Grommes J, Weber C and Schober A. MicroRNA-155 promotes atherosclerosis by repressing Bcl6 in macrophages. *The Journal of clinical investigation*. 2012;122:4190-202.
75. O'Connell RM, Taganov KD, Boldin MP, Cheng G and Baltimore D. MicroRNA-155 is induced during the macrophage inflammatory response. *Proc Natl Acad Sci U S A*. 2007;104:1604-9.
76. Hulsmans M, De Keyzer D and Holvoet P. MicroRNAs regulating oxidative stress and inflammation in relation to obesity and atherosclerosis. *FASEB journal : official publication of the Federation of American Societies for Experimental Biology*. 2011;25:2515-27.
77. Ronald JA, Chen JW, Chen Y, Hamilton AM, Rodriguez E, Reynolds F, Hegele RA, Rogers KA, Querol M, Bogdanov A, Weissleder R and Rutt BK. Enzyme-sensitive magnetic resonance imaging targeting myeloperoxidase identifies active inflammation in experimental rabbit atherosclerotic plaques. *Circulation*. 2009;120:592-9.
78. Fleissner F, Jazbutyte V, Fiedler J, Gupta SK, Yin X, Xu Q, Galuppo P, Kneitz S, Mayr M, Ertl G, Bauersachs J and Thum T. Short communication: asymmetric dimethylarginine impairs angiogenic progenitor cell function in patients with coronary artery disease through a microRNA-21-dependent mechanism. *Circ Res*. 2010;107:138-43.
79. Cole JE, Georgiou E and Monaco C. The expression and functions of toll-like receptors in atherosclerosis. *Mediators of inflammation*. 2010;2010:393946.

80. Tall AR and Yvan-Charvet L. Cholesterol, inflammation and innate immunity. *Nat Rev Immunol*. 2015;15:104-16.
81. Rayner KJ, Suarez Y, Davalos A, Parathath S, Fitzgerald ML, Tamehiro N, Fisher EA, Moore KJ and Fernandez-Hernando C. MiR-33 contributes to the regulation of cholesterol homeostasis. *Science*. 2010;328:1570-3.
82. Rayner KJ, Sheedy FJ, Esau CC, Hussain FN, Temel RE, Parathath S, van Gils JM, Rayner AJ, Chang AN, Suarez Y, Fernandez-Hernando C, Fisher EA and Moore KJ. Antagonism of miR-33 in mice promotes reverse cholesterol transport and regression of atherosclerosis. *The Journal of clinical investigation*. 2011;121:2921-31.
83. Wei Y, Zhu M, Corbalan-Campos J, Heyll K, Weber C and Schober A. Regulation of Csf1r and Bcl6 in Macrophages Mediates the Stage-Specific Effects of MicroRNA-155 on Atherosclerosis. *Arterioscl Throm Vas*. 2015;35:796-803.
84. Shang YY, Fang NN, Wang F, Wang H, Wang ZH, Tang MX, Peng J, Zhang Y, Zhang W and Zhong M. MicroRNA-21, induced by high glucose, modulates macrophage apoptosis via programmed cell death 4. *Molecular medicine reports*. 2015;12:463-9.
85. Xu R, Bi C, Song J, Wang L, Ge C, Liu X and Zhang M. Upregulation of miR-142-5p in atherosclerotic plaques and regulation of oxidized low-density lipoprotein-induced apoptosis in macrophages. *Molecular medicine reports*. 2015;11:3229-34.
86. Lagos-Quintana M, Rauhut R, Lendeckel W and Tuschl T. Identification of novel genes coding for small expressed RNAs. *Science*. 2001;294:853-8.
87. Cheng Y and Zhang C. MicroRNA-21 in cardiovascular disease. *J Cardiovasc Transl Res*. 2010;3:251-5.
88. Thum T, Gross C, Fiedler J, Fischer T, Kissler S, Bussen M, Galuppo P, Just S, Rottbauer W, Frantz S, Castoldi M, Soutschek J, Koteliansky V, Rosenwald A, Basson MA, Licht JD, Pena JT, Rouhanifard SH, Muckenthaler MU, Tuschl T, Martin GR, Bauersachs J and Engelhardt S. MicroRNA-21 contributes to myocardial disease by stimulating MAP kinase signalling in fibroblasts. *Nature*. 2008;456:980-4.
89. Ji R, Cheng Y, Yue J, Yang J, Liu X, Chen H, Dean DB and Zhang C. MicroRNA expression signature and antisense-mediated depletion reveal an essential role of MicroRNA in vascular neointimal lesion formation. *Circ Res*. 2007;100:1579-88.
90. Maegdefessel L, Azuma J, Toh R, Deng A, Merk DR, Raiesdana A, Leeper NJ, Raaz U, Schoelmerich AM, McConnell MV, Dalman RL, Spin JM and Tsao PS. MicroRNA-21 blocks abdominal aortic aneurysm development and nicotine-augmented expansion. *Sci Transl Med*. 2012;4:122ra22.
91. Seeger T, Fischer A, Muhly-Reinholz M, Zeiher AM and Dimmeler S. Long-term inhibition of miR-21 leads to reduction of obesity in db/db mice. *Obesity (Silver Spring)*. 2014;22:2352-60.
92. Weber M, Baker MB, Moore JP and Searles CD. MiR-21 is induced in endothelial cells by shear stress and modulates apoptosis and eNOS activity. *Biochemical and Biophysical Research Communications*. 2010;393:643-8.
93. Sheedy FJ, Palsson-McDermott E, Hennessy EJ, Martin C, O'Leary JJ, Ruan Q, Johnson DS, Chen Y and O'Neill LA. Negative regulation of TLR4 via targeting of the

- proinflammatory tumor suppressor PDCD4 by the microRNA miR-21. *Nature immunology*. 2010;11:141-7.
94. Barnett RE, Conklin DJ, Ryan L, Keskey RC, Ramjee V, Sepulveda EA, Srivastava S, Bhatnagar A and Cheadle WG. Anti-inflammatory effects of miR-21 in the macrophage response to peritonitis. *Journal of leukocyte biology*. 2015.
95. Gurung P, Li B, Subbarao Malireddi RK, Lamkanfi M, Geiger TL and Kanneganti TD. Chronic TLR Stimulation Controls NLRP3 Inflammasome Activation through IL-10 Mediated Regulation of NLRP3 Expression and Caspase-8 Activation. *Scientific reports*. 2015;5:14488.
96. Moore KW, de Waal Malefyt R, Coffman RL and O'Garra A. Interleukin-10 and the interleukin-10 receptor. *Annu Rev Immunol*. 2001;19:683-765.
97. Wei Y, Nazari-Jahantigh M, Chan L, Zhu M, Heyll K, Corbalan-Campos J, Hartmann P, Thiemann A, Weber C and Schober A. The microRNA-342-5p fosters inflammatory macrophage activation through an Akt1- and microRNA-155-dependent pathway during atherosclerosis. *Circulation*. 2013;127:1609-19.
98. Wei Y, Nazari-Jahantigh M, Chan L, Zhu M, Heyll K, Corbalan-Campos J, Hartmann P, Thiemann A, Weber C and Schober A. The microRNA-342-5p Fosters Inflammatory Macrophage Activation Through an Akt1-and microRNA-155-Dependent Pathway During Atherosclerosis. *Circulation*. 2013;127:1609-+.
99. Thulasigam S, Massilamany C, Gangaplara A, Dai H, Yarbaeva S, Subramaniam S, Riethoven JJ, Eudy J, Lou M and Reddy J. miR-27b*, an oxidative stress-responsive microRNA modulates nuclear factor-kB pathway in RAW 264.7 cells. *Mol Cell Biochem*. 2011;352:181-8.
100. Yang K, He YS, Wang XQ, Lu L, Chen QJ, Liu J, Sun Z and Shen WF. MiR-146a inhibits oxidized low-density lipoprotein-induced lipid accumulation and inflammatory response via targeting toll-like receptor 4. *FEBS letters*. 2011;585:854-860.
101. Kim TW, Jeong JH and Hong SC. The impact of sleep and circadian disturbance on hormones and metabolism. *Int J Endocrinol*. 2015;2015:591729.
102. Martino TA and Young ME. Influence of the cardiomyocyte circadian clock on cardiac physiology and pathophysiology. *Journal of biological rhythms*. 2015;30:183-205.
103. Paschos GK. Circadian clocks, feeding time, and metabolic homeostasis. *Frontiers in pharmacology*. 2015;6:112.
104. Dibner C, Schibler U and Albrecht U. The mammalian circadian timing system: organization and coordination of central and peripheral clocks. *Annu Rev Physiol*. 2010;72:517-49.
105. Harrington M. Location, location, location: important for jet-lagged circadian loops. *The Journal of clinical investigation*. 2010;120:2265-7.
106. Yamamoto T, Nakahata Y, Soma H, Akashi M, Mamime T and Takumi T. Transcriptional oscillation of canonical clock genes in mouse peripheral tissues. *BMC molecular biology*. 2004;5:18.

107. Lowrey PL and Takahashi JS. Mammalian circadian biology: elucidating genome-wide levels of temporal organization. *Annual review of genomics and human genetics*. 2004;5:407-41.
108. Bersten DC, Sullivan AE, Peet DJ and Whitelaw ML. bHLH-PAS proteins in cancer. *Nat Rev Cancer*. 2013;13:827-41.
109. Hogenesch JB, Gu YZ, Jain S and Bradfield CA. The basic-helix-loop-helix-PAS orphan MOP3 forms transcriptionally active complexes with circadian and hypoxia factors. *Proc Natl Acad Sci U S A*. 1998;95:5474-9.
110. Gekakis N, Staknis D, Nguyen HB, Davis FC, Wilsbacher LD, King DP, Takahashi JS and Weitz CJ. Role of the CLOCK protein in the mammalian circadian mechanism. *Science*. 1998;280:1564-9.
111. Jin X, Shearman LP, Weaver DR, Zylka MJ, de Vries GJ and Reppert SM. A molecular mechanism regulating rhythmic output from the suprachiasmatic circadian clock. *Cell*. 1999;96:57-68.
112. Curtis AM, Bellet MM, Sassone-Corsi P and O'Neill LA. Circadian clock proteins and immunity. *Immunity*. 2014;40:178-86.
113. Takahashi JS, Hong HK, Ko CH and McDearmon EL. The genetics of mammalian circadian order and disorder: implications for physiology and disease. *Nature reviews Genetics*. 2008;9:764-75.
114. Rutter J, Reick M and McKnight SL. Metabolism and the control of circadian rhythms. *Annual review of biochemistry*. 2002;71:307-31.
115. Bass J and Takahashi JS. Circadian integration of metabolism and energetics. *Science*. 2010;330:1349-54.
116. Mohawk JA, Green CB and Takahashi JS. Central and peripheral circadian clocks in mammals. *Annual review of neuroscience*. 2012;35:445-62.
117. Kornmann B, Schaad O, Reinke H, Saini C and Schibler U. Regulation of circadian gene expression in liver by systemic signals and hepatocyte oscillators. *Cold Spring Harb Symp Quant Biol*. 2007;72:319-30.
118. Filipinski E, Delaunay F, King VM, Wu MW, Claustrat B, Grechez-Cassiau A, Guettier C, Hastings MH and Francis L. Effects of chronic jet lag on tumor progression in mice. *Cancer Res*. 2004;64:7879-85.
119. Davidson AJ, Sellix MT, Daniel J, Yamazaki S, Menaker M and Block GD. Chronic jet-lag increases mortality in aged mice. *Current biology : CB*. 2006;16:R914-6.
120. Penev PD, Kolker DE, Zee PC and Turek FW. Chronic circadian desynchronization decreases the survival of animals with cardiomyopathic heart disease. *Am J Physiol*. 1998;275:H2334-7.
121. Millar-Craig MW, Bishop CN and Raftery EB. Circadian variation of blood-pressure. *Lancet*. 1978;1:795-7.
122. Panza JA, Epstein SE and Quyyumi AA. Circadian variation in vascular tone and its relation to alpha-sympathetic vasoconstrictor activity. *N Engl J Med*. 1991;325:986-90.

123. Cohen MC, Rohtla KM, Lavery CE, Muller JE and Mittleman MA. Meta-analysis of the morning excess of acute myocardial infarction and sudden cardiac death. *Am J Cardiol.* 1997;79:1512-6.
124. Elliott WJ. Circadian variation in the timing of stroke onset: a meta-analysis. *Stroke; a journal of cerebral circulation.* 1998;29:992-6.
125. van Amelsvoort LG, Schouten EG and Kok FJ. Impact of one year of shift work on cardiovascular disease risk factors. *J Occup Environ Med.* 2004;46:699-706.
126. Thomas C and Power C. Shift work and risk factors for cardiovascular disease: a study at age 45 years in the 1958 British birth cohort. *European journal of epidemiology.* 2010;25:305-14.
127. Anea CB, Zhang M, Stepp DW, Simkins GB, Reed G, Fulton DJ and Rudic RD. Vascular disease in mice with a dysfunctional circadian clock. *Circulation.* 2009;119:1510-7.
128. Kunieda T, Minamino T, Miura K, Katsuno T, Tateno K, Miyauchi H, Kaneko S, Bradfield CA, FitzGerald GA and Komuro I. Reduced nitric oxide causes age-associated impairment of circadian rhythmicity. *Circ Res.* 2008;102:607-14.
129. Lin C, Tang X, Zhu Z, Liao X, Zhao R, Fu W, Chen B, Jiang J, Qian R and Guo D. The rhythmic expression of clock genes attenuated in human plaque-derived vascular smooth muscle cells. *Lipids in health and disease.* 2014;13:14.
130. Pan X, Jiang XC and Hussain MM. Impaired cholesterol metabolism and enhanced atherosclerosis in clock mutant mice. *Circulation.* 2013;128:1758-69.
131. Ma H, Zhong W, Jiang Y, Fontaine C, Li S, Fu J, Olkkonen VM, Staels B and Yan D. Increased atherosclerotic lesions in LDL receptor deficient mice with hematopoietic nuclear receptor Rev-erbalpha knock- down. *J Am Heart Assoc.* 2013;2:e000235.
132. Silver AC, Arjona A, Hughes ME, Nitabach MN and Fikrig E. Circadian expression of clock genes in mouse macrophages, dendritic cells, and B cells. *Brain Behav Immun.* 2012;26:407-13.
133. Gibbs JE, Blaikley J, Beesley S, Matthews L, Simpson KD, Boyce SH, Farrow SN, Else KJ, Singh D, Ray DW and Loudon AS. The nuclear receptor REV-ERBAlpha mediates circadian regulation of innate immunity through selective regulation of inflammatory cytokines. *Proc Natl Acad Sci U S A.* 2012;109:582-7.
134. Liston P, Fong WG, Kelly NL, Toji S, Miyazaki T, Conte D, Tamai K, Craig CG, McBurney MW and Korneluk RG. Identification of XAF1 as an antagonist of XIAP anti-Caspase activity. *Nature cell biology.* 2001;3:128-33.
135. Arora V, Cheung HH, Plenchette S, Micali OC, Liston P and Korneluk RG. Degradation of survivin by the X-linked inhibitor of apoptosis (XIAP)-XAF1 complex. *The Journal of biological chemistry.* 2007;282:26202-9.
136. Zou B, Chim CS, Pang R, Zeng H, Dai Y, Zhang R, Lam CS, Tan VP, Hung IF, Lan HY and Wong BC. XIAP-associated factor 1 (XAF1), a novel target of p53, enhances p53-mediated apoptosis via post-translational modification. *Molecular carcinogenesis.* 2012;51:422-32.

137. Zhu LM, Shi DM, Dai Q, Cheng XJ, Yao WY, Sun PH, Ding Y, Qiao MM, Wu YL, Jiang SH and Tu SP. Tumor suppressor XAF1 induces apoptosis, inhibits angiogenesis and inhibits tumor growth in hepatocellular carcinoma. *Oncotarget*. 2014;5:5403-15.
138. Bai Y, Ahmad U, Wang Y, Li JH, Choy JC, Kim RW, Kirkiles-Smith N, Maher SE, Karras JG, Bennett CF, Bothwell AL, Pober JS and Tellides G. Interferon-gamma induces X-linked inhibitor of apoptosis-associated factor-1 and Noxa expression and potentiates human vascular smooth muscle cell apoptosis by STAT3 activation. *The Journal of biological chemistry*. 2008;283:6832-42.
139. Shin S, Moon KC, Park KU and Ha E. MicroRNA-513a-5p mediates TNF-alpha and LPS induced apoptosis via downregulation of X-linked inhibitor of apoptotic protein in endothelial cells. *Biochimie*. 2012;94:1431-6.
140. Nauta AJ, Raaschou-Jensen N, Roos A, Daha MR, Madsen HO, Borrias-Essers MC, Ryder LP, Koch C and Garred P. Mannose-binding lectin engagement with late apoptotic and necrotic cells. *European journal of immunology*. 2003;33:2853-63.
141. Nakamura N, Nonaka M, Ma BY, Matsumoto S, Kawasaki N, Asano S and Kawasaki T. Characterization of the interaction between serum mannan-binding protein and nucleic acid ligands. *J Leukoc Biol*. 2009;86:737-48.
142. Ogden CA, deCathelineau A, Hoffmann PR, Bratton D, Ghebrehiwet B, Fadok VA and Henson PM. C1q and mannose binding lectin engagement of cell surface calreticulin and CD91 initiates macropinocytosis and uptake of apoptotic cells. *The Journal of experimental medicine*. 2001;194:781-95.
143. Madsen HO, Videm V, Svejgaard A, Svennevig JL and Garred P. Association of mannose-binding-lectin deficiency with severe atherosclerosis. *Lancet*. 1998;352:959-60.
144. Best LG, Davidson M, North KE, MacCluer JW, Zhang Y, Lee ET, Howard BV, DeCroo S and Ferrell RE. Prospective analysis of mannose-binding lectin genotypes and coronary artery disease in American Indians: the Strong Heart Study. *Circulation*. 2004;109:471-5.
145. Saevarsdottir S, Oskarsson OO, Aspelund T, Eiriksdottir G, Vikingsdottir T, Gudnason V and Valdimarsson H. Mannan binding lectin as an adjunct to risk assessment for myocardial infarction in individuals with enhanced risk. *The Journal of experimental medicine*. 2005;201:117-25.
146. Matthijsen RA, de Winther MP, Kuipers D, van der Made I, Weber C, Herias MV, Gijbels MJ and Buurman WA. Macrophage-specific expression of mannose-binding lectin controls atherosclerosis in low-density lipoprotein receptor-deficient mice. *Circulation*. 2009;119:2188-95.
147. Fraser DA and Tenner AJ. Innate immune proteins C1q and mannan-binding lectin enhance clearance of atherogenic lipoproteins by human monocytes and macrophages. *J Immunol*. 2010;185:3932-9.
148. Patrick DM, Montgomery RL, Qi X, Obad S, Kauppinen S, Hill JA, van Rooij E and Olson EN. Stress-dependent cardiac remodeling occurs in the absence of microRNA-21 in mice. *The Journal of clinical investigation*. 2010;120:3912-6.

149. Rehmsmeier M, Steffen P, Hochsmann M and Giegerich R. Fast and effective prediction of microRNA/target duplexes. *RNA (New York, NY)*. 2004;10:1507-17.
150. He M, Liu Y, Wang X, Zhang MQ, Hannon GJ and Huang ZJ. Cell-type-based analysis of microRNA profiles in the mouse brain. *Neuron*. 2012;73:35-48.
151. Liu G and Abraham E. MicroRNAs in immune response and macrophage polarization. *Arteriosclerosis, thrombosis, and vascular biology*. 2013;33:170-7.
152. Graff JW, Dickson AM, Clay G, McCaffrey AP and Wilson ME. Identifying functional microRNAs in macrophages with polarized phenotypes. *The Journal of biological chemistry*. 2012;287:21816-25.
153. Banerjee S, Xie N, Cui H, Tan Z, Yang S, Icyuz M, Abraham E and Liu G. MicroRNA let-7c regulates macrophage polarization. *J Immunol*. 2013;190:6542-9.
154. Zhang Y, Zhang M, Zhong M, Suo Q and Lv K. Expression profiles of miRNAs in polarized macrophages. *International journal of molecular medicine*. 2013;31:797-802.
155. Caescu CI, Guo X, Tesfa L, Bhagat TD, Verma A, Zheng D and Stanley ER. Colony stimulating factor-1 receptor signaling networks inhibit mouse macrophage inflammatory responses by induction of microRNA-21. *Blood*. 2015.
156. Wang Z, Brandt S, Medeiros A, Wang S, Wu H, Dent A and Serezani CH. MicroRNA 21 Is a Homeostatic Regulator of Macrophage Polarization and Prevents Prostaglandin E2-Mediated M2 Generation. *PloS one*. 2015;10:e0115855.
157. Mosser DM and Edwards JP. Exploring the full spectrum of macrophage activation. *Nature Reviews Immunology*. 2008;8:958-969.
158. Tedgui A and Mallat Z. Cytokines in atherosclerosis: pathogenic and regulatory pathways. *Physiol Rev*. 2006;86:515-81.
159. Amar J, Fauvel J, Drouet L, Ruidavets JB, Perret B, Chamontin B, Boccalon H and Ferrieres J. Interleukin 6 is associated with subclinical atherosclerosis: a link with soluble intercellular adhesion molecule 1. *J Hypertens*. 2006;24:1083-8.
160. Huber SA, Sakkinen P, Conze D, Hardin N and Tracy R. Interleukin-6 exacerbates early atherosclerosis in mice. *Arterioscler Thromb Vasc Biol*. 1999;19:2364-7.
161. Schieffer B, Selle T, Hilfiker A, Hilfiker-Kleiner D, Grote K, Tietge UJ, Trautwein C, Luchtefeld M, Schmittkamp C, Heeneman S, Daemen MJ and Drexler H. Impact of interleukin-6 on plaque development and morphology in experimental atherosclerosis. *Circulation*. 2004;110:3493-500.
162. Martino F, Carlomosti F, Avitabile D, Persico L, Picozza M, Barilla F, Arca M, Montali A, Martino E, Zanoni C, Parrotto S and Magenta A. Circulating miR-33a and miR-33b are up-regulated in familial hypercholesterolaemia in paediatric age. *Clinical science*. 2015;129:963-72.
163. Khaidakov M and Mehta JL. Oxidized LDL triggers pro-oncogenic signaling in human breast mammary epithelial cells partly via stimulation of MiR-21. *PloS one*. 2012;7:e46973.
164. Chan JA, Krichevsky AM and Kosik KS. MicroRNA-21 is an antiapoptotic factor in human glioblastoma cells. *Cancer Res*. 2005;65:6029-33.

165. Volinia S, Calin GA, Liu CG, Ambs S, Cimmino A, Petrocca F, Visone R, Iorio M, Roldo C, Ferracin M, Prueitt RL, Yanaihara N, Lanza G, Scarpa A, Vecchione A, Negrini M, Harris CC and Croce CM. A microRNA expression signature of human solid tumors defines cancer gene targets. *Proc Natl Acad Sci U S A*. 2006;103:2257-61.
166. Han H, Qu G, Han C, Wang Y, Sun T, Li F, Wang J and Luo S. MiR-34a, miR-21 and miR-23a as potential biomarkers for coronary artery disease: a pilot microarray study and confirmation in a 32 patient cohort. *Exp Mol Med*. 2015;47:e138.
167. Nazari-Jahantigh M, Wei Y, Noels H, Akhtar S, Zhou Z, Koenen RR, Heyll K, Gremse F, Kiessling F, Grommes J, Weber C and Schober A. MicroRNA-155 promotes atherosclerosis by repressing Bcl6 in macrophages. *Journal of Clinical Investigation*. 2012;122:4190-4202.
168. Das A, Ganesh K, Khanna S, Sen CK and Roy S. Engulfment of apoptotic cells by macrophages: a role of microRNA-21 in the resolution of wound inflammation. *J Immunol*. 2014;192:1120-9.
169. Sheedy FJ. Turning 21: Induction of miR-21 as a Key Switch in the Inflammatory Response. *Frontiers in immunology*. 2015;6:19.
170. Keophiphath M, Rouault C, Divoux A, Clement K and Lacasa D. CCL5 promotes macrophage recruitment and survival in human adipose tissue. *Arterioscler Thromb Vasc Biol*. 2010;30:39-45.
171. Seimon T and Tabas I. Mechanisms and consequences of macrophage apoptosis in atherosclerosis. *Journal of lipid research*. 2009;50 Suppl:S382-7.
172. Nakashima Y, Plump AS, Raines EW, Breslow JL and Ross R. ApoE-deficient mice develop lesions of all phases of atherosclerosis throughout the arterial tree. *Arteriosclerosis and thrombosis : a journal of vascular biology / American Heart Association*. 1994;14:133-40.
173. Reddick RL, Zhang SH and Maeda N. Atherosclerosis in mice lacking apo E. Evaluation of lesional development and progression. *Arteriosclerosis and thrombosis : a journal of vascular biology / American Heart Association*. 1994;14:141-7.
174. Zhao Y, Ye D, Wang J, Calpe-Berdiel L, Azzis SB, Van Berkel TJ and Van Eck M. Stage-specific remodeling of atherosclerotic lesions upon cholesterol lowering in LDL receptor knockout mice. *The American journal of pathology*. 2011;179:1522-32.
175. Tangirala RK, Rubin EM and Palinski W. Quantitation of atherosclerosis in murine models: correlation between lesions in the aortic origin and in the entire aorta, and differences in the extent of lesions between sexes in LDL receptor-deficient and apolipoprotein E-deficient mice. *Journal of lipid research*. 1995;36:2320-8.
176. Swirski FK and Nahrendorf M. Leukocyte behavior in atherosclerosis, myocardial infarction, and heart failure. *Science*. 2013;339:161-6.
177. Hansson GK and Libby P. The immune response in atherosclerosis: a double-edged sword. *Nat Rev Immunol*. 2006;6:508-19.
178. Tabas I and Glass CK. Anti-inflammatory therapy in chronic disease: challenges and opportunities. *Science*. 2013;339:166-72.

179. Paulson KE, Zhu SN, Chen M, Nurmohamed S, Jongstra-Bilen J and Cybulsky MI. Resident intimal dendritic cells accumulate lipid and contribute to the initiation of atherosclerosis. *Circ Res.* 2010;106:383-90.
180. Johnson JL and Newby AC. Macrophage heterogeneity in atherosclerotic plaques. *Current opinion in lipidology.* 2009;20:370-378.
181. Lessner SM, Prado HL, Waller EK and Galis ZS. Atherosclerotic lesions grow through recruitment and proliferation of circulating monocytes in a murine model. *The American journal of pathology.* 2002;160:2145-55.
182. Swirski FK. Monocyte accumulation in mouse atherogenesis is progressive and proportional to extent of disease. *Proceedings of the National Academy of Sciences.* 2006;103:10340-10345.
183. Najafi Z, Sharifi M and Javadi G. Degradation of miR-21 induces apoptosis and inhibits cell proliferation in human hepatocellular carcinoma. *Cancer Gene Ther.* 2015.
184. Galkina E and Ley K. Immune and inflammatory mechanisms of atherosclerosis (*). *Annu Rev Immunol.* 2009;27:165-97.
185. Soehnlein O. Multiple roles for neutrophils in atherosclerosis. *Circ Res.* 2012;110:875-88.
186. Guasti L, Dentali F, Castiglioni L, Maroni L, Marino F, Squizzato A, Ageno W, Gianni M, Gaudio G, Grandi AM, Cosentino M and Venco A. Neutrophils and clinical outcomes in patients with acute coronary syndromes and/or cardiac revascularisation. A systematic review on more than 34,000 subjects. *Thrombosis and haemostasis.* 2011;106:591-9.
187. Drechsler M, Megens RT, van Zandvoort M, Weber C and Soehnlein O. Hyperlipidemia-triggered neutrophilia promotes early atherosclerosis. *Circulation.* 2010;122:1837-45.
188. Zernecke A, Bot I, Djalali-Talab Y, Shagdarsuren E, Bidzhekov K, Meiler S, Krohn R, Schober A, Sperandio M, Soehnlein O, Bornemann J, Tacke F, Biessen EA and Weber C. Protective role of CXC receptor 4/CXC ligand 12 unveils the importance of neutrophils in atherosclerosis. *Circulation Research.* 2008;102:209-217.
189. Weber C, Zernecke A and Libby P. The multifaceted contributions of leukocyte subsets to atherosclerosis: lessons from mouse models. *Nat Rev Immunol.* 2008;8:802-15.
190. Weber C and Noels H. Atherosclerosis: current pathogenesis and therapeutic options. *Nat Med.* 2011;17:1410-22.
191. Buscaglia LE and Li Y. Apoptosis and the target genes of microRNA-21. *Chinese journal of cancer.* 2011;30:371-80.
192. Stary HC, Blankenhorn DH, Chandler AB, Glagov S, Insull W, Jr., Richardson M, Rosenfeld ME, Schaffer SA, Schwartz CJ, Wagner WD and et al. A definition of the intima of human arteries and of its atherosclerosis-prone regions. A report from the Committee on Vascular Lesions of the Council on Arteriosclerosis, American Heart Association. *Circulation.* 1992;85:391-405.
193. Stary HC, Chandler AB, Glagov S, Guyton JR, Insull W, Jr., Rosenfeld ME, Schaffer SA, Schwartz CJ, Wagner WD and Wissler RW. A definition of initial, fatty streak, and

- intermediate lesions of atherosclerosis. A report from the Committee on Vascular Lesions of the Council on Arteriosclerosis, American Heart Association. *Arteriosclerosis and thrombosis : a journal of vascular biology / American Heart Association*. 1994;14:840-56.
194. Ross R and Glomset JA. The pathogenesis of atherosclerosis (second of two parts). *The New England journal of medicine*. 1976;295:420-5.
195. Stary HC, Chandler AB, Dinsmore RE, Fuster V, Glagov S, Insull W, Jr., Rosenfeld ME, Schwartz CJ, Wagner WD and Wissler RW. A definition of advanced types of atherosclerotic lesions and a histological classification of atherosclerosis. A report from the Committee on Vascular Lesions of the Council on Arteriosclerosis, American Heart Association. *Circulation*. 1995;92:1355-74.
196. Bertelsen S. Chemical studies on the arterial wall in relation to atherosclerosis. *Annals of the New York Academy of Sciences*. 1968;149:643-54.
197. Levene CI and Poole JC. The collagen content of the normal and atherosclerotic human aortic intima. *Br J Exp Pathol*. 1962;43:469-71.
198. Daugherty A and Rateri DL. T lymphocytes in atherosclerosis: the yin-yang of Th1 and Th2 influence on lesion formation. *Circ Res*. 2002;90:1039-40.
199. Jonasson L, Holm J, Skalli O, Bondjers G and Hansson GK. Regional accumulations of T cells, macrophages, and smooth muscle cells in the human atherosclerotic plaque. *Arteriosclerosis*. 1986;6:131-8.
200. Emeson EE and Robertson AL, Jr. T lymphocytes in aortic and coronary intimas. Their potential role in atherogenesis. *The American journal of pathology*. 1988;130:369-76.
201. Roselaar SE, Kakkanathu PX and Daugherty A. Lymphocyte populations in atherosclerotic lesions of apoE ^{-/-} and LDL receptor ^{-/-} mice. Decreasing density with disease progression. *Arterioscler Thromb Vasc Biol*. 1996;16:1013-8.
202. Dietrich J, Neisig A, Hou X, Wegener AM, Gajhede M and Geisler C. Role of CD3 gamma in T cell receptor assembly. *The Journal of cell biology*. 1996;132:299-310.
203. Hansson GK, Jonasson L, Lojstjed B, Stemme S, Kocher O and Gabbiani G. Localization of T lymphocytes and macrophages in fibrous and complicated human atherosclerotic plaques. *Atherosclerosis*. 1988;72:135-41.
204. Ammirati E, Cianflone D, Vecchio V, Banfi M, Vermi AC, De Metrio M, Grigore L, Pellegatta F, Pirillo A, Garlaschelli K, Manfredi AA, Catapano AL, Maseri A, Palini AG and Norata GD. Effector Memory T cells Are Associated With Atherosclerosis in Humans and Animal Models. *Journal of the American Heart Association*. 2012;1:27-41.
205. Mallat Z, Taleb S, Ait-Oufella H and Tedgui A. The role of adaptive T cell immunity in atherosclerosis. *Journal of lipid research*. 2009;50 Suppl:S364-9.
206. Meisgen F, Xu N, Wei T, Janson PC, Obad S, Broom O, Nagy N, Kauppinen S, Kemeny L, Stahle M, Pivarcsi A and Sonkoly E. MiR-21 is up-regulated in psoriasis and suppresses T cell apoptosis. *Exp Dermatol*. 2012;21:312-4.
207. Carissimi C, Carucci N, Colombo T, Piconese S, Azzalin G, Cipolletta E, Citarella F, Barnaba V, Macino G and Fulci V. miR-21 is a negative modulator of T-cell activation. *Biochimie*. 2014;107 Pt B:319-26.

208. Febbraio M, Podrez EA, Smith JD, Hajjar DP, Hazen SL, Hoff HF, Sharma K and Silverstein RL. Targeted disruption of the class B scavenger receptor CD36 protects against atherosclerotic lesion development in mice. *The Journal of clinical investigation*. 2000;105:1049-56.
209. Chen Y, Kennedy DJ, Ramakrishnan DP, Yang M, Huang W, Li Z, Xie Z, Chadwick AC, Sahoo D and Silverstein RL. Oxidized LDL-bound CD36 recruits an Na⁺/K⁺-ATPase-Lyn complex in macrophages that promotes atherosclerosis. *Science signaling*. 2015;8:ra91.
210. Shashkin P, Dragulev B and Ley K. Macrophage differentiation to foam cells. *Curr Pharm Des*. 2005;11:3061-72.
211. Boshuizen MC, Hoeksema MA, Neele AE, van der Velden S, Hamers AA, Van den Bossche J, Lutgens E and de Winther MP. Interferon-beta promotes macrophage foam cell formation by altering both cholesterol influx and efflux mechanisms. *Cytokine*. 2015.
212. Brasaemle DL, Dolios G, Shapiro L and Wang R. Proteomic analysis of proteins associated with lipid droplets of basal and lipolytically stimulated 3T3-L1 adipocytes. *The Journal of biological chemistry*. 2004;279:46835-42.
213. Londos C, Sztalryd C, Tansey JT and Kimmel AR. Role of PAT proteins in lipid metabolism. *Biochimie*. 2005;87:45-9.
214. Persson J, Degerman E, Nilsson J and Lindholm MW. Perilipin and adipophilin expression in lipid loaded macrophages. *Biochem Biophys Res Commun*. 2007;363:1020-6.
215. Faber BC, Cleutjens KB, Niessen RL, Aarts PL, Boon W, Greenberg AS, Kitslaar PJ, Tordoir JH and Daemen MJ. Identification of genes potentially involved in rupture of human atherosclerotic plaques. *Circ Res*. 2001;89:547-54.
216. Ortega-Gomez A, Perretti M and Soehnlein O. Resolution of inflammation: an integrated view. *EMBO molecular medicine*. 2013;5:661-74.
217. Gautier EL, Ivanov S, Lesnik P and Randolph GJ. Local apoptosis mediates clearance of macrophages from resolving inflammation in mice. *Blood*. 2013;122:2714-22.
218. Kockx MM, De Meyer GR, Muhring J, Jacob W, Bult H and Herman AG. Apoptosis and related proteins in different stages of human atherosclerotic plaques. *Circulation*. 1998;97:2307-15.
219. Guo Q, Zhang H, Zhang L, He Y, Weng S, Dong Z, Wang J, Zhang P and Nao R. MicroRNA-21 regulates non-small cell lung cancer cell proliferation by affecting cell apoptosis via COX-19. *Int J Clin Exp Med*. 2015;8:8835-41.
220. P MR, M BA, A LS, P MB, C MPR and R EC. Inhibition of NF-kappaB by deoxycholic acid induces miR-21/PDCD4-dependent hepatocellular apoptosis. *Scientific reports*. 2015;5:17528.
221. Byun DS, Cho K, Ryu BK, Lee MG, Kang MJ, Kim HR and Chi SG. Hypermethylation of XIAP-associated factor 1, a putative tumor suppressor gene from the 17p13.2 locus, in human gastric adenocarcinomas. *Cancer Res*. 2003;63:7068-75.
222. Chen XY, He QY and Guo MZ. XAF1 is frequently methylated in human esophageal cancer. *World J Gastroenterol*. 2012;18:2844-9.

223. Kim MA, Lee HE, Lee HS, Yang HK and Kim WH. Expression of apoptosis-related proteins and its clinical implication in surgically resected gastric carcinoma. *Virchows Arch.* 2011;459:503-10.
224. Zhang F, Wu LM, Zhou L, Chen QX, Xie HY, Feng XW and Zheng SS. Predictive value of expression and promoter hypermethylation of XAF1 in hepatitis B virus-associated hepatocellular carcinoma treated with transplantation. *Ann Surg Oncol.* 2008;15:3494-502.
225. Tang J, Lobatto ME, Hassing L, van der Staay S, van Rijs SM, Calcagno C, Braza MS, Baxter S, Fay F, Sanchez-Gaytan BL, Duivenvoorden R, Sager H, Astudillo YM, Leong W, Ramachandran S, Storm G, Perez-Medina C, Reiner T, Cormode DP, Strijkers GJ, Stroes ES, Swirski FK, Nahrendorf M, Fisher EA, Fayad ZA and Mulder WJ. Inhibiting macrophage proliferation suppresses atherosclerotic plaque inflammation. *Science advances.* 2015;1.
226. Tabas I, Seimon T, Timmins J, Li G and Lim W. Macrophage apoptosis in advanced atherosclerosis. *Annals of the New York Academy of Sciences.* 2009;1173 Suppl 1:E40-5.
227. Schrijvers DM, De Meyer GR, Herman AG and Martinet W. Phagocytosis in atherosclerosis: Molecular mechanisms and implications for plaque progression and stability. *Cardiovascular research.* 2007;73:470-80.
228. Schrijvers DM, De Meyer GR, Kockx MM, Herman AG and Martinet W. Phagocytosis of apoptotic cells by macrophages is impaired in atherosclerosis. *Arterioscler Thromb Vasc Biol.* 2005;25:1256-61.
229. Ball RY, Stowers EC, Burton JH, Cary NR, Skepper JN and Mitchinson MJ. Evidence that the death of macrophage foam cells contributes to the lipid core of atheroma. *Atherosclerosis.* 1995;114:45-54.
230. Tabas I. Apoptosis and efferocytosis in mouse models of atherosclerosis. *Curr Drug Targets.* 2007;8:1288-96.
231. Thorp E, Cui D, Schrijvers DM, Kuriakose G and Tabas I. MERTK receptor mutation reduces efferocytosis efficiency and promotes apoptotic cell accumulation and plaque necrosis in atherosclerotic lesions of apoE^{-/-} mice. *Arterioscler Thromb Vasc Biol.* 2008;28:1421-8.
232. Ait-Oufella H, Poursmail V, Simon T, Blanc-Brude O, Kinugawa K, Merval R, Offenstadt G, Leseche G, Cohen PL, Tedgui A and Mallat Z. Defective mer receptor tyrosine kinase signaling in bone marrow cells promotes apoptotic cell accumulation and accelerates atherosclerosis. *Arterioscler Thromb Vasc Biol.* 2008;28:1429-31.
233. Wei Y, Zhu M, Corbalan-Campos J, Heyll K, Weber C and Schober A. Regulation of Csf1r and Bcl6 in macrophages mediates the stage-specific effects of microRNA-155 on atherosclerosis. *Arteriosclerosis, thrombosis, and vascular biology.* 2015;35:796-803.
234. Fujita T. Evolution of the lectin-complement pathway and its role in innate immunity. *Nat Rev Immunol.* 2002;2:346-53.
235. Hegele RA, Ban MR, Anderson CM and Spence JD. Infection-susceptibility alleles of mannose-binding lectin are associated with increased carotid plaque area. *J Investig Med.* 2000;48:198-202.

236. Linnell V, Aittoniemi J, Vaarala O, Lehtimäki T, Laine S, Virtanen V, Palosuo T and Miettinen A. Association of mannan-binding lectin deficiency with venous bypass graft occlusions in patients with coronary heart disease. *Cardiology*. 2002;98:123-6.
237. Vengen IT, Madsen HO, Garred P, Platou C, Vatten L and Videm V. Mannose-binding lectin deficiency is associated with myocardial infarction: the HUNT2 study in Norway. *PloS one*. 2012;7:e42113.
238. Nauta AJ, Castellano G, Xu W, Woltman AM, Borrias MC, Daha MR, van Kooten C and Roos A. Opsonization with C1q and mannose-binding lectin targets apoptotic cells to dendritic cells. *J Immunol*. 2004;173:3044-50.
239. Hamada M, Nakamura M, Tran MT, Moriguchi T, Hong C, Ohsumi T, Dinh TT, Kusakabe M, Hattori M, Katsumata T, Arai S, Nakashima K, Kudo T, Kuroda E, Wu CH, Kao PH, Sakai M, Shimano H, Miyazaki T, Tontonoz P and Takahashi S. MafB promotes atherosclerosis by inhibiting foam-cell apoptosis. *Nature communications*. 2014;5:3147.
240. Lee RH and Vazquez G. Reduced size and macrophage content of advanced atherosclerotic lesions in mice with bone marrow specific deficiency of alpha 7 nicotinic acetylcholine receptor. *PloS one*. 2015;10:e0124584.
241. Andres V, Pello OM and Silvestre-Roig C. Macrophage proliferation and apoptosis in atherosclerosis. *Current opinion in lipidology*. 2012;23:429-38.
242. Biwa T, Hakamata H, Sakai M, Miyazaki A, Suzuki H, Kodama T, Shichiri M and Horiuchi S. Induction of murine macrophage growth by oxidized low density lipoprotein is mediated by granulocyte macrophage colony-stimulating factor. *The Journal of biological chemistry*. 1998;273:28305-13.
243. Park YM, Febbraio M and Silverstein RL. CD36 modulates migration of mouse and human macrophages in response to oxidized LDL and may contribute to macrophage trapping in the arterial intima. *The Journal of clinical investigation*. 2009;119:136-45.
244. van Gils JM, Derby MC, Fernandes LR, Ramkhelawon B, Ray TD, Rayner KJ, Parathath S, Distel E, Feig JL, Alvarez-Leite JI, Rayner AJ, McDonald TO, O'Brien KD, Stuart LM, Fisher EA, Lacy-Hulbert A and Moore KJ. The neuroimmune guidance cue netrin-1 promotes atherosclerosis by inhibiting the emigration of macrophages from plaques. *Nature immunology*. 2012;13:136-143.
245. Ramkhelawon B, Yang Y, van Gils JM, Hewing B, Rayner KJ, Parathath S, Guo L, Oldebeken S, Feig JL, Fisher EA and Moore KJ. Hypoxia induces netrin-1 and Unc5b in atherosclerotic plaques: mechanism for macrophage retention and survival. *Arterioscler Thromb Vasc Biol*. 2013;33:1180-8.
246. Thum T, Chau N, Bhat B, Gupta SK, Linsley PS, Bauersachs J and Engelhardt S. Comparison of different miR-21 inhibitor chemistries in a cardiac disease model. *The Journal of clinical investigation*. 2011;121:461-2; author reply 462-3.
247. Schober A, Nazari-Jahantigh M, Wei Y, Bidzhikov K, Gremse F, Grommes J, Megens RT, Heyll K, Noels H, Hristov M, Wang S, Kiessling F, Olson EN and Weber C. MicroRNA-126-5p promotes endothelial proliferation and limits atherosclerosis by suppressing Dlk1. *Nat Med*. 2014;20:368-76.

248. Sood P, Krek A, Zavolan M, Macino G and Rajewsky N. Cell-type-specific signatures of microRNAs on target mRNA expression. *Proc Natl Acad Sci U S A*. 2006;103:2746-51.
249. Kuchenbauer F, Mah SM, Heuser M, McPherson A, Ruschmann J, Rouhi A, Berg T, Bullinger L, Argiropoulos B, Morin RD, Lai D, Starczynowski DT, Karsan A, Eaves CJ, Watahiki A, Wang Y, Aparicio SA, Ganser A, Krauter J, Dohner H, Dohner K, Marra MA, Camargo FD, Palmqvist L, Buske C and Humphries RK. Comprehensive analysis of mammalian miRNA* species and their role in myeloid cells. *Blood*. 2011;118:3350-8.
250. McCullagh KA and Balian G. Collagen characterisation and cell transformation in human atherosclerosis. *Nature*. 1975;258:73-5.
251. Roselaar SE, Schonfeld G and Daugherty A. Enhanced development of atherosclerosis in cholesterol-fed rabbits by suppression of cell-mediated immunity. *The Journal of clinical investigation*. 1995;96:1389-94.
252. Emeson EE and Shen ML. Accelerated atherosclerosis in hyperlipidemic C57BL/6 mice treated with cyclosporin A. *The American journal of pathology*. 1993;142:1906-15.
253. Waltmann MD, Basford JE, Konanah ES, Weintraub NL and Hui DY. Apolipoprotein E receptor-2 deficiency enhances macrophage susceptibility to lipid accumulation and cell death to augment atherosclerotic plaque progression and necrosis. *Biochim Biophys Acta*. 2014;1842:1395-405.
254. Chang BH and Chan L. Regulation of Triglyceride Metabolism. III. Emerging role of lipid droplet protein ADFP in health and disease. *Am J Physiol Gastrointest Liver Physiol*. 2007;292:G1465-8.
255. Hou L, Lu C, Huang Y, Chen S, Hua L and Qian R. Effect of hyperlipidemia on the expression of circadian genes in apolipoprotein E knock-out atherosclerotic mice. *Lipids in health and disease*. 2009;8:60.
256. Xu C, Lu C, Hua L, Jin H, Yin L, Chen S and Qian R. Rhythm changes of clock genes, apoptosis-related genes and atherosclerosis-related genes in apolipoprotein E knockout mice. *The Canadian journal of cardiology*. 2009;25:473-9.
257. Keller M, Mazuch J, Abraham U, Eom GD, Herzog ED, Volk HD, Kramer A and Maier B. A circadian clock in macrophages controls inflammatory immune responses. *Proc Natl Acad Sci U S A*. 2009;106:21407-12.
258. Hayashi M, Shimba S and Tezuka M. Characterization of the molecular clock in mouse peritoneal macrophages. *Biological & pharmaceutical bulletin*. 2007;30:621-6.
259. Curtis AM, Fagundes CT, Yang G, Palsson-McDermott EM, Wochal P, McGettrick AF, Foley NH, Early JO, Chen L, Zhang H, Xue C, Geiger SS, Hokamp K, Reilly MP, Coogan AN, Vigorito E, FitzGerald GA and O'Neill LA. Circadian control of innate immunity in macrophages by miR-155 targeting Bmal1. *Proc Natl Acad Sci U S A*. 2015.
260. Kinoshita C, Aoyama K, Matsumura N, Kikuchi-Utsumi K, Watabe M and Nakaki T. Rhythmic oscillations of the microRNA miR-96-5p play a neuroprotective role by indirectly regulating glutathione levels. *Nature communications*. 2014;5:3823.
261. Li A, Lin X, Tan X, Yin B, Han W, Zhao J, Yuan J, Qiang B and Peng X. Circadian gene Clock contributes to cell proliferation and migration of glioma and is directly regulated by tumor-suppressive miR-124. *FEBS letters*. 2013;587:2455-60.

262. Lee KH, Kim SH, Lee HR, Kim W, Kim DY, Shin JC, Yoo SH and Kim KT. MicroRNA-185 oscillation controls circadian amplitude of mouse Cryptochrome 1 via translational regulation. *Molecular biology of the cell*. 2013;24:2248-55.
263. Cheng HY, Papp JW, Varlamova O, Dziema H, Russell B, Curfman JP, Nakazawa T, Shimizu K, Okamura H, Impey S and Obrietan K. microRNA modulation of circadian-clock period and entrainment. *Neuron*. 2007;54:813-29.
264. Liu K and Wang R. MicroRNA-mediated regulation in the mammalian circadian rhythm. *J Theor Biol*. 2012;304:103-10.
265. Xu S, Witmer PD, Lumayag S, Kovacs B and Valle D. MicroRNA (miRNA) transcriptome of mouse retina and identification of a sensory organ-specific miRNA cluster. *The Journal of biological chemistry*. 2007;282:25053-66.
266. Ohno T, Onishi Y and Ishida N. A novel E4BP4 element drives circadian expression of mPeriod2. *Nucleic acids research*. 2007;35:648-55.
267. Ohno T, Onishi Y and Ishida N. The negative transcription factor E4BP4 is associated with circadian clock protein PERIOD2. *Biochem Biophys Res Commun*. 2007;354:1010-5.
268. Na YJ, Sung JH, Lee SC, Lee YJ, Choi YJ, Park WY, Shin HS and Kim JH. Comprehensive analysis of microRNA-mRNA co-expression in circadian rhythm. *Exp Mol Med*. 2009;41:638-47.
269. Arvey A, Larsson E, Sander C, Leslie CS and Marks DS. Target mRNA abundance dilutes microRNA and siRNA activity. *Molecular systems biology*. 2010;6:363.
270. Lee S, Donehower LA, Herron AJ, Moore DD and Fu L. Disrupting circadian homeostasis of sympathetic signaling promotes tumor development in mice. *PloS one*. 2010;5:e10995.
271. Fu L, Pelicano H, Liu J, Huang P and Lee C. The circadian gene Period2 plays an important role in tumor suppression and DNA damage response in vivo. *Cell*. 2002;111:41-50.
272. Gery S, Komatsu N, Baldjyan L, Yu A, Koo D and Koeffler HP. The circadian gene per1 plays an important role in cell growth and DNA damage control in human cancer cells. *Molecular cell*. 2006;22:375-82.
273. Mehta N and Cheng HY. Micro-managing the circadian clock: The role of microRNAs in biological timekeeping. *Journal of molecular biology*. 2013;425:3609-24.

7 Acknowledgements

My sincere gratitude goes to my supervisor and mentor Prof. Dr. med. Andreas Schober who gave me the opportunity to work with him and on this project. His ideas, suggestions and mentorship were indispensable for the success of this project. I also wish to thank Dr. Maliheh Nazari-Jahantigh whose supervision, contributions, and suggestions during my training and research, have helped in producing this work.

I will also like to acknowledge Dr. Yuanyuan Wei, Dr. Lucia Natarelli, and Dr. Ela Karshovska who have also contributed significantly to my work and training. I want to as well thank my fellow PhD students: Mengyu Zhu, Petra Hartmann and Farima Zahedi who also helped, encouraged and contributed in various ways to this project. I acknowledge also, the support and contributions of our technicians: Kathrin Hyell, Claudia Geißler, Judith Campos and Lourdes Luiz-Heinrich.

I will like thank the Deutscher Akademischer Austausch Dienst (DAAD) and the Ministry of Education, Government of Ghana, for the funding during my Doctoral training and Karola Rügamer-Biese for her support and administrative work.

Finally, my deepest gratitude goes to my family for their support and prayers and to my two best friends Nana Oye Ewuraba Williams and Isaac Ankumah for always being there.